Universität Stuttgart
IER Institut für Energiewirtschaft
und Rationelle Energieanwendung

Forschungsbericht

Modelling the energy yield of bifacial photovoltaic plants and their integration into European power supply systems

Dimitrij Chudinzow

Band 149

Modelling the energy yield of bifacial photovoltaic plants and their integration into European power supply systems

Von der Fakultät Energie-, Verfahrens- und Biotechnik der Universität Stuttgart zur Erlangung der Würde eines Doktor-Ingenieurs (Dr.-Ing.) genehmigte Abhandlung

vorgelegt von
Dimitrij Chudinzow, M.Sc. RWTH
geboren in
Kisinev, Republik Moldova

Hauptberichter: Prof. Dr.-Ing. Kai Hufendiek
Mitberichter: Prof. Dr.-Ing. Hendrik Lens

Tag der Einreichung: 20.10.2021
Tag der mündlichen Prüfung: 13.04.2022

Institut für Energiewirtschaft und Rationelle Energieanwendung, Universität Stuttgart
Heßbrühlstr. 49a, 70565 Stuttgart
Prof. Dr.-Ing. Kai Hufendiek
Abteilung: Systemanalyse und Erneuerbare Energien (SEE)
Dr. sc. agr. Ludger Eltrop

2022

ISSN 0938-1228

D93 (Dissertation der Universität Stuttgart)

"If I have seen further, it is by standing on the shoulders of Giants."

Sir Isaac Newton

Acknowledgement

This doctorate was created during my time as a research assistant at the IER from 2015-2020, an exciting time with ups and downs, during which I was able to learn a lot and which I would not want to miss. Many people have supported me during my doctorate, whom I would like to thank at this point with all my heart.

I would like to thank my doctoral supervisor Prof. Dr.-Ing. Kai Hufendiek, who has always supported me and provided me with useful advice and asked exactly the right critical questions in the doctoral seminars and follow-up meetings. It was a good preparation for the defence.

I would like to express my sincere thanks to Prof. Dr.-Ing. Hendrik Lenk for taking over the co-report and Prof. Dr.-Ing. Günter Scheffknecht for taking over the chair of the examination.

My thanks of course go to my head of department, Dr. Ludger Eltrop, whose team always had a positive, friendly and constructive atmosphere. I appreciate the fact that you, Ludger, have given me a lot of freedom in choosing my doctoral thesis topic.

I would also like to express my special thanks to Dr. Markus Klenk from the Zurich University of Applied Science, who provided me with significant support in the validation of the simulation model.

I would like to express my deepest thanks to all current and former employees in the administration who keep the IER running. Many thanks to Claudia Heydorn, Nicole Lampa, Andriy Chut, Nadine-Denise Auwärter, Adelheid Flauss, Angelika Zimmermann and Martin Spengler. I would also like to thank Ralph Schelle, who always helped without hesitation with very practical problems such as replacing a broken light bulb.

My doctorate would never have been possible without my great colleagues, who have become friends over the years and who have always supported me in word and deed. The whole college at the IER is wonderful, but my special thanks go to Natalia Matiz Rubio, my long-time office colleague, whose positive attitude motivated not only me, but the whole IER. It is with great amusement that I will remember our struggle to find the right level of office lighting.

Many thanks to Joshua Güsewell, with whom I could share my passion for beautiful Matlab plots and who was always ready to share his knowledge and skills with everyone.

Many thanks to Sylvio Nagel, with whom I always enjoyed working together, especially when working on our joint article. With pleasure I will also remember the little football breaks.

Many thanks to Samah Gouya, for whose fighting spirit I have great respect, both in sport and in her professional development, keep it up!

Many thanks to Christoph Bahret, who was able to juggle several projects at once and with whom the cooperation was always constructive and a lot of fun.

Acknowledgement

Many thanks to Jannik Vetter-Gindele. The interesting business trips to Rwanda and Vietnam will always remain in my memory.

I would like to thank my friends Christina, Roman, Sophie and Felix Janulik, who have so often proved that "love goes through the stomach". Many thanks for the countless beautiful and delicious moments together, during which I was able to switch off so wonderfully.

From the bottom of my heart I thank my beloved wife Dr. Yiqing Yan. Thanks to you I could always refuel at home and then give my best at work. You also gave me a lot of wise and helpful advice for my doctorate. Thanks for always standing behind me!

My dear sister Elena Lindenmann, I thank you with all my heart that you are always there for me. No matter whether it is picking me up from kindergarten or your support in difficult times - I can always rely on you. You can't imagine how great it was to visit you regularly in Aarau, to play with the little ones and to remember what really counts in life. Thanks for everything.

My dear mother Olga Kettler, words cannot express how much I owe you. If I were to try, this acknowledgement of thanks would be longer than the actual promotion. Therefore, I only want to say how much I love you and that without your strength and love all this would never have happened. Thanks!

Finally, I would like to dedicate this work to my beloved grandparents, through whose love I was able to develop the courage to believe in myself and strive for more - Николай Николаевич Петрашов, Мария Григорьевна Петрашова, Виктор Павлович Худынцов and Анна Соломоновна Худынцова.

Stuttgart, May 2022

Dimitrij Chudinzow

Abstract

Bifacial photovoltaic systems (B-PV) offer the advantage over conventional, monofacial photovoltaic systems (C-PV) that the irradiation hitting the back can also be converted into electricity. Thanks to this property, B-PV offer the possibility of significantly increasing the energy yield and reducing the cost of electricity. Furthermore, vertically installed bifacial PV systems (VBPV) facing east and west can achieve a generation profile complementary to C-PV, which can help to increase the economic efficiency of market-oriented PV systems and reduce integration costs in national power supply systems. Despite these promising features, B-PV has long played a minor role in research, development and application, leaving knowledge gaps in the areas of "energy yield simulation", "field design" and "integration into power supply systems". The present thesis contributes to closing these knowledge gaps.

In the **first step**, the state of the art in energy yield modelling of B-PV as of 2016 was analysed. It was found that the adequate modelling of cast ground shadows, the irradiation absorbed from the front and the back, as well as the yield-reducing effects of the module rows on each other, represents a knowledge gap. Using a newly developed energy yield model, methods were developed to address this knowledge gap. This was essentially achieved by combining three-dimensional modelling of the PV system and methods from the field of irradiation exchange. This approach made it possible to quantify and classify the influence of important irradiation and installation parameters on the energy yield. In addition, a breakdown of the total absorbed irradiation into eight components became possible, which allows a site-dependent identification of the most important irradiation contributions. As a result, it was shown, among other things, that the presence of ground shadows can reduce the backside contribution to electricity generation by almost 30 % and the total annual electricity generation by up to 4 %. This illustrates the importance of thorough modelling of ground-reflected irradiance for a sound energy yield prediction.

While decades of experience in field design of C-PV have led to reliable design guidelines on how to achieve minimum cost of electricity, this level of knowledge is not yet available to the same extent for B-PV. To contribute closing this knowledge gap, the **second step** was to use the newly developed model to investigate for eight European sites how different installation parameters affect the energy yield and cost of electricity of non-tracking and single-axis tracking B-PV. From this, general recommendations for the field design were derived, depending on latitude and irradiation conditions. The results showed, among other things, that with increasing latitude of the investigated site, an increase in the row spacing leads to an ever

higher energy yield gain. If the energy yield is to be achieved by brightening the soil (e.g. with bright gravel), which is associated with additional costs, a reduction in the electricity generation costs is possible with a suitable overall configuration of the PV field. This illustrates that the complex interactions of radiation absorption must always be investigated holistically in order to find the cost optimum. A validation of the simulation model showed that the angle-dependent **absorption of irradiation** on the front side is well represented by the simulation model. Only at a tilt angle of 90° do larger deviations occur. The angle-dependent **electricity generation** (front + rear side) is also well captured by the model, with larger deviations occurring at a tilt angle of 0° (module is parallel to the ground). At cloudy weather, the model tends to overestimate the electricity generation by approx. 5 %, at sunnier weather the electricity generation is underpredicted by 10 %-15 %. The highest underprediction of generated electricity was observed at a tilt angle of 0° with a 20 % deviation.

National power supply systems with high shares of installed C-PV capacity face the challenge of nearly simultaneous power generation from these systems because they are generally oriented towards the equator. This results in a generation peak at midday, while in the mornings and afternoons electricity generation is usually significantly lower. On the one hand, this simultaneity leads to decreasing electricity prices on the stock exchange, which endangers the profitability of PV systems. On the other hand, the total costs of power supply systems increase due to the need to maintain power plant reserves and electricity storage. VBPV enables feed-in profiles that have a peak in the morning and a peak in the afternoon. Consequently, in the **third step**, it was investigated which energetic and economic advantages could result from the use of VBPV compared to C-PV. The economic analyses from a business perspective were carried out for twelve locations in four European countries, while the cost-reducing effects in a power supply system were investigated with the help of a cost-minimising electricity market model using Germany as an example. It could be shown that above a latitude of 50°, VBPV always has a higher annual electricity generation than C-PV. An analysis of historical electricity prices in Germany showed that although C-PV always had a higher net present value, the difference to VBPV constantly decreased with decreasing electricity prices, which indicates an increasing competitiveness of VBPV. At the system level, VBPV was found to play an essential role in a cost-minimal electricity system with a high share of renewables and a high CO_2-reduction. In the most ambitious of the climate scenarios investigated, VBPV would account for about 70 % of the total installed PV capacity and enable an annual system cost reduction of about 0.6 %.

Kurzfassung

Bifaciale Photovoltaiksysteme (B-PV) bieten gegenüber konventionellen, monofacialen Photovoltaiksystemen (C-PV) den Vorteil, dass auch die rückseitig auftreffende Strahlung in Elektrizität umgewandelt werden kann. Dank dieser Eigenschaft bieten B-PV die Möglichkeit, die Energieausbeute deutlich zu erhöhen und Stromgestehungskosten zu senken. Weiterhin lässt sich mit vertikal aufgestellten, nach Osten und Westen ausgerichteten bifacialen PV Anlagen (VBPV) ein zur konventionellen PV komplementäres Erzeugungsprofil erreichen, dass dabei helfen kann die Wirtschaftlichkeit von marktorientierten PV Anlagen zu erhöhen und die Integrationskosten in nationale Stromversorgungssysteme zu senken. Trotz dieser vielversprechenden Eigenschaften hatte die B-PV lange Zeit eine untergeordnete Rolle in Forschung, Entwicklung und Anwendung gespielt, sodass Wissenslücken in den Bereichen „Energieertragssimulation“, „Felddesign“ und „Integration in Stromversorgungssysteme“ bestehen. Die vorliegende Arbeit leistet einen Beitrag zur Schließung dieser Wissenslücken.

Im **ersten Schritt** wurde der Stand der Technik des Jahres 2016 bei der Energieertragsmodellierung von B-PV analysiert. Dabei hat sich herausgestellt, dass die adäquate Modellierung der Schattenwürfe, der vorderseitig und hinterseitig absorbierten Strahlung sowie der ertragsmindernden Effekte der Modulreihen untereinander eine Wissenslücke darstellt. Mithilfe eines eigens entwickelten Energieertragsmodells wurden Methoden entwickelt, wie die genannte Wissenslücke geschlossen werden kann. Dies wurde im Wesentlichen durch die Kombination einer dreidimensionalen Modellierung der PV Anlage und Methoden zur Berechnung von Strahlungsaustausch erreicht. Dadurch konnte der Einfluss wichtiger Strahlungs- und Installationsparameter auf den Energieertrag quantifiziert und eingeordnet werden. Zusätzlich wurde eine Aufschlüsselung der gesamten absorbierten Strahlung in acht Komponenten möglich, was eine standortabhängige Identifizierung der wichtigsten Strahlungsbeiträge erlaubt. Im Ergebnis konnte unter anderem gezeigt werden, dass die Anwesenheit von Bodenschatten den rückseitigen Beitrag zur Stromerzeugung um knapp 30 % und die gesamte jährliche Stromerzeugung um bis zu 4 % verringern kann. Dies veranschaulicht die Wichtigkeit einer sorgfältigen Modellierung von bodenreflektierter Strahlung für eine solide Energieertragsmodellierung.

Während die jahrzehntelange Erfahrung im Felddesign von C-PV zu verlässlichen Entwurfsrichtlinien geführt hat, wie sich minimale Stromgestehungskosten erreichen lassen, sind diese Erfahrungen für B-PV noch nicht in gleichem Maße verfügbar. Zur Schließung dieser Wissenslücke wurde im **zweiten Schritt** mithilfe des neu entwickelten Modells für acht

europäische Standorte untersucht, wie sich unterschiedliche Installationsparameter auf den Energieertrag und die Stromerzeugungskosten von nicht nachgeführter und einachsig nachgeführter B-PV auswirken. Daraus wurden allgemeingültige Empfehlungen für das Felddesign abgeleitet, wie, je nach Breitengrad und Strahlungsbedingungen, niedrigere Stromgestehungskosten und höhere Energieerträge erreicht werden können. Im Ergebnis hat sich unter anderem gezeigt, dass mit zunehmendem Breitengrad des untersuchten Standortes eine Erhöhung des Reihenabstandes zu einem immer höheren Ertragsgewinn führt. Soll der Energieertrag durch eine mit zusätzlichen Kosten verbundene Aufhellung des Bodens erzielt werden (bspw. durch hellen Kies), so ist bei einer geeigneten Gesamtkonfiguration des PV-Feldes eine Reduktion der Stromgestehungskosten möglich. Dies veranschaulicht, dass die komplexen Wechselwirkungen der Strahlungsabsorbtion stets ganzheitlich untersucht werden müssen, um das Kostenoptimum zu finden. Eine Validierung des Simulationsmodells ergab, dass die winkelabhängige Strahlungsabsorption auf der Vorderseite durch das Simulationsmodell gut abgebildet wird. Nur bei einem Neigungswinkel von 90° kommt es zu größeren Abweichungen. Auch die winkelabhängige Stromerzeugung (Vorderseite + Rückseite) wird durch das Modell gut wiedergegeben, wobei größere Abweichungen bei einem Neigungswinkel von 0° (Modul steht parallel zum Boden) auftreten. Bei bewölktem Wetter neigt das Modell dazu, die Stromerzeugung um ca. 5 % zu überschätzen, bei sonnigerem Wetter wird die Stromerzeugung um 10 %-15 % unterschätzt. Die höchste Abweichung der erzeugten Elektrizität wurde bei einem Neigungswinkel von 0° mit einer Unterschätzung von 20 % festgestellt.

Nationale Stromversorgungssysteme mit hohen Anteilen installierter C-PV Kapazität stehen vor der Herausforderung der nahezu gleichzeitigen Stromerzeugung dieser Systeme, weil diese grundsätzlich in Richtung Äquator ausgerichtet werden. Dadurch ergibt sich eine Erzeugungsspitze zur Mittagszeit, während vormittags und nachmittags die Stromerzeugung in der Regel deutlich geringer ist. Dieser Gleichzeitigkeitseffekt führt zum einen zu fallenden Börsenstrompreisen, was die Rentabilität von PV Systemen gefährdet. Zum anderen steigen durch den Bedarf von vorzuhaltenden Kraftwerksreserven und Stromspeichern die Gesamtsystemkosten. VBPV ermöglicht Einspeiseprofile, die einen Peak am Vormittag und einen Peak an Nachmittag aufweisen. Folglich wurde im **dritten Schritt** untersucht, welche energetischen und wirtschaftlichen Vorteile sich aus dem Einsatz der VBPV gegenüber C-PV ergeben können. Dabei wurden die betriebswirtschaftlichen Analysen für zwölf Standorte in vier europäischen Ländern durchgeführt, während die kostensenkenden Effekte in einem Stromversorgungssystem mithilfe eines kostenminimierenden Strommarktmodells am Beispiel

Deutschlands untersucht wurden. Es konnte gezeigt werden, oberhalb eines Breitengrades von 50°, VBPV stets eine höhere jährliche Stromproduktion aufweist als C-PV. Eine Analyse historischer Börsenstrompreise in Deutschland hat ergeben, dass C-PV zwar stets einen höheren Barwert aufwies, der Unterschied zur VBPV mit sinkenden Börsenstrompreisen jedoch konstant abnahm, was auf eine steigende Wettbewerbsfähigkeit von VBPV hinweist. Auf Systemebene hat sich herausgestellt, dass VBPV eine wesentliche Rolle in einem kostenminimalen Stromsystem mit einem hohen Anteil von erneuerbaren Energien und einer hohen CO_2-Reduktion einnehmen kann. Im ambitioniertesten der untersuchten Klimaszenarien würde VBPV ca. 70 % der gesamten installierten PV-Kapazität ausmachen und eine jährliche Systemkostenreduktion von ca. 0.6 % ermöglichen.

Table of content

List of figures

List of tables

Nomenclature

Abbreviation	Explanation
AT	A single-axis tracked PV system with a north-south axis, whose modules follow the azimuth angle of the sun (azimuth-tracked, AT).
BG_{el}	Bifacial gain in generated electricity.
BIFOROT	„Bifacial Outdoor Rotor Tester“ experimental facility in Winterthur.
C-PV	Conventional PV power plant (monofacial, equator-oriented, optimally tilted according to the latitude)
DHI	Diffuse horizontal irradiance.
DNI	Direct normal irradiance.
ET	A single-axis tracked PV system with an east-west axis, whose modules follow the elevation angle of the sun (elevation-tracked, ET).
FT	Fixed-tilt PV power plant.
GRI	Ground-reflected irradiance.
LCOE	Levelized cost of electricity.
PV	Photovoltaics.
STC	Standard test conditions (for PV cells and modules).
VBPV	Vertical bifacial PV.
VF	Value factor.

1 Introduction

This chapter describes the initial situation in which the present work has been carried out. For this purpose the introduction is divided. Section 1.1 provides a brief introduction to bifacial photovoltaic technology (B-PV). The technical and economic opportunities associated with B-PV investigated in this work, are described in Section 1.2. Finally, the objectives and structure of the work are presented in Section 1.3.

1.1 A brief introduction to bifacial PV

Bifacial PV cells are anything but a new technology. In fact, in principle every PV cell is bifacial, as long as neither side is completely coated with an opaque layer [1]. Historically, the research, development and application were mainly focused on monofacial cells. Simply put, monofacial cells are designed in such a way that their backside is passivated with an opaque aluminium layer to reduce the recombination of free charge carriers (i.e. reduce efficiency losses) [1]. This procedure improved the electrical efficiency but resulted in the fact that only the light that falls on the front side could be used.

Bifacial PV cells, on the other hand, can also utilize the light hitting the back. This is made possible by omitting the aluminium layer on the back of the bifacial PV cell, in addition to other adjustments in the cell design. Figure 1 shows schematically the differences between a monofacial and bifacial PERC (Passivated Emitter and Rear Cell) cell design[1].

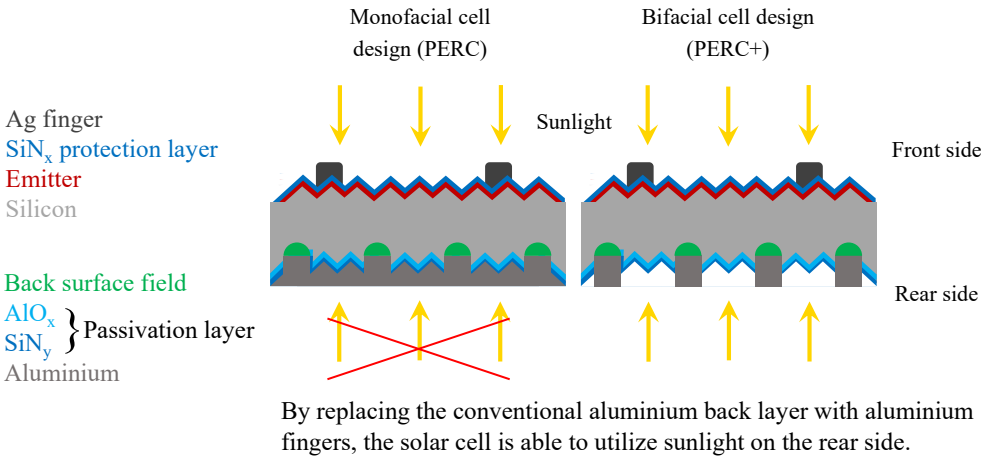

Figure 1: Schematic representation of a monofacial and bifacial PERC cell design (PERC: Passivated Emitter and Rear Cell). Own drawing based on the illustration from [2].

[1] It is important to note that there are numerous other design concepts, applicable both for monofacial and bifacial PV cells. However, PV cell design itself is a huge topic in the scientific and engineering domain and is not in the focus of this work.

Over the years various international research teams (e.g. from Germany, USA, Russia, Spain, Japan, Israel) have worked on the development and improvement of bifacial PV cells [3]. A prominent example of the use of bifacial PV cells is the International Space Station, which has a 10 kW bifacial PV array [3]. In 1980 it was reported that the energy yield of bifacial cells was 50 % higher than that of monofacial cells when placed over a white painted surface and in front of a white painted wall [4]. The observation of the significant additional energy yields achieved in this way strengthened the research activities in the field of bifacial PV.

What applies to bifacial cells naturally also applies to bifacial modules. Nowadays, bifacial PV modules have a transparent and robust encapsulation on both sides (e.g. made of glass and/or a transparent backsheet) [1], so that they too can benefit from irradiation absorption on the rear side. Figure 2 shows in a simplified way how an inclined bifacial module absorbs direct and ground-reflected irradiance (albedo irradiation).

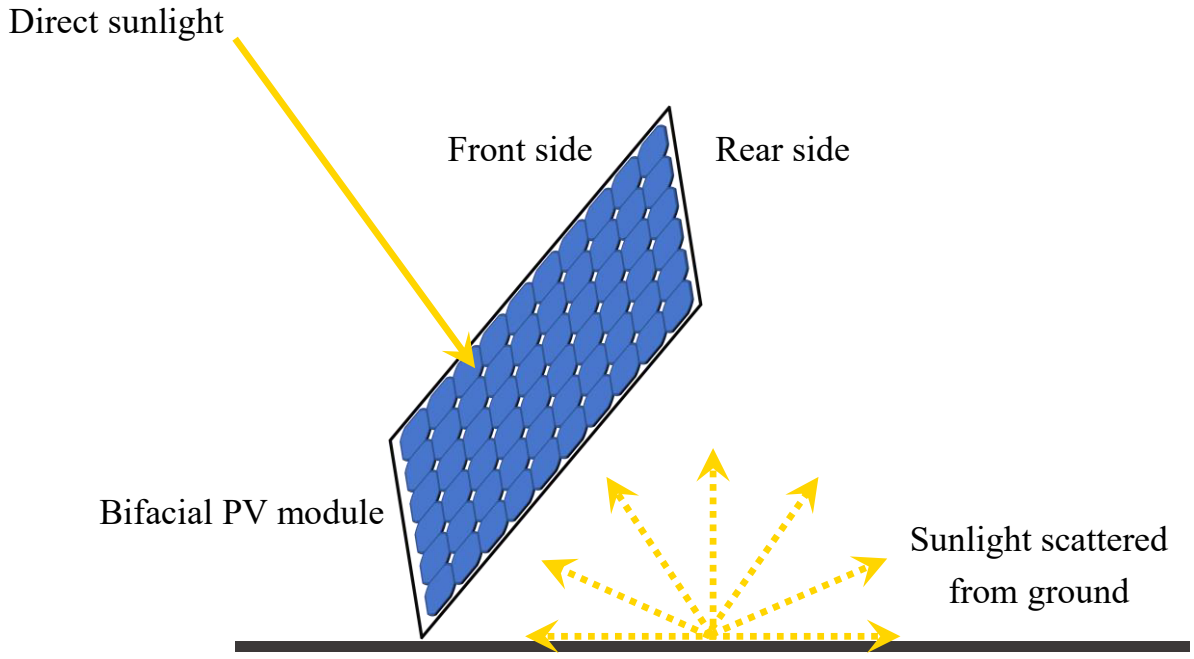

Figure 2: Schematic representation of the light absorption of a bifacial PV module. In contrast to conventional monofacial modules, bifacial modules can also make use of the irradiation hitting the back of the module.

Meanwhile the bifacial PV technology has arrived in global mass application. In 2020 there were over 9 GW of bifacial PV capacity installed worldwide and it is expected that several Gigawatts will be added annually in the next few years [5]. Due to additional backside energy gain, the International Technology Roadmap for Photovoltaic predicts a market share of almost 40 % for bifacial modules in 2028, based on the total volume of crystalline silicon modules [6]. The fact that almost all well-known manufacturers (e.g. LG, Sunpreme, Panasonic, Hanwha Q-

Cells, Trina Solar) now have bifacial PV modules in their product portfolio underlines the growing importance of the bifacial PV technology [1].

1.2 Techno-economic opportunities of bifacial PV systems

The ability of bifacial PV systems to absorb and utilize irradiation from both sides offers huge opportunities for the techno-economic performance of PV systems and national electricity supply systems, which are described in the following.

1. Due to irradiation absorption on both sides, a significantly **higher energy yield** can be expected from bifacial PV systems as compared to monofacial PV systems. Despite the still higher investments for bifacial PV systems, the higher energy yield can therefore lead to **lower levelized costs of electricity** (LCOE).
2. If bifacial PV modules are installed vertically and their two sides are oriented to the east and west (vertical bifacial PV power plant, VBPV), a completely different diurnal feed-in profile can be generated than with conventionally installed monofacial PV power plants (C-PV, oriented to the equator, inclined). This unique feed-in profile of VBPV has one peak in the morning and one peak in the afternoon (see Figure 3).

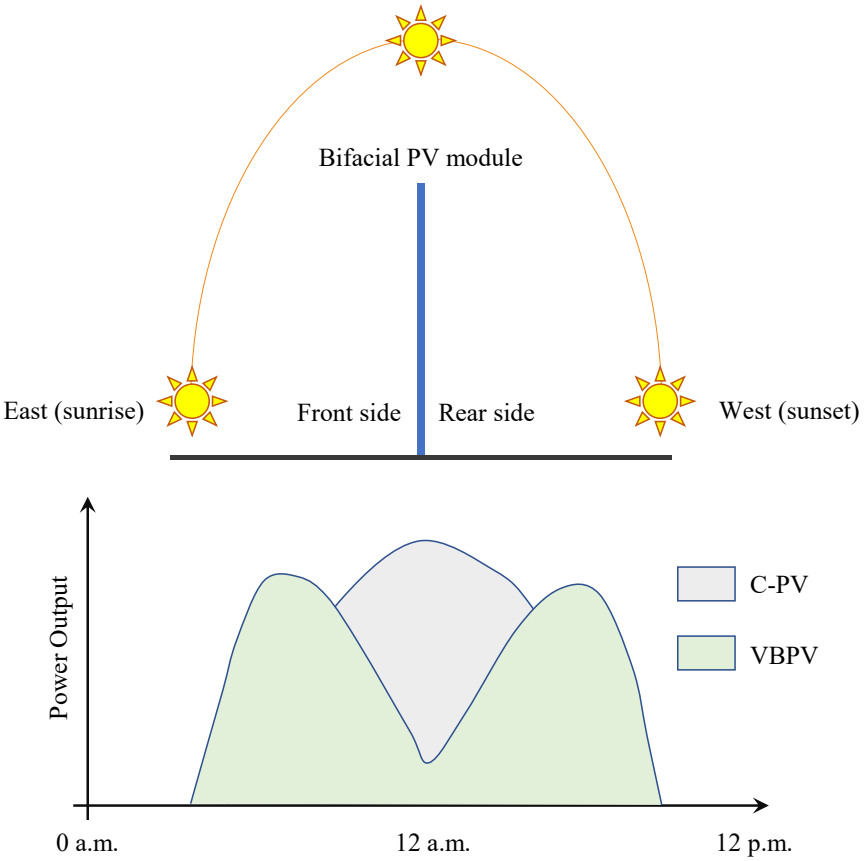

Figure 3: Vertical bifacial PV power plans (VBPV) with an east-west orientation can generate a feed-in profile with one peak in the morning and one peak in the afternoon. In contrast, conventionally installed PV systems (C-PV) have a peak around noon.

Against the background of the continuously increasing capacities of C-PV power plants in many national power supply systems (e.g. Germany), there is the opportunity of achieving two positive effects with VBPV:

2.1 With an increasing share of C-PV in total installed capacity, the generation peak of C-PV at noon leads to a corresponding decrease in electricity prices on electricity markets. As a result, the profitability and unsubsidized operation of C-PV is more difficult to achieve [7]. The unique generation profile of VBPV can **increase the market income** of plant operators and thus lead to an **improvement in profitability**.

2.2 The fact that the power generation profiles of C-PV systems are almost identical over time creates additional demand for cost-related ancillary services (e.g. electricity storage). By smoothing the feed-in curve of C-PV with the feed-in curve of VBPV, there is the opportunity to **reduce the need for ancillary services and thus save costs in the power supply system**.

1.3 Objectives and structure of the work

Based on the described status quo, none of the previously mentioned opportunities could be fully analysed and evaluated. Therefore, in the nexus described, the following two objectives were initially defined for this work:

1. Analysis of the optimal field design of non-tracked and tracked bifacial PV systems with regard to increasing the energy yield and reducing the LCOE.
2. Analysis of VBPV with regard to the increase of the profit and the contribution to the reduction of system costs in a national power supply system.

At the beginning of the analyses in the year 2016, it became apparent very early on that there is no adequate energy yield model available for bifacial PV systems, which is indispensable for the analysis of both objectives. Due to the decades of market dominance of monofacial PV systems, only few rudimentary simulation tools for bifacial PV systems have been available at that time. For example, the market leader for commercial PV simulation tools PVSyst has only started to consider bifacial PV systems since 2017 [8]. Another widely used, freely available simulation tool is the System Advisor Model, which is being developed by the National Renewable Energy Laboratory in the USA. It has only been possible to simulate the energy yield of a bifacial PV system since 2018 [9]. For this reason a third objective was added for this work:

3. Development of a suitable energy yield model for bifacial PV systems to investigate the research goals formulated above.

Based on the simulation models available at that time, the following key improvements were identified and implemented in the new model:

- The calculation of absorbed irradiation for both sides of each cell string originating from eight irradiance contributions was included: DNI_{front}, DNI_{rear}, DHI_{front}, DHI_{rear}, $GRI_{DNI\text{-}front}$, $GRI_{DNI\text{-}rear}$, $GRI_{DHI\text{-}front}$, $GRI_{DHI\text{-}rear}$, whereby GRI stands for ground-reflected irradiance. This decomposition of absorbed irradiation is a novelty in the modelling of bifacial PV systems.

- Avoiding the assumption of infinitely long module rows for calculating GRI. Instead, the view factors[2] between the relevant ground area and a cell string were computed with a numerical algorithm in three-dimensional space. This allowed for quantification of the impact of the ground size located at the sides of the module rows on the energy yield, also called “edge effects”.
- Instead of considering each individual module row in isolation, the introduction of so-called “view fields” allows the interactions of the module rows to be considered and quantified in the absorption of GRI. This holistic approach is another novelty in the modelling of bifacial PV systems.

Each of the three objectives was dealt with in a separate scientific paper and published. The structure of the thesis is therefore based on the three papers and is as follows:

Section 2 gives a summary of the first paper, which analysed the status quo in energy yield modelling of bifacial PV systems and dealt with the development and testing of the newly developed energy yield model. The published version of the first paper is given in Section 2.2. The author contributions for the first paper are given in Section 2.2.1.

Section 3 gives a summary of the second paper, which dealt with the optimal field design of fixed and single-axis tracked bifacial PV systems and which also provides a validation of the presented energy yield model. The published version of the second paper is given in Section 3.2. The author contributions for the second paper are given in Section 3.2.1.

Section 4 gives a summary of the third paper, which investigated the technical and economic properties of vertical bifacial PV systems from a business and electricity system perspective. The published version of the third paper is given in Section 4.2. The author contributions for the third paper are given in Section 4.2.1.

A graphic representation of this thesis’ structure is shown in Figure 4.

[2] The principle of view factors originates from the field of heat transfer by radiation and allows (under the assumption of an isotropic radiation distribution) to determine the radiation exchange between two surfaces A_1 and A_2 positioned arbitrarily to each other in space. Here, the value of the view factor φ_{12} indicates the share of radiant energy emitted by surface A_1 that reaches surface A_2. Consequently, the value of a view factor always takes on values between 0 and 1.

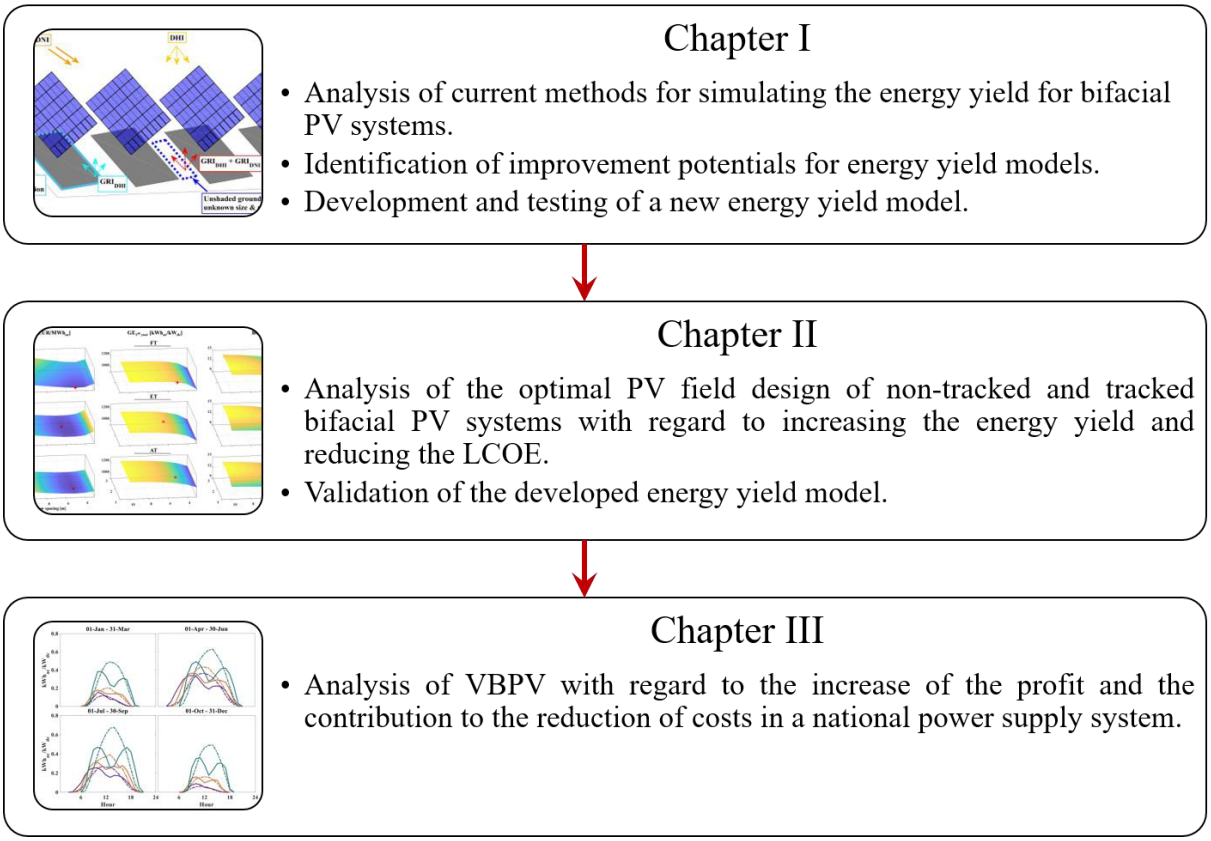

Figure 4: Structure of the thesis.

2 Chapter I – Development of an energy yield model for bifacial PV systems

2.1 Summary of Paper 1

Basically, an energy yield simulation model for PV systems consists of three submodels: an optical, a thermal and an electrical model. The optical model calculates the amount of incident radiation on the module. The thermal model considers the influence of the module temperature on the electrical efficiency of the module. The electrical model calculates the electrical power output based on the outputs of the optical and thermal sub-model. The first publication focuses on the further development of the optical model for the energy yield simulation of bifacial PV systems. Since the further development of the other two sub-models would go beyond the scope of this work, the thermal and electrical models used were taken from the literature without any major changes [10].

The development of the new energy yield model was based on the state of the art described in the literature at that time (2016-2017). It was found that there is significant potential for improvement in the representation of ground-reflected irradiance.

Most of the energy yield models investigated use two-dimensionally calculated view factors. The principle of view factors can be used to calculate the radiation exchange between the ground and the PV module [11]. The advantage of using 2D view factors is that the calculation

can be performed very quickly using an analytical formula [12]. The disadvantage is that this procedure, transferred to PV systems, is based on the assumption of infinitely long module rows. This eliminates the possibility of quantifying the contribution of the ground segments located laterally next to the module rows to the total energy yield ("edge effects"). By implementing a numerical calculation of three-dimensional view factors in the energy yield model [13], the possibility to investigate edge effects was created. For example, it could be shown that a uniform enlargement of the laterally located soil segments contributing to the energy yield leads to a slight asymptotic increase in the amount of absorbed radiation (Figure 16 (Figure 9 in Paper 1)). In practice, this finding means, for example, that in the case of soil brightening measures that are associated with costs (e.g. covering the ground with bright gravel), the focus should be on the soil segments located in the immediate vicinity, while the lightening of soil segments further away may be uneconomical.

A further implemented improvement was the differentiation of the absorbed irradiation contributions. The three-dimensional modelling of the module rows and their cast ground shadows made it possible to distinguish a total of eight irradiation contributions: DNI_{front}, DNI_{rear}, DHI_{front}, DHI_{rear}, $GRI_{DNI\text{-}front}$, $GRI_{DNI\text{-}rear}$, $GRI_{DHI\text{-}front}$, $GRI_{DHI\text{-}rear}$, where GRI stands for ground-reflected irradiance. Such a breakdown of irradiation contributions has not been found in the sighted literature so far. The benefit of this breakdown is to be able to determine for each location how important (or unimportant) an irradiation contribution is in order to carry out energy yield-increasing measures, as described in Chapter II.

A further approach, which is recurrent in many energy yield models, is that in the calculation of GRI a module row is considered in isolation. However, since depending on the field design and location, the cast ground shadows can become long and attenuate the radiation reflected by the ground, the isolated consideration of one module row can lead to an overestimation of the energy yield. This common technique was replaced by a method in which so-called "view fields" were defined for both sides of each module row. The irradiation incident on these finite-sized view fields directly determines the amount of GRI absorbed. It was taken into account that the shadows of each module row can extend into the front and rear view field of any other module row. This approach allowed the energy yield-reducing effect of the ground shadows to be considered more thoroughly. It could be shown that at sites with a high proportion of DNI irradiance, the annual energy yield could be almost 4 % higher if there were no ground shadows. This shows that future energy yield models should adequately account for the effect of ground shadows.

In summary, key contributions to the state of the art can be presented as follows:

1. The breakdown of the absorbed irradiation into eight contributions allows to quantify the site-dependent significance of irradiation type.
2. The three-dimensional calculation of the ground-reflected irradiance made it possible to abandon the otherwise frequently used simplification of infinitely long module rows and to quantify edge effects.
3. A method was presented how the energy yield-reducing effect of the cast ground shadows on the energy yield of all module rows can be considered, which improves the quality of obtained results.

It should be noted that the validation of the simulation model is presented in Chapter II.

2.2 Paper 1

SIMULATING THE ENERGY YIELD OF A BIFACIAL PHOTOVOLTAIC POWER PLANT

Authors: Dimitrij Chudinzow[3], Jannik Haas, Gustavo Díaz-Ferrán, Simón Moreno-Leiva, Ludger Eltrop

Published in: Solar Energy, Volume 183, 1 May 2019, Pages 812-822

DOI: https://doi.org/10.1016/j.solener.2019.03.071

2.2.1 Author contributions for the first paper

The following Figure 5 shows the contributions of the co-authors to the first paper, using the "CRediT author statement" system [14]. The first paper was written in the context from a German-Chilean research project ("Solar Mining Chile") in which the Chilean partners Jannik Haas, Gustavo Díaz-Ferrán and Simón Moreno-Leiva participated by reviewing the submitted manuscript. Ludger Eltrop reviewed the submitted manuscript as well.

	Simulating the energy yield of a bifacial photovoltaic power plant				
	Dimitrij Chudinzow	Jannik Haas	Gustavo Díaz-Ferrán	Simón Moreno-Leiva	Ludger Eltrop
Conceptualization	✓				
Methodology	✓				
Software	✓				
Validation					
Formal analysis	✓				
Investigation	✓				
Resources					
Data Curation	✓				
Writing - Original Draft	✓				
Writing - Review & Editing		✓	✓	✓	✓
Visualization	✓				
Project administration	✓				

Figure 5: Author contributions for the first paper.

[3] Main author

Solar Energy 183 (2019) 812–822

Contents lists available at ScienceDirect

Solar Energy

journal homepage: www.elsevier.com/locate/solener

Simulating the energy yield of a bifacial photovoltaic power plant

Dimitrij Chudinzow[a,*], Jannik Haas[b], Gustavo Díaz-Ferrán[c], Simón Moreno-Leiva[a], Ludger Eltrop[a]

[a] Institute of Energy Economics and Rational Energy Use (IER), University of Stuttgart, Heßbrühlstraße 49a, 70565 Stuttgart, Germany
[b] Department of Stochastic Simulation and Safety Research for Hydrosystems (IWS/SC SimTech), University of Stuttgart, Pfaffenwaldring 5a, 70569 Stuttgart, Germany
[c] Energy Center, Department of Electrical Engineering, University of Chile, Tupper 2007, Santiago, Chile

ARTICLE INFO

Keywords:
PV
Optical model
Ground-reflected irradiance
Albedo
Chile

ABSTRACT

Bifacial photovoltaics (bifacial PV) offer higher energy yields as compared to monofacial PV. The development of appropriate models for simulating the energy yield of bifacial PV power plants is a major topic in both research and industry. In particular, the adequate calculation of the energy yield from ground-reflected irradiance (GRI) is challenging. The purpose of this work is to investigate the currently available energy yield models and suggest areas for improvement. A new model with the proposed enhancements is used to investigate the behaviour of bifacial PV power plants in more detail. The model calculates the absorbed irradiation originating from eight irradiance contributions for the front and rear of each cell string: DNI, DHI, GRI from DHI (GRI_{DHI}) and GRI from DNI (GRI_{DNI}). The model was tested using a defined case study power plant. The breakdown of absorbed irradiation (subscript "ab") into its contributions revealed that while in summer months $GRI_{DNI\text{-}ab\text{-}rear}$ is significantly larger than $GRI_{DHI\text{-}ab\text{-}rear}$, both are roughly the same in winter months. Furthermore, for the calculation of GRI the common simplification of infinitely long module rows was avoided by implementing an algorithm for the view factor calculation for a three-dimensional space. This procedure allowed for the assessment of impact of the ground size on the annual energy yield. In a sensitivity analysis, it has been shown that the extension of the relevant ground area resulted in an asymptotical increase of the energy yield. Additionally, the impact of ground shadows on the power plant's performance was quantified. The presence of ground shadows reduced the annual electricity generation by almost 4%, compared to a hypothetical scenario where no ground shadows existed. Finally, five different ground surfaces and the resulting bifacial gains were analysed. The results show that while dry asphalt (12% reflectivity) gave less than 6% of bifacial gain related to generated electricity (BG_{el}), the use of a white membrane (70%) would result in 29% of BG_{el}.

1. Introduction

Although bifacial PV is known since the 1950s, it was considered as a niche technology for decades (Kopecek, 2014). The main advantage of this technology is its ability to utilize irradiation on the back of a PV cell, thereby increasing the energy yield per unit of land use. For example, the experimental 1.25 MW fixed-tilt bifacial Hokuto PV power plant in Japan showed a bifacial gain related to generated electricity (BG_{el}) of almost 20% over the course of more than two years (Ishikawa, 2016). Nevertheless, the interest in bifacial PV is growing. The worldwide installed bifacial PV capacity was at 1 GW by the end of 2017 (Kopecek and Libal, 2018). The "International Technology Roadmap for Photovoltaic" predicted that 30% of annually sold c-Si PV modules will be bifacial by the year 2030 (VDMA, 2017).

A significant barrier for the further propagation of bifacial PV systems is the lack of established methods to predict the energy yield of bifacial PV systems (Meydbray, 2018). Reliable yield predictions are mandatory for a bank to finance a new power plant. Yield predictions, which are associated with a higher uncertainty, lead to a higher risk premium and consequently to higher project costs (Richter, 2017). Ultimately, this issue has been stalling a more extensive use of bifacial PV technology. To overcome this, a fundamental understanding of the behaviour of bifacial PV systems is essential to support the development of more reliable yield models. Below, we give a brief overview of the related studies, highlight the main assumptions and explore the potential for improvements.

The annual energy yield of ground-mounted fixed-tilt bifacial PV arrays and one-axis tracked stand-alone bifacial modules was simulated by Shoukry et al. (2016). To calculate the bifacial gain related to generated electricity (BG_{el}), the ground area was divided into two segments: shaded and unshaded. The shaded ground segment reflected diffuse irradiance only, whereas the unshaded ground reflected both

* Corresponding author.
E-mail address: dimitrij.chudinzow@ier.uni-stuttgart.de (D. Chudinzow).

https://doi.org/10.1016/j.solener.2019.03.071
Received 22 June 2018; Received in revised form 18 March 2019; Accepted 19 March 2019
Available online 27 March 2019
0038-092X/

Nomenclature

Abbreviation and explanation

$DNI_{ab\text{-}front/rear}$, $DHI_{ab\text{-}front/rear}$, $GRI_{DNI\text{-}ab\text{-}front/rear}$, $GRI_{DHI\text{-}ab\text{-}front/rear}$ *Absorbed irradiation:* Absorbed irradiation (subscript "ab") from corresponding irradiance contribution (Wh)

T_{amb} *Ambient air temperature:* Temperature of ambient air. Taken from "Typical Meteorological Year" (TMY) dataset (°C)

θ, θ_Z *Angle of incidence of beam irradiance:* Angle of incidence θ on an inclined surface (module) and on a horizontal surface (ground) θ_Z (DEG)

$A_{String,\ unshaded}$, $A_{String,\ shaded}$ *Area of an unshaded or shaded cell string:* $A_{String,\ unshaded} = \frac{\text{Module area}}{\text{Number of cell strings per module}}$. If a cell string is partly shaded, $A_{string,\ shaded}$ is the remaining unshaded area of the cell string. If a cell string is fully shaded, $A_{string,\ shaded}$ is zero (m^2)

$A_{FVF/RFV_{complete/reduced}}$ *Area of complete/reduced front view field/rear view field:* A "complete" view field describes the rectangular view field of a module row, whose edges do not overlap with a ground shadow. When the edges of a view field overlap with ground shadow(s), the shape of the original view field minus the part(s) of ground shadow(s) that overlap(s) with the view field defines a "reduced" view field (m^2)

BG_{ab} *Bifacial gain related to absorbed irradiation:* $\frac{\text{Absorbed irradiation by rear of bifacial PV system}}{\text{Absorbed irradiation by front of bifacial PV system}}$ (–)

BG_{el} *Bifacial gain related to generated electricity:* $\frac{\text{Generated electricity by rear of bifacial PV system}}{\text{Generated electricity by front of bifacial PV system}}$ (–)

ϕ_{PV} *Bifaciality:* Ratio of rear and front electrical efficiency; $\phi_{PV} = \frac{\eta_{PV,\,el,\,rear}}{\eta_{PV,\,el,\,front}}$. In this work $\phi_{PV} = 0.85$ (–)

T_0 *Critical temperature:* Temperature at which η_{PV} is zero. Set to 270 °C (Dubey et al., 2013) (°C)

DHI *Diffuse horizontal irradiance:* Direct horizontal irradiance; this irradiance contribution is considered isotropic (Duffie and Beckman, 2013) ($\frac{W}{m^2}$)

DNI *Direct normal irradiance:* Direct normal irradiance ($\frac{W}{m^2}$)

$\eta_{PV,\,front/rear}$ *Electrical efficiency:* Electrical efficiency of PV module (–)

GE *Generated electricity:* Generated electricity by the bifacial PV power plant (Wh)

GR *Ground reflectivity:* $\frac{\text{Reflected irradiance by the ground}}{\text{Received irradiance by the ground}}$, $[0 \le GR \le 1]$ (–)

GRI_{DHI} *Ground-reflected DHI:* Diffuse horizontal irradiance, which is reflected by the ground. This irradiance contribution is considered isotropic ($\frac{W}{m^2}$)

GRI_{DNI} *Ground-reflected DNI:* Direct normal irradiance, which is reflected by the ground. This irradiance contribution is diffuse and considered isotropic ($\frac{W}{m^2}$)

I_{NOCT} *Irradiance at NOCT:* Irradiance at which NOCT is measured ($I_{NOCT} = 800\ W/m^2$) ($\frac{W}{m^2}$)

α_{PV} *Irradiation absorption factor of PV module:* $\frac{\text{Absorbed irradiation by PV module}}{\text{Received irradiation by PV module}}$, $[0 \le \alpha_{PV} \le 1]$. In this work = 0.95 (–)

NOCT *Nominal operating cell temperature:* PV cell temperature at I_{NOCT} and 25 °C ambient air temperature. In this work $T_{NOCT} = 43$ °C

T_{ref} *Reference temperature:* Temperature at which $\eta_{PV,\,el,\,ref}$ is given. In this work $T_{ref} = 25$ °C

SEY *Specific electricity yield:* Generated electricity per installed front-side capacity ($\frac{Wh_{dc}}{W_{front}}$)

β *Temperature coefficient of* η_{PV}: $\frac{1}{T_0 - T_{ref}}$ ($\frac{1}{°C}$)

$E_{ab_{String,\,front/rear}}$, $E_{el_{String}}$ *Total absorbed irradiation and generated electricity by cell string:* Total absorbed irradiation and generated electricity by a cell string. If a string is partially or fully shaded, the generated electricity is zero due to activated bypass diode (Wh, Wh_{dc})

I_{sum} *Total irradiance:* Sum of all irradiance contributions ($\frac{W}{m^2}$)

$V_{Cell\ String \rightarrow Sky}$ *View factor from cell string to sky:* View factor of a cell string to the sky. For front side of first row and rear side of last row calculated according to (Yusufoglu et al., 2014). View factors for front sides of second till last row and rear sides of first till penultimate row calculated following (Maor and Appelbaum, 2012), $[0 \le V_i \le 1]$ (–)

$V_{FVF/RVF_{complete/reduced} \rightarrow Cell\ String}$ *View factor from view field to cell string:* View factor of a complete or reduced view field to a cell string. $0 \le V_{FVF/RVF_{complete/reduced} \rightarrow Cell\,string} \le 1$. View factors calculated numerically using (Lauzier, 2004) (–)

VF width factor *View fields' width factor:* Describes by which factor the width of a view field is enlarged to the left and to the right hand side of a module row. A value of zero means, that the width of a view field equals the length of a module row. Setting the value, for example, to 0.5 would mean that the width is enlarged by 50% of a module row's length to the left and to the right hand side. The resulting total width of the view field would be 200% of a module row's length (–)

beam and diffuse irradiance. The ratio of ground-reflected irradiance (GRI) that reached a cell on the back was calculated using the concept of view factors (Stephan et al., 2010), assuming that ground shadows are always rectangular (Gross et al., 1981). Considering the shape of ground shadows to be mostly oblique parallelograms is one option to increase the precision of energy yield models. Furthermore, the authors assumed that the GRI of a row is influenced by the two adjacent rows only. Since the investigated PV array had three rows, the middle row was influenced by the two other rows, while the other two were influenced by the middle row only. As we will show in Section 2.3, it can happen that a module row's energy yield is affected by more than two rows. This understanding provides further possibility for the improvement of energy yield models. Finally, GRI was neglected for the front, thus underestimating the total energy yield.

A simulation tool for the power generation of a fixed-tilt bifacial PV power plant was developed by Chiodetti et al. (2015). The investigated power plant had three rows, each with 14 modules. The power generation of the back row was calculated by differentiating between shaded and unshaded ground areas and applying the corresponding view factors. In order to reduce computation time, view factors were calculated for one day per month and interpolated. The relative error on annual energy yield was calculated for different slopes and locations and showed that the maximum error was below 0.2%. Nevertheless, with other module slopes or at other locations, the error might be higher. Avoiding interpolation of view factors can eliminate a source of uncertainty.

The annual absorbed irradiation and bifacial gain related to absorbed irradiation (BG_{ab}) of vertically mounted and optimally inclined bifacial arrays were investigated by Appelbaum (2016). Since the ground was not subdivided into shaded and unshaded areas, the obtained results very likely overestimated the energy yield. Therefore, the distinction of shaded and unshaded ground for calculating GRI is considered as a necessity for all energy yield models.

An approach to simulate the energy yield per unit of used land of vertically mounted bifacial PV arrays was presented by Khan et al. (2017). The annual energy yield of optimally tilted (tilt angle of module rows correspond to the latitude) monofacial and vertically mounted bifacial PV arrays was compared for several locations worldwide,

particularly taking into account the latitude and local irradiance conditions. While the GRI was considered for bifacial PV arrays, it was neglected for the monofacial ones, thus making the comparison somewhat unbalanced. The calculation of view factors related to GRI was based on the assumption of infinitely long module rows. While this is a common assumption since it allows for the analytical (and therefore quick) calculation of view factors, one cannot investigate some important parameters (e.g., effect of increasing the ground area, which contributes to GRI).

NREL's System Advisor Model (SAM) is a well-known tool to model and evaluate renewable energy technologies. Currently, SAM's technology portfolio is being enhanced with bifacial PV power plants (DiOrio and Deline, 2018). Keeping the computation time of view factors low was crucial to the developers; therefore, the assumption of infinitely long module rows was applied. The calculation of GRI is performed by meshing the space between two rows into *n* segments, labelling each segment as either shaded or unshaded, and finally applying view factors both to shaded and unshaded segments (Marion et al., 2017). It is a principal question, whether a model shall be particularly fast or precise. As the understanding of bifacial PV systems' behaviour grows, the decision about which parameter needs to be modelled in more or less detail will be made simpler.

PVsyst is probably the most popular commercial simulation software for PV systems. In 2017, PVsyst's approach to implement bifacial PV systems was presented in Mermoud and Wittmer (2017). For the fast computation of GRI, PVsyst also makes use of the two-dimensional view factor calculation. Using masking angles, the amount of irradiance hitting the ground from sky is calculated in a two-dimensional manner. It remains unclear which time resolution was used for the view factor calculation and whether or not the user can edit it. Based on a sensitivity analysis, the authors recommend slightly higher tilt angles for bifacial than for monofacial PV systems for achieving maximum energy yield.

MoBiDiG is another tool to predict the energy yield of bifacial systems and to calculate the levelized cost of electricity (Berrian et al., 2017). It calculates the absorbed irradiation according to the aforementioned work from Shoukry et al. (2016) as well as the current and voltage at the maximum power point for each module. The model was validated against a test system installed on a building roof. The reported mismatch of modelled and measured power from five aggregated days was 4.9%.

A three-dimensional calculation of view factors for calculating GRI was implemented in the tool BIGEYE (Janssen et al., 2018). BIGEYE accounts for self-shading, shading from nearby objects and homogeneous transparency of the modules. Additionally, energy yield simulations for one-axis tracked systems are possible. Using an experimental rooftop installation in Zurich, the model was validated against generated electricity for a sunny day for different tilt angles. The relative deviations were below 4%, although it should be noted that using data from a single day only might be insufficient.

In summary, for an adequate simulation of bifacial PV power plants the distinction of shaded and unshaded ground segments is mandatory. To account for GRI, the theory of view factors seems to be the method of choice. Although the assumption of infinitely long module rows is convenient, since it allows using analytical functions for the quick calculation of view factors, a three-dimensional calculation of view factors might provide deeper insights into the behaviour of bifacial PV systems.

This work aims to provide a deeper understanding about the behaviour of bifacial PV power plants by including the following considerations:

1. The calculation of absorbed irradiation for both sides of each cell string originating from eight irradiance contributions: DNI_{front}, DNI_{rear}, DHI_{front}, DHI_{rear}, $GRI_{DNI\text{-}front}$, $GRI_{DNI\text{-}rear}$, $GRI_{DHI\text{-}front}$, $GRI_{DHI\text{-}rear}$, as well as generated electricity (direct current). The breakdown of the absorbed irradiation into its components indicates the importance of each contribution to the energy yield.
2. Avoiding the assumption of infinitely long module rows for calculating GRI. Instead, the view factor between the relevant ground area and a cell string was computed with a numerical algorithm in three-dimensional space. This allowed for quantification of the impact of the ground size on the energy yield.
3. The quantification of the impact of cast ground shadows on the power plant's performance.
4. Comparing five ground surfaces (and the corresponding reflectivity), the potential of increasing the energy yield through ground treatment is shown.

In order to make this work more transparent, all analyses were performed for a defined case study of a bifacial PV power plant, which is based on the characteristics of the Chilean bifacial PV power plant La Hormiga (Joanny et al., 2017). The following Section 2 presents the methodological approach. Results are discussed in Section 3. Finally, Section 4 contains a conclusion and an outlook for further research.

2. Method

The basic structure of the model can be subdivided in three parts (Model Inputs, Model Calculations and Results) and is shown in Fig. 1. The model was written in Matlab.

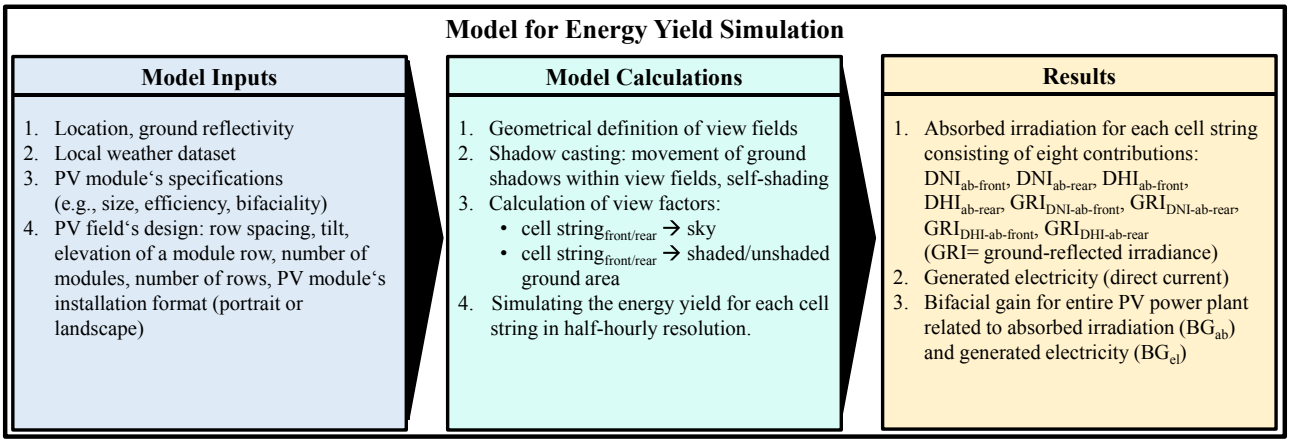

Fig. 1. Structure of the model.

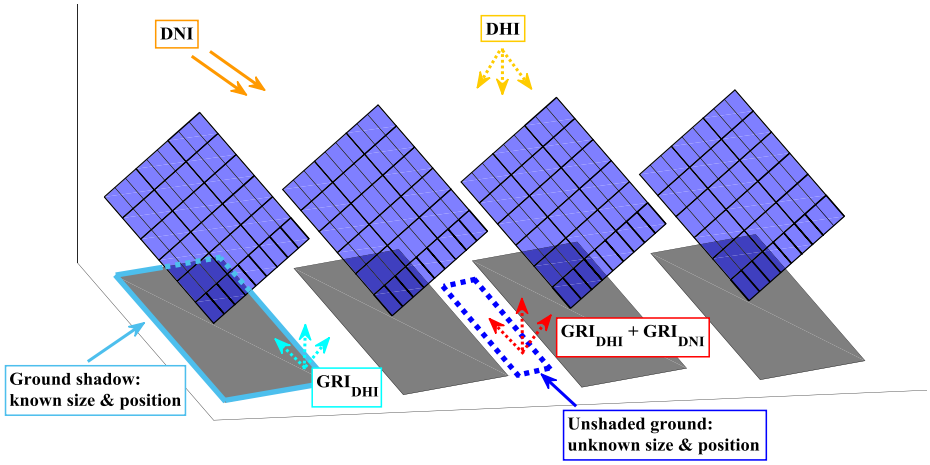

Fig. 2. Irradiance contributions in a bifacial PV array: DNI, DHI, GRI_{DHI} and GRI_{DNI}.

2.1. Irradiance contributions

First, we are going to examine the most relevant irradiance contributions for power generation of bifacial PV systems. In this work, we assumed that the modules were completely opaque; therefore, their cast ground shadows did not receive any beam irradiance (DNI). The isotropic sky diffuse model was used, which means that diffuse irradiance is uniform for the sky dome (Duffie and Beckman, 2013). Fig. 2 shows that only diffuse horizontal irradiance (DHI) is reflected from shaded parts of the ground, thereby producing GRI_{DHI}. In contrast, the unshaded parts of the ground reflect both direct and diffuse irradiance, yielding GRI_{DHI} and GRI_{DNI}. While the position and size of cast ground shadows are relatively easy to simulate, the size and position of the unshaded ground parts is unknown and therefore need to be dealt with differently. To calculate the ground shadows, the spatial position of the modules' corners and the sun's celestial path are the only inputs needed. The simulation of the sun's movement was performed according to Duffie and Beckman (2013). In our model, any configuration of module rows is possible, as long as all module rows are symmetric. The next Section 2.2 describes how the unshaded ground area was accounted for.

2.2. Definition of view fields

To consider for both GRI_{DHI} and GRI_{DNI}, a rectangular ground segment for each side of a module row was defined. We expressed these ground segments as "front view field" and "rear view field". One of our central assumptions is that GRI, which is created outside any view field, does not contribute to absorbed irradiation.

Fig. 3 depicts an example of how the front and rear view fields for module row 3 are defined. The length of the front view field is defined with the pink[1] (PL1, PL2) and green (GL1, GL2) lines in such a way that GRI can hit the top edge of module row 3. The resulting cone, which encloses the space of radiative energy exchange between the front view field and third module row, is coloured green. Accordingly, the pink (PL1, PL2) and turquoise (TL1, TL2) coloured lines define the length of third row's rear view field. The resulting cone, which encloses the space of radiative energy exchange between the rear view field and third module row, is coloured turquoise. The front view field of the first row and the rear view field of the last row are considered to be larger, since they are not obstructed from either side by adjacent module rows. In this work, the length of the first front view field and the last rear view field was defined as 150% of the length of inner view fields. Furthermore, the width of all view fields is equal. The width of the view fields' was defined as the 1.5-fold length of a module row by prolongation of the view fields both to the left and to right by 25% of a module row's length. By performing a sensitivity analysis in Section 3.3, the impact of the view field's width on annual energy yield was investigated.

2.3. Definition of shading constellations

There are two distinct shading constellations: without and with self-shading among the module rows. When there is no self-shading, the shadows on the ground are separated (Fig. 4a). One can also see that a cast ground shadow of a row overlaps with multiple view fields (Fig. 4b), thereby reducing the amount of absorbed GRI_{DNI} for the whole array. As mentioned in Section 1, Fig. 4b illustrates that the cast shadow of a specific module row may easily reduce absorbed $GRI_{DNI\text{-}ab\text{-}front/rear}$ by any other module row: the green ground shadow overlaps with all four front view fields. This effect becomes especially prominent with a lower elevation of the sun's angle and narrow row distances. When self-shading occurs, the cast ground shadows of the equidistantly placed module rows merge into one single shadow segment (Fig. 5a). This single shadow overlaps with three rear view fields and one front view field (Fig. 5b). The shadow part, which is shown in yellow in Fig. 5b, does not contribute to absorbed irradiation, since it is not part of any view field. The described interaction among ground shadows and view fields discourages from analysing isolated module rows. Instead, the PV field should be considered in a holistic manner. The presented model accounts for interactions among any ground shadow, any module row and any view field.

2.4. Calculation of absorbed irradiation

The definition of view fields and the distinction of shaded and unshaded areas of each view field allow the application of the concept of view factors for calculating $GRI_{DNI\text{-}ab\text{-}front/rear}$ and $GRI_{DHI\text{-}ab\text{-}front/rear}$. Both irradiation contributions were calculated for each cell string for both sides, and the corresponding view factors were computed using the numeric algorithm from (Lauzier, 2004), which allows the calculation of view factors for arbitrarily shaped planar surfaces in three-dimensional space. The amount of $DHI_{ab\text{-}front/rear}$ was calculated for each module row as a whole, whereby the corresponding view factors were determined analytically according to Maor and Appelbaum (2012). Finally, the amount of $DNI_{ab\text{-}front/rear}$ was calculated according to Duffie and Beckman (2013). To avoid additional complexity, it was assumed that the view factor from a view field to the sky is always one,

[1] For interpretation of color in Fig. 3, Fig. 4b, Fig. 5a and Fig. 5b, the reader is referred to the web version of this article.

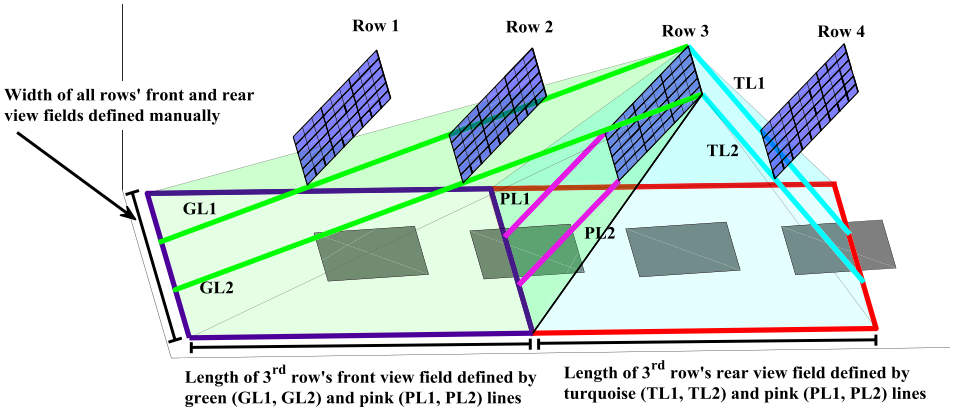

Fig. 3. Example definition of the view fields of module row 3.

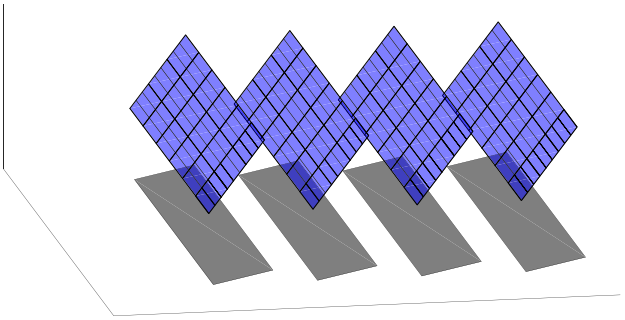

Fig. 4a. Array without self-shading. A single ground shadow is (mostly) shaped as an oblique parallelogram. All ground shadows are separated.

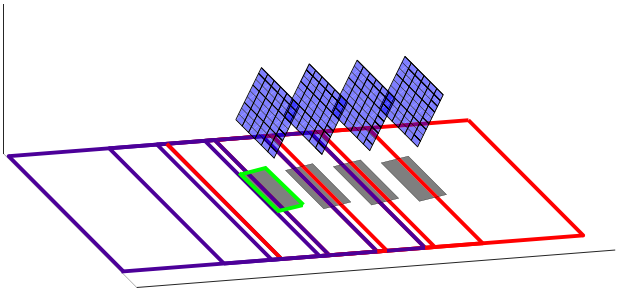

Fig. 4b. Interaction of cast ground shadows with front (purple) and rear (red) view fields at time with no self-shading. The green-contoured shadow overlaps with all four front view fields.

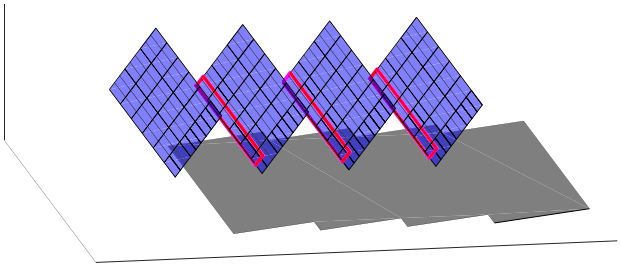

Fig. 5a. Array with self-shading. Cast ground shadows merged into a single shadow polygon. The magenta rectangles indicate shadows on the module rows (self-shading).

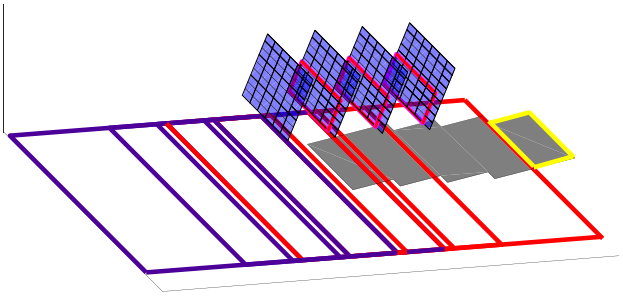

Fig. 5b. Interaction of cast ground shadows, which merged into a single shadow, with front (purple) and rear (red) view fields at time with self-shading. The yellow-contoured shadow area does not contribute to absorbed irradiation, since it is not part of any view field. The magenta rectangles indicate shadows on the module rows (self-shading).

irrespective of adjacent module rows. The main formulas used to calculate the energy yield are given in Section 6, Table 2.

2.5. Calculation of generated electricity

The model checks each cell string whether the front or rear is shaded or not, thereby emulating a bypass diode. If a string is shaded (fully or partially) by another module row, the corresponding bypass diode is forward biased, thus the power generation of the cell string is zero during the corresponding time step. The simulation was performed in a half-hourly resolution, where the hourly typical meteorological year (TMY) data was interpolated linearly. Losses due to inverters, wiring, soiling etc. were considered zero. For simplicity, the efficiency of maximum power point trackers was considered always as one.

2.6. Testing the model using a case study

The Chilean bifacial PV power plant La Hormiga in San Felipe (latitude = –32.7159°, longitude = −70.7221°) was taken as the reference for our case study (Fig. 6). La Hormiga incorporates 9,180 bifacial modules (270 W_p), as well as 240 monofacial modules[2] (ISC Konstanz, 2015). The technical parameters of the bifacial modules were taken from the "BiSoN MBA-GG60-270 W_p" datasheet (Megacell, 2015). According to photographs of the site (Joanny et al., 2017; Kopecek, 2018), the ground is covered with white gravel along the

[2] Because the focus of this work is on bifacial PV, the monofacial modules were neglected.

Fig. 6. Photograph of La Hormiga, taken in 2017 (Kopecek, 2018).

whole length of a module row in order to increase the energy yield. The ground surface to the left and right of a module row has not been modified. Since we had no possibility to measure the ground reflectivity onsite, a value of 40% was used for white gravel (Bretz et al., 1998). Furthermore, La Hormiga has three modules in landscape format along the short side of a row with a tilt angle of approximately 30°. The array's front is oriented towards the equator, the modules' installation height is roughly 0.5 m and the row spacing is approximately 5 m. This corresponds to a ground coverage ratio of 0.59, whereby this ratio is defined as the (usually) short side of a module row divided by the row spacing (Doubleday et al., 2016). A TMY dataset for San Felipe in hourly resolution was taken from (Ministerio de Energía, 2017). Since the simulation was carried out for both sides of each cell string, it would have been computationally too time-consuming to consider all modules of La Hormiga. Therefore, a downscaled PV power plant was simulated, which had four rows. Each row incorporated 18 modules in landscape format, with three modules along the short side and six along the bottom. In total, the investigated bifacial PV system had 72 bifacial modules with a front-side capacity of 19.44 kW_p.

3. Results & discussion

3.1. Absorbed irradiation & generated electricity

The energy yield was simulated over the course of one year. Fig. 7 shows the energy yield in terms of absorbed irradiation (subscript "ab"),

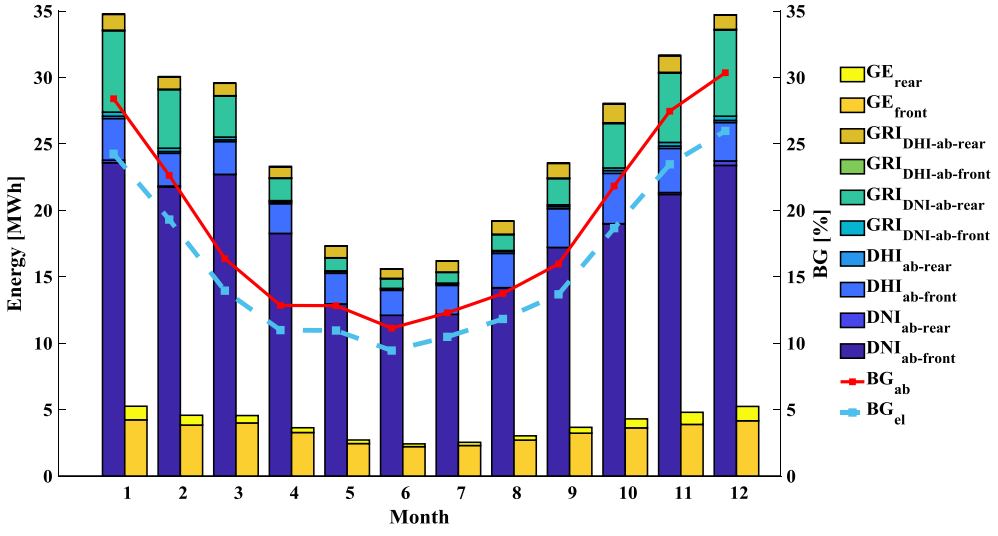

Fig. 7. Simulated absorbed irradiation, generated electricity (GE) and bifacial gains (BG_{ab}, BG_{el}) of a 19.44 kW_p bifacial PV power plant, located in San Felipe, Chile. Subscripts: "ab" = absorbed irradiation from corresponding irradiance contribution, "el" = electrical.

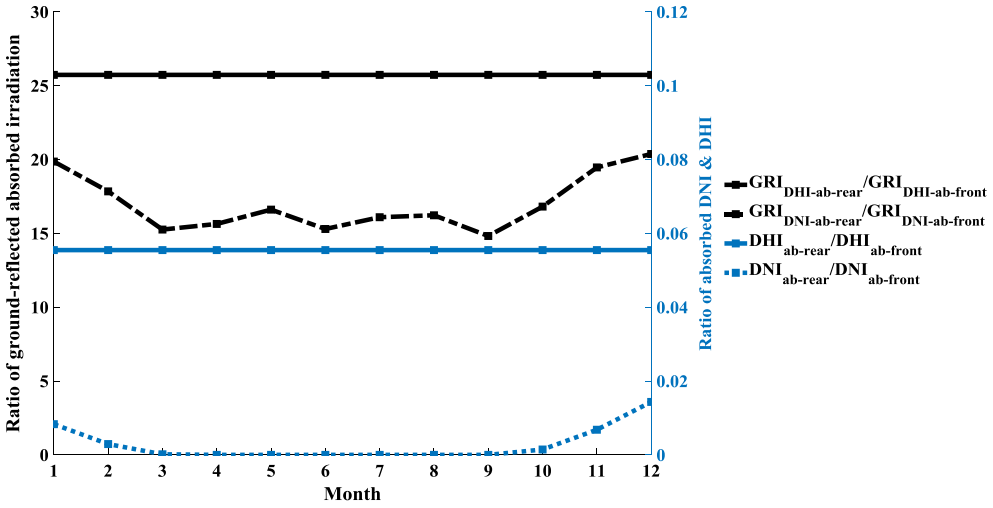

Fig. 8. Simulated monthly ratios of rear and front irradiation contributions.

generated electricity (GE) as well as bifacial gains. One can see that BG_{ab} and BG_{el} were higher in the summer months than in the wintertime.[3] This happens, because the sun's elevation angle is lower in winter and therefore reduces the intensity of GRI_{DNI}. Additionally, shadows are longer in winter and GRI_{DNI} is further reduced. The differences between BG_{ab} and BG_{el} arose, because both are coupled through the relationship: bifaciality $\varphi_{PV} = BG_{el}/BG_{ab}$ (when neglecting electrical losses). The major reason for the described divergence in both BG is that the bifaciality of the analysed modules is 0.85. Two electrical losses led to further decrease of the generated electricity. Firstly, the absorbed irradiation on the rear heated up the modules more, thus reducing the electrical efficiency. Secondly, partly shaded strings did absorb irradiation, but did not contribute to power generation due to the activated bypass diode. For the whole year, the loss in power generation due to self-shading was 0.2%. It should be noted, that this figure represents losses due to self-shading of the module rows only; shadows from mounting, junction boxes, nearby objects etc. were not considered in this work. Furthermore, Fig. 7 illustrates that in summer $GRI_{DNI\text{-}ab\text{-}rear}$ is significantly larger than $GRI_{DHI\text{-}ab\text{-}rear}$, while both contributions are roughly the same in winter months. This can be attributed to longer ground shadows in the winter as well, as well as to the use of an isotropic sky diffuse model. As expected, $DNI_{ab\text{-}front}$ constituted the greatest share of absorbed irradiation in every month, which is always true in sunny regions. The annual bifacial gains were BG_{ab} = 20.1% and BG_{el} = 17.1%. For optimized bifacial PV installations, a BG_{el} up to 30% can be expected (Kopecek and Libal, 2018). The "Bifacial Design Guide" from LG reports, that at a ground reflectivity of 90%, a BG_{el} of almost 29% is achievable (LG, 2017). For larger arrays with adverse interactions between module rows and ground shadows, lower values in the range of 5–15% can be expected, whereby these values strongly depend on the array design, location and especially the ground reflectivity (Reise and Schmidt, 2015). For the entire year, the specific electricity yields (SEY) were SEY_{front} = 2051 kWh_{dc}/kW_{front}, SEY_{rear} = 351 kWh_{dc}/kW_{front} and $SEY_{front+rear}$ = 2402 kWh_{dc}/kW_{front}.

3.2. Seasonality of rear and front irradiation contributions

Fig. 8 shows the monthly ratios of rear and front irradiation contributions. Both ratios from $GRI_{DHI\text{-}ab\text{-}rear/front}$ and $DHI_{ab\text{-}rear/front}$ were constant throughout the year, because they depended on the module slope angle only. The ratio of $DNI_{ab\text{-}rear/front}$ is characterized by a smooth course over the year, rising in summer and dropping in winter. This is due to the DNI only rarely hitting the rear and only for short periods during sunrise and sunset, which led to a minimal increase in $DNI_{ab\text{-}rear}$. The annual course of $GRI_{DNI\text{-}ab\text{-}rear/front}$ is characterized by a zigzag contour. This is based on two effects: firstly, when the sun is lower, the cast ground shadows are further away from the array, leading to fewer interactions between the ground shadows and the view fields. Secondly, when interaction takes place, the rear view fields are affected more often than the front view fields, because the array is oriented towards the equator and ground shadows were only rarely in front of the array (more precisely: when the beam irradiance hit the rear). One can also see that the rear contributes relatively more to $GRI_{DNI\text{-}ab\text{-}rear}$ in the summer months when the sun elevation angle is high. In summary, although $GRI_{DNI\text{-}ab\text{-}rear}$ and $GRI_{DHI\text{-}ab\text{-}rear}$ are significantly larger than $GRI_{DNI\text{-}ab\text{-}front}$ and $GRI_{DHI\text{-}ab\text{-}front}$ (provided that the modules are not installed vertically), the energy yield of the front might tip the scale when it comes to bankability considerations. It is therefore advisable to consider GRI_{front} in all yield predictions.

3.3. Influence of ground size on the energy yield

As previously mentioned, we defined front and rear view fields, which represent the ground contributing to GRI. The width of all view fields (VF) was initially defined as the 1.5-fold length of a module row by expanding its width by 25% to the left and the right of a module row. This corresponded to a VF width factor of 0.25 (a VF width factor of zero would mean that the width of all view fields is exactly the length of a module row). In order to investigate the impact of the view fields' width on the energy yield, a sensitivity analysis was conducted. Fig. 9 shows, that the enlargement of the VF width factor from zero to 0.25 gave the largest increase in energy yield. A further increase of the VF width factor promoted the energy yield insignificantly. This result reveals, that although the area of the view fields was increased proportionally, the course of the energy yield showed an asymptotical behaviour. This is because the longer the distance from a view field's segment to a module, the smaller the corresponding view factor. In conclusion, in order to boost the energy yield by increasing the ground reflectivity (e.g., using bright ground cover material), it might be enough to consider the ground in close vicinity only, thereby saving costs.

3.4. Influence of ground shadows on the energy yield

Based on the previously mentioned assumptions regarding completely opaque modules, cast ground shadows do not reflect DNI, thus reducing the energy yield of the power plant. In order to assess the magnitude of this effect, a second scenario was simulated. In this

[3] In the southern hemisphere, the seasons are the other way around than in the northern hemisphere.

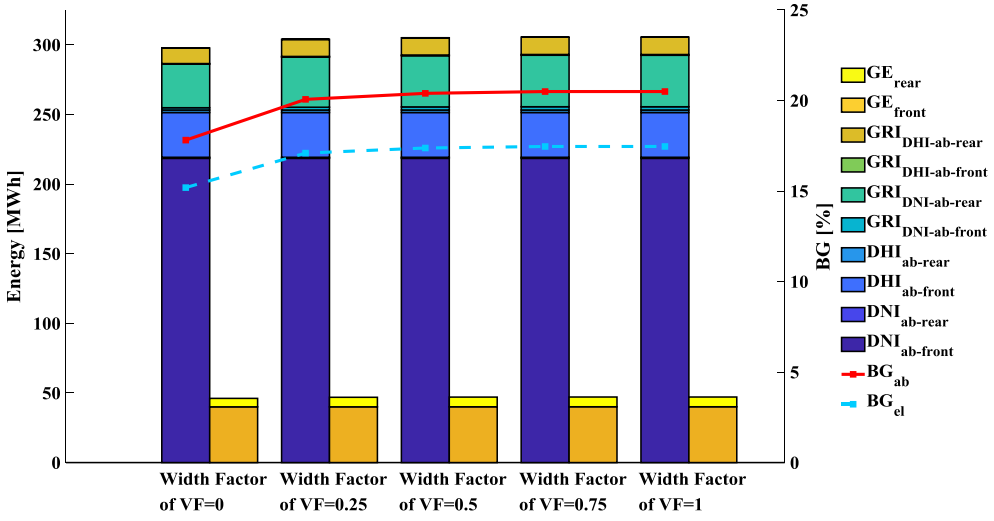

Fig. 9. Impact of the view fields' width on the annual energy yield and bifacial gains.

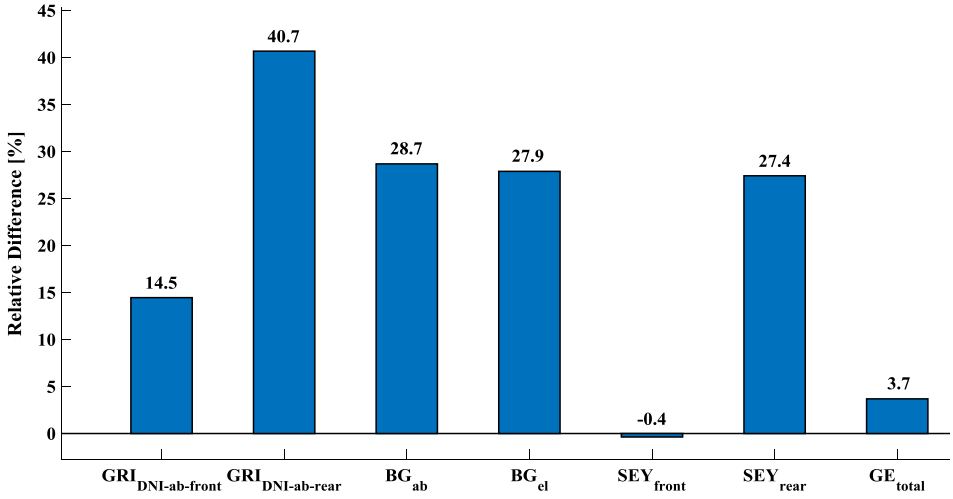

Fig. 10. Relative difference of selected parameters based on two scenarios: 1. Cast ground shadows do not exist; 2. Cast ground shadows exist.

Table 1
Different ground surfaces and their reflectivity.

Ground surface	Ground reflectivity [%]	Reference
Dry Asphalt	12	PVsyst (n.d.)
Grass	20	PVsyst (n.d.)
Dry Grassland	25	Intelligent Systems Laboratory (n.d.)
White Gravel	40	Bretz et al. (1998)
White Membrane	70	Bretz et al. (1998)

second scenario, all boundary conditions were unchanged except one: there were no ground shadows, (i.e., all view fields were always unshaded). However, self-shading among the module rows still occurred. Through the comparison of this second scenario with the primary one, we derived the influence of the ground shadows on the power plant's performance. Fig. 10 shows the relative difference[4] of selected parameters related to a whole year. It reveals that cast ground shadows affected $GRI_{DNI\text{-}ab\text{-}rear}$ the most, reducing its contribution by more than 40%. Interestingly, SEY_{front} was slightly lower when there were no ground shadows. This happened, because the effect of additional heating of the modules, which reduced the electrical efficiency, outweighed the amount of additional $GRI_{DNI\text{-}ab\text{-}front}$. SEY_{rear} would have been 27% higher if there were no ground shadows. In addition, the total annual electricity generation GE_{total} would have grown by 3.7%. It is worth mentioning that all values highly depend on the view fields' size and ground reflectivity. Nevertheless, the magnitude of results show that cast shadows can have a significant impact on a bifacial PV power plant's performance and their adequate modelling is advisable.

3.5. Increasing the energy yield with bright ground covering

The ground reflectivity is one of the most important parameters for the energy yield of a bifacial PV power plant. The power plant's operator can artificially adjust this parameter for maximizing the energy yield. In order to quantify the change in energy yield when using different ground surfaces, a sensitivity analysis with five different ground surfaces (Table 1) was performed. The resulting annual energy yield and bifacial gains are presented in Fig. 11. The comparison of different ground surfaces illustrates that the use of bright ground cover materials (white gravel, white membrane) significantly increases the annual electricity yield.

[4] Relative Difference = ($Parameter_{no\ ground\ shadows}$ - $Parameter_{with\ ground\ shadows}$)/$Parameter_{with\ ground\ shadows}$.

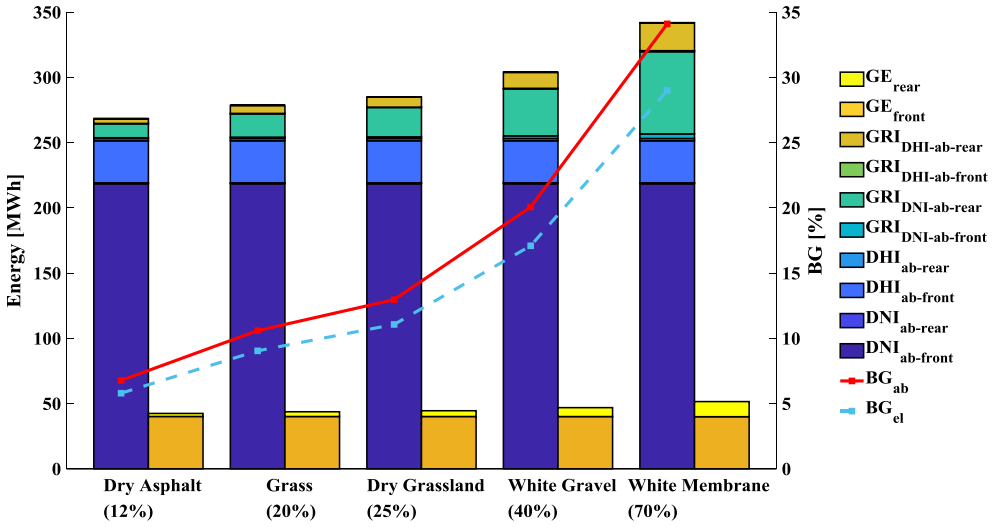

Fig. 11. Sensitivity analysis of ground reflectivity.

4. Conclusion & outlook

Based on a review of existing models to simulate the energy yield of bifacial PV power plants, this work explores options to improve the quality of energy yield models. The presented opportunities for improvement were implemented in an own simulation model, where the influence of ground size, cast ground shadows as well as ground reflectivity on the energy yield were investigated. The breakdown of absorbed irradiation originating from eight irradiance contributions ($DNI_{front/rear}$, $DHI_{front/rear}$, $GRI_{DHI\text{-}front/rear}$ and $GRI_{DNI\text{-}front/rear}$, whereby GRI stands for ground-reflected irradiance) allowed for the identification of the most significant contributions to the total energy yield. The presented method shows how the influence of ground shadows on the entire PV array can be accounted for in a holistic way. This means that it should be accounted for that the cast ground shadows of any module row may have an impact on absorbed GRI by any other row.

A 19.44 kW_p bifacial PV power plant, based on technical characteristics of the Chilean bifacial PV power plant La Hormiga was used as a case study to test the model. The results showed that the monthly bifacial gain regarding absorbed irradiation (BG_{ab}) was on average two percentage points higher than the bifacial gain regarding generated electricity (BG_{el}). Annual BG_{el} and BG_{ab} were 17.1% and 20.1%, respectively, where the ground surface was white gravel with a reflectivity of 40%.

To evaluate the impact of the ground size on the energy yield, a sensitivity analysis was conducted. The results showed that the extension of ground area, which contributes to ground-reflected irradiation, resulted in a slight, asymptotical increase of the energy yield.

In order to investigate the impact of ground shadows on the power plant's performance, a scenario without ground shadows was simulated. It was possible to show that $GRI_{DNI\text{-}ab\text{-}rear}$ was reduced more than any other irradiation contribution and would have been around 40% higher if there were no ground shadows. Annual electricity generation would have risen by nearly 4%.

Finally, the influence of ground reflectivity on the energy yield was investigated. Using five different ground surfaces (dry asphalt, grass, dry grassland, white gravel and white membrane), the change in annual energy yield and bifacial gains was analysed. It became apparent, that the use of bright ground cover materials significantly increased the annual energy yield: in the case of white membrane (70% reflectivity), BG_{el} grew to 29%.

Future improvements of the presented simulation model can be achieved by allowing spatial (e.g., partially covering the ground with bright gravel) and temporal (season-dependent) variations of the ground reflectivity. Furthermore, it should be taken into account that bifacial modules are semi-opaque. Finally, provided that necessary datasets will become available, the model should be validated against real field measurements.

Acknowledgement

The authors are grateful for the support of the German Federal Ministry of Education and Research through Grant number 01DN15008 and the support of the Chilean Council of Scientific and Technological Research through the Solar Energy Research Center SERC-Chile (CONICYT/FONDAP/15110019) and the Solar Mining project (Program for International Cooperation/CONICYT-BMBF/20140019). Simón Moreno-Leiva would like to thank the support of the German Academic Exchange Service (DAAD) and the National Commission for Scientific and Technological Research of Chile (CONICYT) through the "Becas Chile-DAAD" program.

Appendix

Table 2 shows the main formulas to calculate the energy yield for the case that beam irradiance comes from the front. For the case of beam light hitting the rear, the same formulas apply (with necessary changes in the subscripts).

Table 2
Formulas for the calculation of absorbed irradiation and generated electricity.

Direct light incidence on the front, cell string is unshaded			
$DNI_{ab\text{-}front}$ & $DHI_{ab\text{-}front}$	$GRI_{ab\text{-}front}$	$GRI_{ab\text{-}rear}$	Generated Electricity
$E_{abCell\ String,front} = [DNI{\cdot}\cos(\Theta) + DHI{\cdot}V_{Cell\ String\rightarrow Sky}] \cdot A_{String,unshaded}{\cdot}\alpha_{PV}$	$E_{abCell\ String,front,GRI} = [DHI{\cdot}A_{RVF_{complete}}{\cdot}V_{FVF_{complete}\rightarrow Cell\ String} + DNI{\cdot}\cos(\tilde{\theta}_z){\cdot}A_{RVF_{Reduced}}{\cdot}V_{FVF_{Reduced}\rightarrow Cell\ String}]{\cdot}GR{\cdot}\alpha_{PV}$	$E_{abCell\ String,rear,GRI} = [DHI{\cdot}A_{RVF_{complete}}{\cdot}V_{RVF_{complete}\rightarrow Cell\ String} + DNI{\cdot}\cos(\tilde{\theta}_z){\cdot}A_{RVF_{Reduced}}{\cdot}V_{RVF_{Reduced}\rightarrow Cell\ String}]{\cdot}GR{\cdot}\alpha_{PV}$	$E_{el_{Cell\ String}} = \eta_{PV,front}{\cdot}[E_{abCell\ String,front} + E_{abCell\ String,front,GRI} + E_{abCell\ String,rear,GRI}{\cdot}\phi_{PV}]$
Direct light incidence on the front, cell string is shaded			
$DNI_{ab\text{-}front}$ & $DHI_{ab\text{-}front}$	$GRI_{ab\text{-}front}$	$GRI_{ab\text{-}rear}$	Generated Electricity
$E_{abCell\ String,front} = [DNI{\cdot}\cos(\tilde{\theta}) + DHI{\cdot}V_{Cell\ String\rightarrow Sky}] \cdot A_{Cell\ String,shaded}{\cdot}\alpha_{PV}$	see above	see above	0
Calculation of $\eta_{PV,\ front}$			
$\eta_{PV,front} = \eta_{PV,front,ref}{\cdot}[1 - \beta{\cdot}(T_{amb} - T_{ref}) + (T_{NOCT} - T_{amb}){\cdot}\frac{I_{sun}}{I_{NOCT}}]$ Dubey et al. (2013)			

References

Appelbaum, J., 2016. Bifacial photovoltaic panels field. Renew. Energy 85, 338–343.

Berrian, D., Libal, J., Glunz, S., 2017. MoBiDiG: Simulat. LCOE.

Bretz, S., Akbari, H., Rosenfeld, A., 1998. Practical issues for using solar-reflective materials to mitigate urban heat islands. Atmos. Environ. 32 (1), 95–101.

Chiodetti, M., Guédez, R., Lindsay, A., 2015. Bifacial PV Plants: Performance Model Development and Optimization of Their Configuration. KTH Royal Institute of Technology. http://kth.diva-portal.org/smash/get/diva2:848584/FULLTEXT01.pdf. Accessed 15 February 2017.

DiOrio, N., Deline, C., 2018. Bifacial simulation in SAM. Bifacial Workshop 2018. <http://bifipv-workshop.com/fileadmin/images/bifi/denver/presentations/4_Diorio-_Modeling_with_SAM_bifiPV2018.pdf> (Accessed 9 October 2018).

Doubleday, K., Choi, B., Maksimovic, D., Deline, C., Olalla, C., 2016. Recovery of interrow shading losses using differential power-processing submodule DC–DC converters. Sol. Energy 135, 512–517.

Dubey, S., Sarvaiya, J.N., Seshadri, B., 2013. Temperature dependent photovoltaic (PV) efficiency and its effect on PV production in the world – a review. Energy Proc. 33, 311–321.

Duffie, J.A., Beckman, W.A., 2013. Solar Engineering of Thermal Processes, fourth ed.

Gross, U., Spindler, K., Hahne, E., 1981. Shapefactor-equations for radiation heat transfer between plane rectangular surfaces of arbitrary position and size with parallel boundaries. Lett. Heat Mass Transf. 8 (3), 219–227.

Intelligent Systems Laboratory, n.d. Average Ground Reflectance Info. <http://www.intelligence.tuc.gr/renes/fixed/info/reflectanceinfo.html> (Accessed 8 October 2018).

Konstanz, I.S.C., 2015. Largest bifacial PV system by MegaCell with BiSoN modules in Hormiga, Chile. Accessed 6 April 2018. http://isc-konstanz.de/isc/aktuelles/news/article/larges-bifacial-pv-system-build-by-megacell-with-bison-modules-in-hormiga-chile.html.

Ishikawa, N., 2016. World First Large Scale 1.25MW Bifacial PV Power Plant on Snowy Area in Japan. 3rd bifi PV workshop in Miyazaki, Japan. Photovoltaic Technical Solutions. <http://bifipv-workshop.com/fileadmin/images/bifi/miyazaki/presentations/3_1_3_-_ISHIKAWA_-_World_1st_large_scale_Bifacial_PV_power_plant.pdf> (Accessed 15 February 2017).

Janssen, G.J.M., Burgers, A.R., Binani, A., Carr, A.J., van Aken, B.B., Romjin, I., Klenk, M., Nussbaumer, H., Baumann, T., 2018. How to maximize the kWh/kWp ratio: simulations of single-axis tracking in bifacial systems.

Joanny, M., Libal, J., Kopecek, R., Veschetti, Y., Colin, H., 2017. Bifacial Systems Overview. <http://bifipv-workshop.com/fileadmin/layout/images/Konstanz-2017/1_M._Joanny_INES_System_overview.pdf> (Accessed 7 February 2018).

Khan, M.R., Hanna, A., Sun, X., Alam, M.A., 2017. Vertical Bifacial Solar Farms. Physics, Design, and Global Optimization. <http://arxiv.org/pdf/1704.08630>.

Kopecek, R., 2014. Bifacial world – monofacial modules: why do we compromise system power? <http://de.slideshare.net/sandiaecis/2-kopecek-bifi-pvok-60345232> (Accessed 15 February 2017).

Kopecek, R., 2018. Photos from bifacial PV power plant “La Hormiga”. Personal Communication.

Kopecek, R., Libal, J., 2018. Towards large-scale deployment of bifacial photovoltaics. Nat. Energy 3 (6), 443–446.

Lauzier, N., 2004. MATLAB function that calculates view factors between two planar surfaces. <https://de.mathworks.com/matlabcentral/fileexchange/5664-view-factors> (Accessed 14 July 2017).

LG, 2017. Bifacial Design Guide. <http://www.lg-solar.com/downloads/brochures/Bifacial_design_guide_Full_ver.pdf> (Accessed 25 January 2018).

Maor, T., Appelbaum, J., 2012. View factors of photovoltaic collector systems. Sol. Energy 86 (6), 1701–1708.

Marion, B., MacAlpine, S., Deline, C., 2017. A Practical Irradiance Model for Bifacial PV Modules. Preprint. <https://www.nrel.gov/docs/fy17osti/67847.pdf> (Accessed 9 October 2018).

Megacell, 2015. Datasheet BiSoN MBA-GG60 series 270-280Wp. <http://www.mega-group.it/wp-content/uploads/MBA-GG60-270_280B_rev3.pdf> (Accessed 5 April 2018).

Mermoud, A., Wittmer, B., 2017. Bifacial shed simulations with PVsyst. <http://bifipv-workshop.com/fileadmin/layout/images/Konstanz-2017/2_B._Wittmer_PV_SYST_Bifacial_shed_simulations.pdf>.

Meydbray, J., 2018. Barriers to Financing Bifacial PV Projects. <http://bifipv-workshop.com/fileadmin/images/bifi/denver/presentations/1_Meydbrey-_financing_barriers_bifiPV2018.pdf> (Accessed 18 October 2018).

Ministerio de Energía, 2017. Explorador Solar. <http://www.minenergia.cl/exploradorsolar/> (Accessed 14 September 2017).

PVsyst, n.d. Albedo coefficient. <http://files.pvsyst.com/help/albedo.htm>. Accessed 8 October 2018.

Reise, C., Schmidt, A., 2015. Realistic Yield Expectations for Bifacial PV Systems – an Assessment of Announced, Predicted and Observed Benefits. Frauenhofer ISE. <https://www.tuv.com/media/corporate/solar_1/pv_modulworkshop_2/42_Reise_

Realistic_Yield_Expectations_for_Bifacial_PV_Systems.pdf> (Accessed 4 May 2018).
Richter, A., 2017. Bankability. Meyer Burger. <http://bifipv-workshop.com/fileadmin/layout/images/Konstanz-2017/1_A._Richter_MEYER_BURGER_Bankability.pdf> (Accessed 18 October 2018).
Shoukry, I., Libal, J., Kopecek, R., Wefringhaus, E., Werner, J., 2016. Modelling of bifacial gain for stand-alone and in-field installed bifacial PV modules. Energy Proc. 92, 600–608.
Stephan, P., Kabelac, S., Kind, M., Martin, H., Mewes, D., Schaber, K.-H., 2010. VDI Heat Atlas, 2. Springer, Heidelberg u.a XXI, 1585 S.
VDMA, 2017. International Technology Roadmap for Photovoltaic (ITRPV). 2016 Results. <http://www.itrpv.net/Reports/Downloads/> (Accessed 2 July 2017).
Yusufoglu, U.A., Lee, T.H., Pletzer, T.M., Halm, A., Koduvelikulathu, L.J., Comparotto, C., Kopecek, R., Kurz, H., 2014. Simulation of energy production by bifacial modules with revision of ground reflection. Energy Proc. 55, 389–395.

3 Chapter II – Improving the techno-economic performance of bifacial PV systems

3.1 Summary of Paper 2

Due to the decades-long worldwide expansion of monofacial PV systems and the associated learning curve, there are established and approved methods and rules on how a monofacial PV system should be designed to achieve minimum LCOE [15]. This basis of experience is currently not yet available to this extent for bifacial PV systems. Only gradually are design guidelines for bifacial PV systems emerging as a result of international project planning experience gained in recent times [16–18]. A comparison of the worldwide installed capacity illustrates the knowledge advantage of monofacial PV systems: in 2020 there were currently approx. 583 GW of PV capacity in operation worldwide [19]. In addition, countless gigawatts of monofacial PV systems have already been decommissioned. The estimated installed capacity of bifacial PV systems in the same year, however, was around 9 GW [5]. Due to the fact that in bifacial PV systems the rear-side absorbed irradiation makes a significant contribution to the total energy yield, it can be assumed that the design guidelines established for monofacial PV systems cannot be transferred to bifacial PV systems without adaptions.

Against this background, the impact of selected installation parameters of the PV field design on energy yield and LCOE was investigated. Three plant types were examined: a fixed-tilt bifacial PV power plant (FT), a horizontal single-axis tracked bifacial PV power plant with a north-south axis and an east-west axis. Since the modules of a system with an east-west axis follow the elevation angle of the sun and those of a system with a north-south axis follow the azimuth angle of the sun, the systems are referred to as “elevation-tracked” (ET) and “azimuth-tracked” (AT). By extending the analyses to eight European sites, the influence of the location was also considered.

For fixed-tilt bifacial PV systems it was found that doubling the distance between the module rows increases the energy yield, whereby the relative additional energy yield decreases with decreasing latitude. In addition, it was found that if the module elevation is increased and the tilt angle is reduced at the same time, the energy yield increases at all eight locations, but at the same time the bifacial gain in generated electricity (BG_{el}) decreases at six locations. This clearly shows that the popular parameter BG_{el}, which relates the energy yield at the rear to the energy yield at the front, should not be regarded as the only target variable, but always the total energy yield (Figure 24).

Furthermore, it could be shown that the tilt angle of a bifacial PV system should be smaller compared to the otherwise optimally defined tilt angle of a monofacial PV system in order to

increase the energy yield. This is an important finding which shows that the design guidelines for bifacial PV systems cannot be taken from monofacial PV systems without adaptions.

The comparison of the elevation-tracked and azimuth-tracked bifacial PV systems has revealed that the energy yield gain by increasing the module elevation of both technologies increases equally with decreasing latitude. If, on the other hand, the distance between rows is increased, the energetic gain of ET decreases significantly with decreasing latitude. In the case of AT, there was no correlation observed between the latitude of a site and the energetic gain from an increased row spacing.

In addition to the optimisation of the installation parameters, there is the possibility of increasing the yield by artificially brightening the soil. By covering the ground with light-coloured materials, the reflectivity of the ground is increased and with it the amount of ground-reflected irradiance. The gain in energy yield by using light gravel (40 % reflectivity) and a white foil (70 % reflectivity) was investigated. In all three plant designs the absolute energy yield could be increased by approx. 10 % - 20 % depending on the material used, whereby the latitude had no noticeable influence. In contrast, it was found that the relative gain of BG_{el} increases with decreasing latitude for all three plant designs.

Based on the results presented, the influence of a changed field design on the energy yield of three different plant designs can be estimated, which represents a scientific added value. In order to evaluate the impact of a changed field design on the LCOE, cost functions for the used land area, a higher module elevation as well as for the soil brightening were defined and evaluated. It has been found that, as a rule of thumb, the field design with the highest energy yield does not correspond to the field design with the lowest LCOE. This illustrates that in the planning phase of a B-PV system, it must be clearly defined whether maximum energy yield or minimum LCOE is to be achieved.

In addition to the techno-economic analyses, the simulation model developed was validated. Thanks to a good scientific cooperation with the Zurich University of Applied Science, the measurement data of the bifacial test facility BIFOROT (Bifacial Outdoor Rotor Tester) could be used. A special feature of the test facility is that the tilt angle is varied every 5 seconds, so that measurement data for 12 different angles are available.

The validation was carried out on the basis of three days with varying degrees of cloud cover. The comparison of the measured and calculated absorbed irradiation on the front side showed that the simulation model generally shows a similar deviation for all inclination angles, with the accuracy varying on the three days. The smallest deviation was found on the day with the lowest degree of cloudiness, namely 2 % - 7 % depending on the angle of inclination. Larger

deviations were observed on the day with the highest degree of cloudiness, namely 10 % - 15 %. Only with a vertical installation (90° tilt angle) a deviation of 25 % was observed. The comparison of the measured and calculated electricity generation (front + rear side) also showed that the simulation model represents the angular dependence well. Only with angles of 0° and 90° did larger deviations occur (up to 20 % for a tilt angle of 0°). On average, the deviation of the measured and calculated electricity generation on the three days for the different tilt angles was between -12 % and +5 %.

In summary, the most important contributions to the state of the art described in Chapter II can be presented as follows:

1. If the ground is not brightened and covered by grass (20 % reflectivity), the LCOE for all three system designs will always increase if changes are made to the field design that are associated with costs (i.e. an increase in module elevation or row spacing).
2. If changes are made to the field design, which are associated with costs (greater module elevation, greater row spacing), lower LCOE can still be achieved, depending on the location, if soil brightening measures are additionally applied. This is a good example of achieving an economic benefit, provided that the complex interactions within bifacial PV systems are considered holistically.
3. It was calculated how expensive the brightening of the soil may be at a maximum in order not to lead to an increase of the LCOE if the installation parameters are varied. This led to the important finding that depending on the location, some changes in the field design would always lead to higher LCOE, ceteris paribus.
4. To increase the energy yield, the tilt angle of fixed-tilt bifacial PV systems should be smaller than that of monofacial PV systems.
5. The relative additional energy yield for ET and AT due to a greater installation height of the modules increases with decreasing latitude.
6. The relative additional energy yield for FT and ET due to a larger distance between rows decreases with decreasing latitude. No clear tendency was found for AT.
7. The energy yield can be significantly increased for all three system designs, regardless of the degree of latitude, by covering the ground with bright materials.
8. The validation of the simulation model showed that the angle-dependent **absorption of irradiation** on the front side is well represented by the simulation model. Only at a tilt angle of 90° do larger deviations occur. The angle-dependent **electricity generation** (front + rear side) is also well captured by the model, with larger deviations occurring at a tilt angle of 0° (module is parallel to the ground). At cloudy weather, the model tends to overestimate the

electricity generation by approx. 5 %, at sunnier weather the electricity generation is underpredicted by 12 % on average. The highest underprediction of generated electricity was observed at a tilt angle of 0° with a 20 % deviation.

In addition to the content of the presented paper, there are two supplements. The first supplement is given in Section 3.3, which confirms the site-dependent energy yields shown using another simulation model (SAM). Section 3.4 presents the main findings of an international benchmark with the presented and 12 other simulation models.

3.2 Paper 2

IMPACT OF FIELD DESIGN AND LOCATION ON THE TECHNO-ECONOMIC PERFORMANCE OF FIXED-TILT AND SINGLE-AXIS TRACKED BIFACIAL PHOTOVOLTAIC POWER PLANTS

Authors: Dimitrij Chudinzow[4], Markus Klenk, Ludger Eltrop

Published in: Solar Energy, Volume 207, 1 September 2020, Pages 564-578

DOI: https://doi.org/10.1016/j.solener.2020.06.096

3.2.1 Author contributions for the second paper

The following Figure 19 shows the contributions of the co-authors to the second paper, using the "CRediT author statement" system [14]. Markus Klenk is an employee at the ZHAW and is responsible for the BIFOROT test facility. He provided the necessary data for the validation and reviewed the submitted manuscript. Ludger Eltrop reviewed the submitted manuscript.

	Impact of field design and location on the techno-economic performance of fixed-tilt and single-axis tracked bifacial photovoltaic power plants		
	Dimitrij Chudinzow	Markus Klenk	Ludger Eltrop
Conceptualization	✓		
Methodology	✓		
Software	✓		
Validation	✓	✓	
Formal analysis	✓		
Investigation	✓		
Resources		✓	
Data Curation	✓	✓	
Writing - Original Draft	✓		
Writing - Review & Editing		✓	✓
Visualization	✓		
Project administration	✓		

Figure 19: Author contributions for the second paper.

[4] Main author

Solar Energy 207 (2020) 564–578

Contents lists available at ScienceDirect

Solar Energy

journal homepage: www.elsevier.com/locate/solener

Impact of field design and location on the techno-economic performance of fixed-tilt and single-axis tracked bifacial photovoltaic power plants

Dimitrij Chudinzow[a,*], Markus Klenk[b], Ludger Eltrop[a]

[a] Institute of Energy Economics and Rational Energy Use (IER), University of Stuttgart, Heßbrühlstraße 49a, 70565 Stuttgart, Germany
[b] Zurich University of Applied Science, SoE, Institute of Energy Systems and Fluid Engineering, Technikumstrasse 9, 8401 Winterthur, Switzerland

ARTICLE INFO

Keywords:
LCOE
PV field configuration
Energy yield
Ground reflectivity
Latitude
Validation

ABSTRACT

In the design phase of the photovoltaic field for a bifacial photovoltaic power plant (B-PV), the influence of installation parameters on both the energetic and economic performance must be considered, which makes determining the cost-optimal field design a challenge. Although some studies have dealt with this topic, many questions remain unanswered.

Therefore, this work investigated the site-dependent impact of the installation parameters row spacing, module elevation, tilt angle and soil reflectivity of a fixed-tilt and a single-axis tracked B-PV with an east–west and north south-axis on the energy yield, the levelized cost of electricity (LCOE) and the bifacial gain. Based on the results, the magnitude of the influence of an installation parameter on the energy yield and LCOE could be quantified for all three system designs. However, three findings are particularly noteworthy: 1. in the case of the fixed-tilt design, the relative energy yield gain caused by a larger row spacing increases with increasing latitude; 2. depending on PV field's configuration, soil brightening measures can significantly increase the energy yield of all three system designs, practically independent of location, and at the same time reduce the LCOE; 3. the choice of a too high module elevation can lead to small yield losses. Finally, the simulation model used was validated with the Swiss BIFOROT test array.

In summary, it can be said that the complex interactions of installation parameters must be thoroughly investigated in order to avoid energy yield losses and unnecessarily high LCOE.

1. Introduction

The main advantage of bifacial photovoltaic power plants (B-PV) compared to conventional photovoltaic power plants (C-PV) with monofacial modules is the ability to use irradiation on both sides of a module, thereby increasing the energy yield. In contrast to C-PV, the energy yield of B-PV depends to a greater extent on the PV field design. Installation parameters such as row spacing, module elevation and the reflectivity of the ground have a significant impact on the energy yield. When designing the PV field, two objectives can be distinguished: maximizing the energy yield or minimizing the levelized cost of electricity (LCOE). There are a number of measures to maximize the energy yield. One can avoid self-shading by choosing a sufficiently large row spacing. Taking mechanical stability criteria into account (e.g. wind load), the module elevation can be increased to maximize the absorption of ground-reflected irradiation. By applying soil brightening measures (e.g. piling up light-coloured gravel) it is also possible to increase the reflectivity of the soil, which increases the ground-reflected irradiation. A tracking system can also be used instead of a fixed-tilt design. As a rule, however, the second objective is pursued, namely achieving minimum LCOE (International Finance Corporation, 2015). This means that when designing B-PV, the simultaneous effects of the measures on both the energy yield and the LCOE must be carefully evaluated. The complexity of the solar field design is additionally increased by the irradiation conditions and the latitude of the site under consideration. For example, the choice of a row spacing that excludes self-shading would result in higher land costs at high latitudes than at locations closer to the equator.

The following literature review presents some studies on the topic of bifacial PV field design, while economic evaluations were not always carried out.

The impact of installation parameters (tilt angle, module elevation and ground reflectivity) of three bifacial photovoltaic system configurations located in Albuquerque on the energy yield was investigated using a ray tracing model (Asgharzadeh et al., 2018). The considered systems were equator-oriented and had a fixed tilt. The authors selected

* Corresponding author.
E-mail address: dimitrij.chudinzow@ier.uni-stuttgart.de (D. Chudinzow).

https://doi.org/10.1016/j.solener.2020.06.096
Received 28 April 2020; Received in revised form 25 June 2020; Accepted 26 June 2020
Available online 12 July 2020

the row spacing in the simulations so that no self-shading occurred. The procedure made it possible to quantify the influence of the three plant parameters on the energy yield, but no economic aspects were considered.

A global comparison of the energy yield of fixed-tilt bifacial and monofacial modules was carried out by (Sun et al., 2018). The authors considered the influence of several installation parameters on the energy yield depending on the location and visualized the results on a global map. The results can help to install a bifacial module in a way that maximizes the energy yield depending on the location. However, the yield calculations were only carried out for an isolated module, not for installations with several rows, so that the effect of self-shading could not be considered. Cost analyses were not performed.

An approach to minimize the LCOE of a fixed-tilt B-PV is presented in (Tillmann et al., 2020). In a first step, the annual energy yield was calculated in four different climate zones. Based on this, the LCOE was minimized depending on the distance between the rows and the module inclination using the Bayesian method. The costs considered included investments for hardware and the purchase of land. It was found that the well-known rule of thumb, namely to avoid shading at the winter solstice and choosing a module tilt angle corresponding to the geographic latitude, does not yield the minimum LCOE, which is an important finding. For the yield simulations, only one module row in an infinitely extended solar field was considered.

The dependency of the field design and the LCOE, taking into account land costs, module elevation, row spacing and tilt angle, was examined by (Chiodetti et al., 2015). It was found that field designs that lead to a minimum LCOE do not necessarily have the highest energy yield. This makes sense, as there is a trade-off between increasing the power generation and minimizing the overall costs. In order to limit the calculation time in the simulations, the cast ground shadows and corresponding view factors were calculated once a month. However, it was shown that under certain circumstances ground shadows can significantly reduce the energy yield (Chudinzow et al., 2019). Therefore, a more precise calculation of the view factors and the ground shadows is advisable.

A special variant of bifacial systems are vertically installed module rows with a north–south axis. In a study, the technical and economic performance of this type of plant was compared with fixed-tilt monofacial PV power plants at twelve European locations. It turned out that the vertical B-PV have consistently higher LCOE, but can achieve higher energy yields at latitudes above 50° (Chudinzow et al., 2020).

In summary, the presented studies make clear that the established rules for the design of a PV field of C-PV power plants cannot simply be transferred to B-PV systems. Rather, the interdependency of different installation parameters must be considered depending on the location in order to identify the optimal field design.

The goal of this work is to broaden the understanding of how cost-effective B-PV can be designed. For this purpose, three plant types were examined: a fixed-tilt B-PV (FT), a horizontal single-axis tracked B-PV with a north–south axis and an east–west axis. Since the modules of a system with an east–west axis follow the elevation angle of the sun and those of a system with a north–south axis follow the azimuth angle of the sun, we will refer in this article to the tracking with an east–west axis as “elevation-tracked” (ET) and with a north–south axis as “azimuth-tracked” (AT).

The installation parameters investigated include the tilt angle (in the case of FT), the row spacing, the module elevation and two different soil brightening measures. In order to investigate the influence of the site, eight different European cities were considered for the analyses. To determine the uncertainty of the simulation model, it is validated using measurement data from the BIFOROT (Bifacial Outdoor Rotor Tester) test facility located in Winterthur (Switzerland).

The further work is structured as follows: Section 2 deals with the methods used for the energy yield simulation, the applied cost functions for the B-PV and the validation. Section 3 contains the results and discussion, which served for the conclusions in Section 4.

Table 1
Investigated European sites.

Site	Latitude, Longitude [°]
Bergen, Norway	60.3, 5.22
Copenhagen, Denmark	55.63, 12.67
Warsaw, Poland	52.23, 21
Prague, Czech Republic	50.09, 14.42
Stuttgart, Germany	48.63, 8.66
Winterthur, Switzerland	47.5, 8.73
Rome, Italy	41.9, 12.49
Seville, Spain	37.42, −5.9

2. Methodology

2.1. Investigated sites and weather data

In order to investigate the influence of the location on the techno-economic performance of B-PV, eight different European cities were considered for the analyses, which are listed in Table 1 and sorted by descending latitude. Consequently, a meridian area of about 23° was covered, which corresponds to a distance of about 2700 km. The corresponding typical meteorological year (TMY) datasets were taken from (Joint Research Centre, 2019).

2.2. Energy yield simulation

The generated electricity (GE) of the three B-PV designs was calculated with an own simulation model which was presented in (Chudinzow et al., 2019). At the time of publication, only B-PV with a fixed-tilt could be simulated with the model. For the present work the model was extended by single-axis tracked systems. A distinction was made between two tracking principles:

1. The axis of a module row has a north–south orientation. The front sides of the module rows are oriented east in the morning and rotate during the day until they are oriented west in the evening. The PV modules therefore follow the azimuth angle of the sun (azimuth tracking, AT).
2. The axis of a module row has an east–west orientation. The PV modules therefore follow the elevation angle of the sun (elevation tracking, ET).

The algorithms used for the tracking calculations were taken from (Duffie and Beckman, 2013). They were originally developed for C-PV systems and have not been adapted to B-PV systems in the context of this work. Backtracking to avoid self-shading was also not considered in this work.

The energy yield simulations were carried out in hourly resolution for one year. The MBA-GG60-280 W_p BiSoN module was chosen as reference for the technical parameters bifaciality, efficiency, NOCT and module dimensions (Megacell, 2015). The electrical front-side efficiency at STC was 16.9%. The modelled power plant consisted of four rows with five modules each in landscape format along the long side and two modules along the short side of a row. Thus, the B-PV consisted of 40 modules with a total of 11.2 kW_{dc} front-side capacity. For the DC-AC inverter efficiency, an EU-weighted constant value of 0.98 was used (ABB n.d.).

2.2.1. Modelling of ground-reflected irradiance

To consider ground-reflected irradiance (GRI) in the simulation model adequately, so-called “view fields” were defined. Each module row is assigned a front view field and a rear view field. This is shown in Fig. 1 as an example for module row 3. The length of the front view

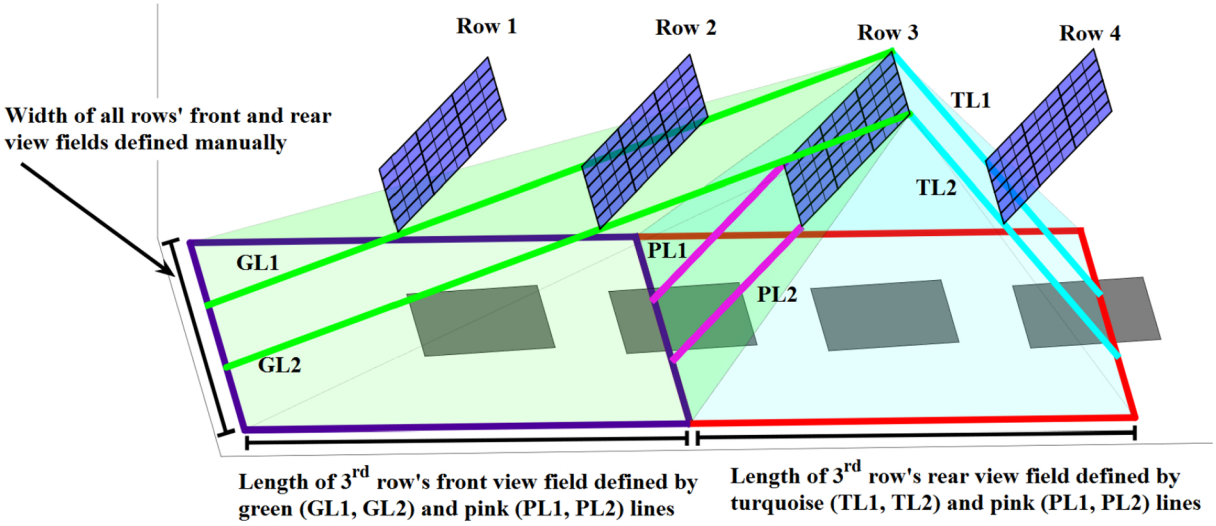

Fig. 1. Definition of front and rear view fields for the consideration of ground-reflected irradiance (Chudinzow et al., 2019).

field is defined with the pink (PL1, PL2) and green (GL1, GL2) lines in such a way that GRI can hit the top edge of module row 3. The resulting cone, which encloses the space of radiative energy exchange between the front view field and the third module row, is coloured green. Accordingly, the pink (PL1, PL2) and turquoise (TL1, TL2) coloured lines define the length of third row's rear view field. The resulting cone, which encloses the space of radiative energy exchange between the rear view field and third module row, is coloured turquoise.

The idea behind the definition of view fields is that in the energy yield simulations only the part of the GRI that originates from a view field is considered. In principle, this approach is also suitable for the analysis of tracked systems, whereby the size and position of the view fields change in each time step. What cannot be evaluated with this approach is the question whether soil brightening measures can be economically meaningful. This is because at times when the tilt angle of the module rows is very flat, the view fields can become several kilometres long and soil brightening would be limited to the adjacent soil. For this reason, two ground zones were introduced in the model for tracked systems and are shown in Fig. 2. The "inner zone" represents the part of the soil that would be brightened. The width of the inner zone corresponds to the width of the view fields, the length is defined manually (see Table 2). The "outer zone" corresponds to the surrounding soil and would not be considered for soil brightening. The reflectivity of both zones can be defined as required.

2.3. Investigated installation parameters

A base configuration of the PV field was defined for each plant design. In addition, certain parameters were varied to determine their influence. Table 2 contains an overview of the parameters considered. The values of the base configuration are printed in bold.

2.4. Economic parameters

The module elevation of B-PV systems has a significant impact on the energy yield. It was therefore particularly important to find a suitable estimate of the costs of the mounting structure, considering the effect of a variable module elevation. The costs for the mounting structure were therefore divided into two parts.

2.4.1. Mounting structure

Based on (Fu et al., 2018), the costs for the mounting structure of the fixed-tilt and single-axis tracked design of a utility-scaled PV power plant is between 87.5 EUR/kW_{dc} and 183.8 EUR/kW_{dc}. Therefore, the lower limit was taken as the mounting structure cost for the fixed-tilt design and the upper limit as the mounting structure cost for both tracked designs. It was further assumed that these basic costs refer to a module elevation of 0.75 m for the FT design and 1 m for the ET and AT designs. To account for the cost increase due to a larger module elevation, an empirical correlation was established between the installed piles and the number of installed modules in a module row. For this purpose, an online image search was used to determine the average number of poles required per installed module, depending on the plant design. For the fixed-tilt and tracked plant designs, 15 exemplary plants were considered in the image evaluation. In addition, the piles were assumed to be U-shaped galvanized steel to withstand adverse weather conditions and wind loads due to the greater construction height. The material costs for the additional installation height were estimated using German wholesale prices (Stahlshop, 2018). This results in the following cost function for the mounting structure (Eq. (1)).

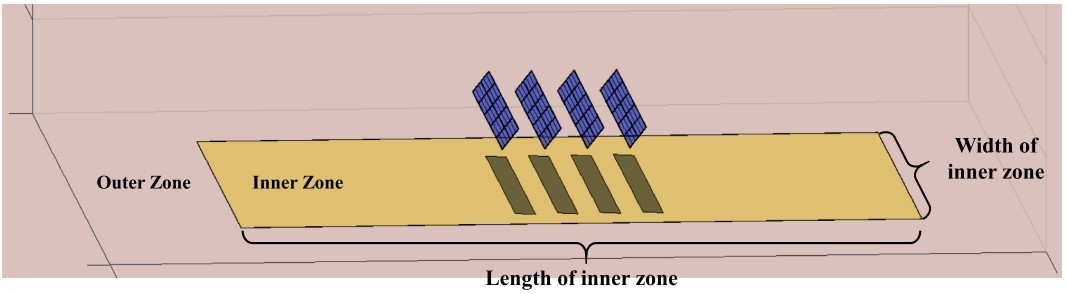

Fig. 2. Definition of the inner zone (yellow) and outer zone for a single-axis tracked B-PV. Soil brightening measures affect the inner zone only. (For interpretation of the references to colour in this figure legend, the reader is referred to the web version of this article.)

Table 2
Parameter values used in the analyses. The values in bold print define the base configuration for the three plant designs.

Parameter	Fixed-tilt plant design	Single-axis tracked plant design	Comment
Tilt angle (TA).	Optimal tilt angle −5°, **optimal tilt angle**, optimal tilt angle +5°	Tilt angle results from the tracking algorithms.	The optimal tilt angle for the bifacial PV system has been approximated to the optimal tilt angle of a monofacial PV system according to (Jacobson and Jadhav, 2018).
Row spacing (RS).	**5 m**, 10 m		
Module elevation (ME).	**0.75 m**, 1.5 m	**1 m**, 2 m	In the case of FT plant design, the module elevation is measured from the ground to the lower edge of a module row. For the ET and AT plant designs, the module elevation is measured from the ground to the rotation axis of a module row.
Ground cover (reflectivity) of inner zone.	**Grass (20%),** white gravel (40%), white foil (70%)		Reflectivity values taken from (PVsyst n.d.) and (Bretz et al., 1998).
Ground cover (reflectivity) of outer zone.	**Grass (20%)**		
Inner zone factor (see Fig. 2).		**1**, 2	The inner zone factor is used to adjust the length of the inner zone. A value of 1 sets the length of the inner zone to the length of the array, where the array length is defined as $(N_{rows} - 1) \cdot Row\ spacing$. Choosing a value of 2 would double the length of the inner zone, while the additional length is evenly distributed between the front and back of the PV array. The size of the inner zone determines the cost of the land lease.

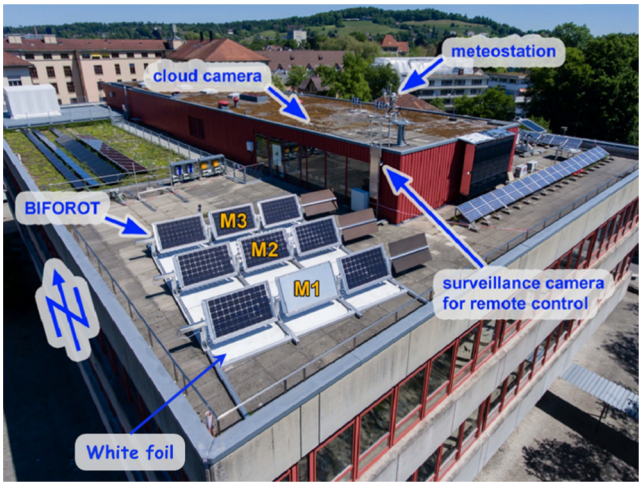

Fig. 3. BIFOROT installation on the roof of the ZHAW in Winterthur. To increase the energy yield, a white foil was placed under the array (Nussbaumer et al., 2020). The performance values of module M2 were used throughout the validation.

$$\text{Mounting costs} = P \cdot [c_0 + (ME - ME_{ref}) \cdot c_1 \cdot c_2 \cdot p] \quad (1)$$

P = Total front-side capacity [kW_{dc}]
c_0 = Base costs for mounting structure. Fixed-tilt design: 87.5 EUR/kW_{dc}, Tracked design: 183.8 EUR/kW_{dc}.
ME = Module elevation.
ME_{ref} = Reference module elevation: 0.75 m for FT, 1 m for ET and AT.
c_1 = Material costs for one meter for a U-shaped galvanized steel pole: 4.93 EUR/m.
c_2 = Average number of poles per module. Fixed-tilt design: 0.36 pole/module, tracked design: 0.2 pole/module.
p = Modules/kW_{dc}

2.4.2. Land lease

The annual land lease was set at 1800 EUR/ha (0.18 EUR/m^2) for all sites in combination with an annual increase of 2% (Leipe and Zill, 2011). It is important to emphasize that a location-dependent land lease was deliberately waived because even within one country the land lease can vary greatly from region to region. Likewise, better conditions may be negotiated for large PV projects than for small projects. In addition, this work should above all show the *differences* of a cost-optimized plant design depending on the climatic conditions of a site. Such a comparison would be opposed by the use of different lease agreements for land.

2.4.3. Further technical and economic values

The technical and economic input values used for the other system components are given in Table 6.

2.5. Validation of the simulation model

As explained in Section 2.2, an own energy yield simulation model for B-PV systems was used, which has not yet been validated. This was mainly due to the difficulty of obtaining sufficiently accurate measurement data that could be used for validation. Using test data of the test facility BIFOROT, which is operated by the Zurich University of Applied Science (ZHAW), a validation is performed in this work. This will also make it possible to estimate the uncertainty of the results of this work.

2.5.1. Experimental setup

The BIFOROT test facility is located on the roof of a ZHAW building (latitude 47.496405°, longitude 8.730359°) and consists of three rows of three modules each (Nussbaumer et al., 2020). The installed bifacial PV module type is MBA-GG60-270 from Megacell (Megacell, 2015). Each module row also has a dummy module to cast an additional shadow on the ground. The system varies the tilt angle every 5 s, so that the system characteristics of the middle module of the second row (M2) are recorded at 12 different tilt angles (see Fig. 3). The validation is carried out using the module M2, which most closely resembles the behaviour of a module in a large PV system. The energy yield simulation was performed in minute resolution. Originally, the simulation model requires the diffuse horizontal irradiance (DHI) and the direct normal irradiance (DNI) as input. However, in the measurement data used, DHI and the global horizontal irradiance (GHI) were available, so DNI was calculated using Eq. (2), where ϑ_Z is the zenith angle of the sun (NREL, 2018).

$$DNI = \frac{GHI - DHI}{\cos(\vartheta_Z)} \quad (2)$$

Table 3 shows an overview of the values for three significant input parameters, namely the electrical front-side efficiency, the bifaciality and the reflectivity of the white foil below the modules. The individual parameters were measured by the ZHAW, which differ from the literature values. The subsequent evaluation of the validation results will show that these parameters have a great influence on the quality of the simulation results.

The comparison of simulated and measured energy yield was

Table 3
Measured values and literature values for three significant input parameters of the BIFOROT test facility.

	Measured value by ZHAW	Literature value and reference	
Front-side efficiency	0.187	0.163	Module datasheet (Megacell, 2015)
Bifaciality	0.78	0.85	Module datasheet (Megacell, 2015)
Reflectivity of white foil	0.51	0.7	(Bretz et al., 1998)

carried out for three days, which differ in the degree of diffuse fraction. The diffuse fraction is the integrated DHI divided by the integrated GHI for a day. A low value stands for a sunny day, a high value for an overcast day. It is worth mentioning that other simulation models (MoBiDig, BIGEYE, PVSyst) have also been validated with BIFOROT on the basis of these three days, so that a comparability between the different simulation models is established (Nussbaumer et al., 2020).

3. Results and discussion

3.1. Electricity generation of fixed-tilt and single-axis tracked bifacial PV power plants

Fig. 4 shows the amount of annually generated electricity by the three plant designs and the BG_{el} at the eight locations. In the case of tracking systems, both parameters refer to the gross values, i.e. the own electricity consumption for the tracking systems was not subtracted. To visualize the influence of the latitude, the sites were sorted by descending latitude. The results shown were simulated for the base configuration (Table 2). The analysis of the amount of generated electricity reveals that at all locations the AT design achieves a higher energy yield than the ET design. AT and ET differ in two main characteristics. First, AT provides a more even feed-in profile throughout the day (the daily electricity generation is also available online as a supplementary video animation). The feed-in profile of ET, on the other hand, is similar to that of equator-oriented fixed-tilt PV systems and has its peak at solar noon. Secondly, ET designs are better suited for locations near the equator, where the shadows cast are short and thus do not significantly reduce performance. This is also reflected in the ratios of the amount of generated electricity by AT and ET. The additional yield of AT relative to ET in Bergen and Seville was 6% and 9% respectively. As expected, the lowest energy yield is achieved with the FT design. A look at the BG_{el} shows that the BG_{el} decreases with decreasing latitude in all system designs (the definition of the BG_{el} is given in Appendix A). This is because with decreasing latitude the modules are tilted in such a way that the rear side "sees" less ground and thus absorbs less ground-reflected irradiation. The climate of the location also plays a role. In places with a lot of direct radiation (Seville), this is more beneficial to the front energy yield than the rear energy yield, so that the BG_{el} decreases. This in turn can be explained by the fact that cast ground shadows can hardly receive direct irradiance and therefore cannot reflect it. Diffuse irradiation, on the other hand, also reaches shaded ground areas and can be reflected onto the back of a module. Therefore, the BG_{el} tends to be larger at locations with a higher diffuse fraction.

3.1.1. Impact of bifacial PV field design on the generated electricity

When designing a B-PV system, several installation parameters can be varied to increase the energy yield. The effects of a single parameter change or several simultaneous changes depend largely on the location. In order to quantify the effects, sensitivity calculations were performed based on the values shown in Table 2. In all calculations the ground was covered with grass (20% reflectivity). The change in the ratio of the amount of generated electricity by a variable PV field configuration (Var. conf.) and by the basic PV field configuration (Base conf.) is shown in the left Fig. 5. The changes of the BG_{el} are shown in the right Fig. 5. Based on the results, the following observations can be made: on the one hand, doubling the row spacing (RS) from 5 m to 10 m always leads to a higher energy yield. It is remarkable that the relative additional yield achieved in this way increases with increasing latitude. This is due to the fact that as latitude increases, the shadows become longer and so does the loss of yield caused by self-shading. Therefore, an increase in row spacing at higher latitudes leads to greater yield advantages in relative terms. Increasing the tilt angle while maintaining the same row spacing resulted in less generated electricity at all locations for both module elevations than in the base configuration (turquoise right-pointing triangle, green cross). Interestingly, the measures have different effects on the GE and the BG_{el}. A simultaneous reduction of the tilt angle and increase of the module elevation (orange diamond)

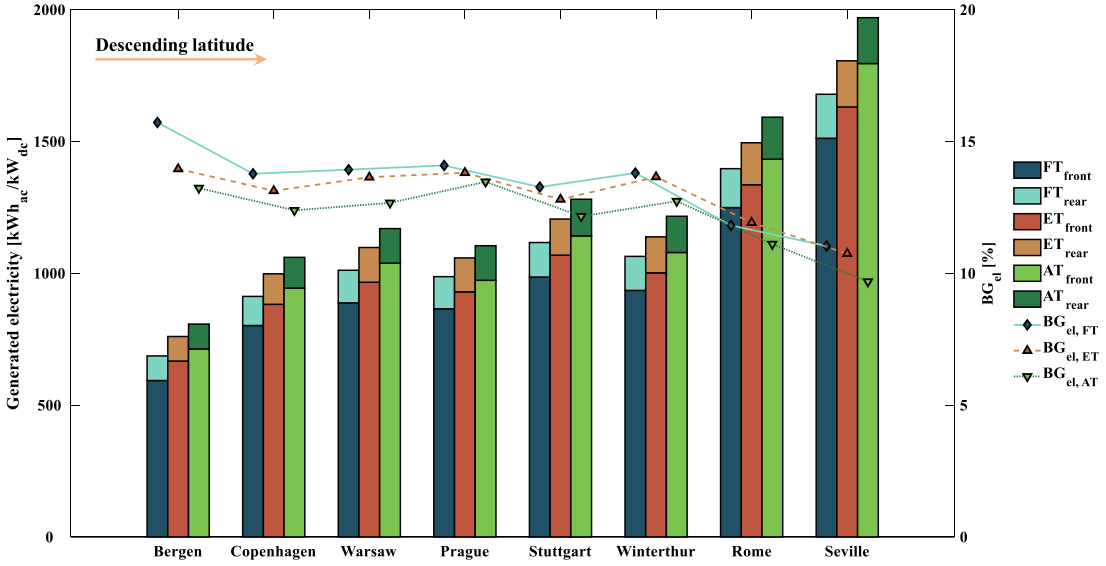

Fig. 4. Generated electricity by the three PV system designs (base configuration) and bifacial gain in generated electricity (BG_{el}) in the eight sites investigated. The amount of generated electricity of AT is always the largest, followed by ET and FT.

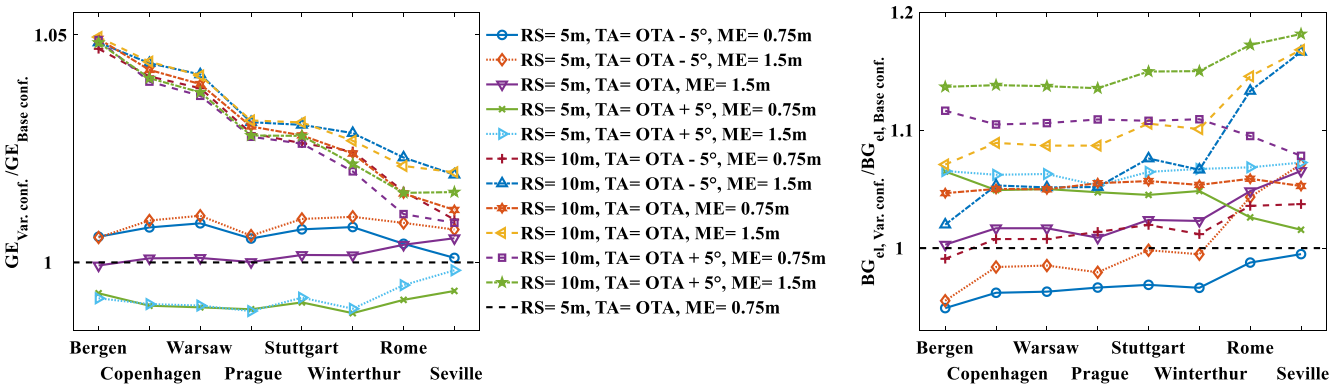

Fig. 5. Impact of field design on the annually generated electricity (GE) (left) and bifacial gain in generated electricity (BG_{el}) (right) for FT. Ground surface is grass with 20% reflectivity. The base configuration is plotted with a black dashed line. RS: Row spacing, TA: Tilt angle, OTA: Optimal tilt angle, ME: Module elevation.

increases the energy yield at all locations, but reduces the BG_{el} at six of the eight locations. Similarly, a reduction in the tilt angle leads to increased GE and reduced BG_{el} at all sites (blue circle). The measures with the greatest gain in BG_{el} were an increase in row spacing, tilt angle and module elevation, with the largest gains being achieved in Seville (green five-pointed star). It also shows that the optimum tilt angle determined for C-PV cannot be transferred one-to-one to B-PV. The results show that a reduction of the location-dependent optimal tilt angle by 5° increases the energy yield. An increase of the optimal tilt angle by 5°, however, reduces the energy yield.

The influence of altered installation parameters on GE for ET and AT is shown in the left plot in Fig. 6. A doubling of the module elevation from 1 m to 2 m (with an unchanged row spacing of 5 m) leads at all locations to a moderate increase in GE for both system designs (turquoise square, orange cross). In the simulation model, an increase in module elevation leads to an enlargement of the view fields, which in turn usually increases the amount of absorbed ground-reflected irradiation. Effects such as self-shading remain unchanged, so that the amount of absorbed irradiation not reflected form the ground does not change. Increasing the row spacing from 5 m to 10 m leads to varying results in the individual locations, depending on the tracking principle. In the case of ET, the additional amount of GE decreases with decreasing latitude (violet diamond, yellow asterisk). This can be explained by the fact that ET at high latitudes is particularly prone to self-shading. This can be reduced considerably by increasing the row spacing. Common to both tracking designs is that an increase in module elevation with decreasing latitude brings a higher additional energy yield. This is a consequence of two effects. First, a greater module elevation increases the size of the view fields. Secondly, shadows cast are shorter at lower latitudes, so that the additional size of the view fields leads to an even greater increase in energy yield. When analysing the changes in BG_{el} (Fig. 6, right plot), it is noticeable that the highest gain is achieved by an increased row spacing and module elevation (violet diamond, blue upward-pointing triangle). Interestingly, an increase in row spacing with unchanged module elevation leads to an almost constant increase in BG_{el} at all locations (yellow asterisk, red six-pointed star). It is important to emphasize that a configuration that can lead to a significant increase in BG_{el} does not necessarily increase the GE to the same extent (turquoise square, orange cross).

An additional possibility to increase the energy yield of a bifacial PV system is to increase the reflectivity of the soil. Fig. 7 shows the influence of higher soil reflectivity on the GE (left plot) and on the BG_{el} (right plot) for FT, ET and AT. Again, the base configuration was used as a reference (Table 2). As expected, the energy yield can be significantly increased by using materials with higher reflectivity. By using a white foil, the energy yield at all locations could be increased by approx. 20%, while white gravel would increase the energy yield by 6–7%. It can be seen that the impact of higher ground reflectivity on GE is not particularly dependent on the site. The increase in BG_{el}, however, is greater at low latitudes. This is due to the fact that with decreasing latitude the energy yield at the rear side decreases relatively (Fig. 4), so that higher soil reflectivity causes the BG_{el} to rise overproportionally. Since FT by definition has a constant tilt angle, an increase in ground reflectivity leads to the largest increases for GE and BG_{el} at all sites for the FT plant design (yellow asterisk, red plus).

3.2. Levelized cost of electricity of fixed-tilt and tracked bifacial PV systems

This section examines how the LCOE changes depending on location and system design and which measures are suitable to reduce the LCOE. The calculated LCOE for all sites for the three plant designs based on the base configuration are shown in Fig. 8. For a better readability the sites were sorted by descending latitude. Based on the results, some basic conclusions can be drawn. Firstly, FT achieves the lowest LCOE in all

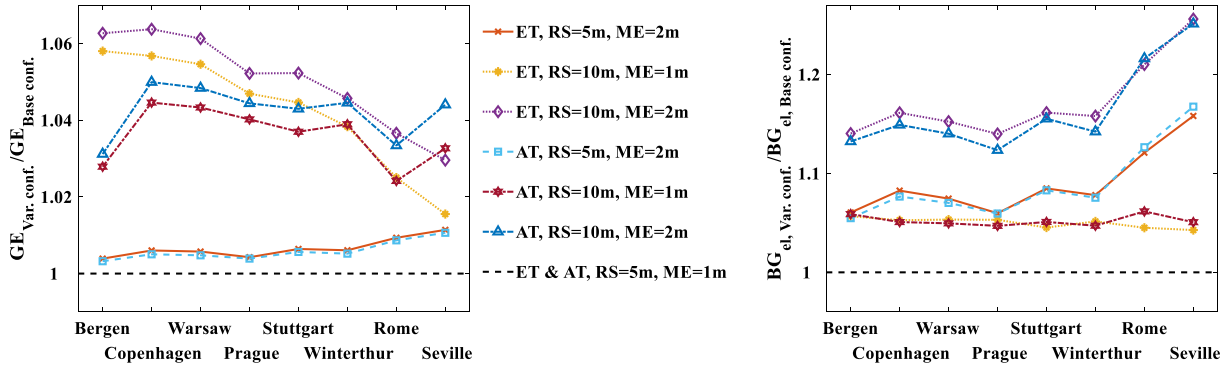

Fig. 6. Impact of design parameters on the annually generated electricity (GE) (left) and bifacial gain in generated electricity (BG_{el}) (right) for ET and AT. The base configuration is plotted with a black dashed line. Ground surface is grass with 20% reflectivity. RS: Row spacing, ME: Module elevation.

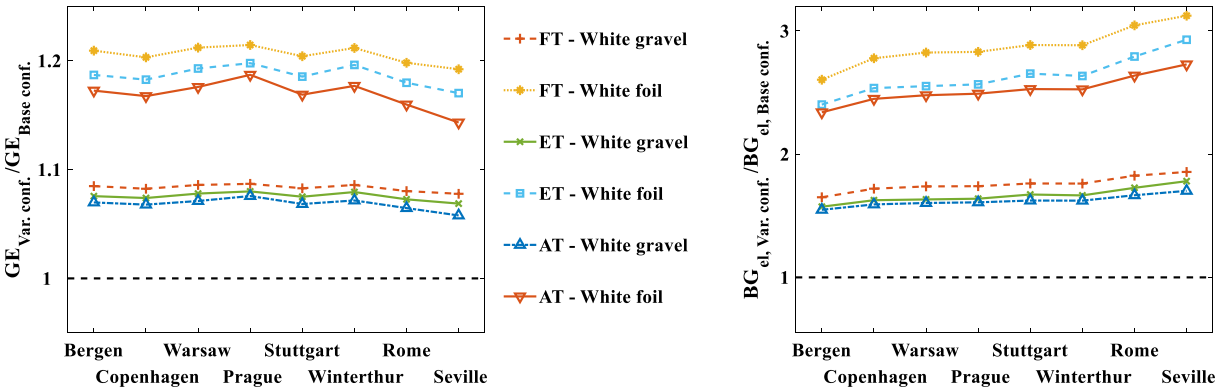

Fig. 7. Influence of different ground covers and their corresponding reflectivity on generated electricity (GE) (left) and bifacial gain in generated electricity (BG_{el}) (right) for all three system designs. The reference is the base configuration for each field design with the ground cover grass (black dashed line).

locations except Rome and Seville. This means that, based on the cost data used in this work, the additional costs for tracked bifacial PV systems are only offset in sunny locations. However, it should be noted that the LCOE is by no means the only factor that determines the economic profitability of a PV system. When the electricity generated is sold on an electricity market, the time course of the electricity generation is a key factor determining profitability (Chudinzow et al., 2020). The LCOE of ET is 5–11% higher in comparison to AT (right Y-axis). This is because ET is better suited for near-equator areas than areas at higher latitudes. The latitude-dependent suitability of different tracking technologies for monofacial PV systems was investigated by (Bahrami et al., 2016; Bahrami and Okoye, 2018) and their findings are consistent with the arrangement of the three system designs shown here.

3.2.1. *Impact of design parameters on the levelized cost of electricity*

In order to investigate how individual installation parameters and soil brightening measures affect the LCOE of FT, sensitivity calculations were carried out, the results of which are shown in Fig. 9. Here the LCOE of a variable field configuration is related to the LCOE of the base configuration with the soil surface grass. The estimated costs for soil brightening measures are shown in Table 6. It is important to emphasise that these costs are only indicative. Depending on the supplier, the quantity purchased, the country and other factors, these costs can vary considerably. However, since the costs used here were determined from the perspective of a private customer, it can be assumed that these costs represent an upper bound. The soil surface "Grass" means that no soil brightening measures were carried out. The following observations can be made on the changes in LCOE for grass (left plot). There is no measure that can significantly reduce the LCOE. Only by increasing the tilt angle can the LCOE in southern locations be reduced marginally (green cross). It is important to note that in the simulation model the tilt angle is used to calculate the area requirement of the plant. A flatter tilt angle results in a higher area requirement, because the front and rear view fields of the module rows are increased (see Fig. 1). As a result, although a flatter tilt angle leads to higher energy yield (Fig. 5), the associated additional cost of land lease means that this measure increases the LCOE slightly (blue circle). The effects of some combined measures are almost the same for all locations, such as varying the tilt angle and increasing the module elevation (turquoise right-pointed triangle, orange diamond). Furthermore, if the row spacing is doubled, the additional LCOE is greater with descending latitude. On the one hand, this is due to the fact that a larger row spacing prevents more self-shading as the latitude increases. On the other hand, as mentioned above, the shadows cast are longer the higher the latitude. Since it was assumed in the simulation model that shadows do not reflect DNI, a shadow reduces the energy yield in the north more than in the south. Accordingly, a larger row spacing lowers the LCOE in the north more than in the south. If the ground is covered with white gravel (centre plot) and the row spacing is kept constant, the LCOE can be lowered at all locations as compared to the base configuration. By using a white foil (right plot), the LCOE can be lowered at all locations as long as

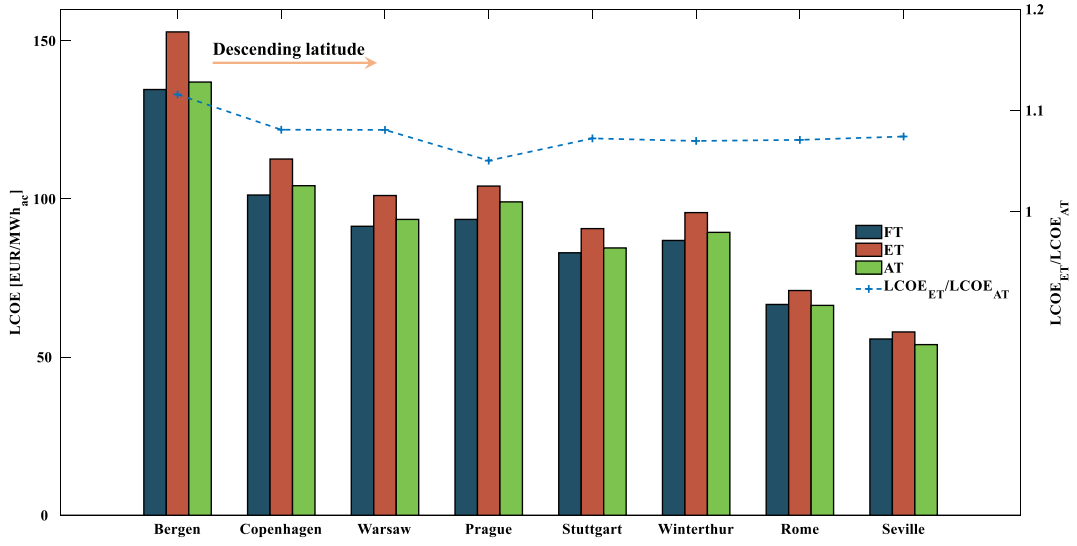

Fig. 8. Calculated LCOE in all sites for the base configuration (left Y-axis) and ratio of the LCOE of ET and AT (right Y-axis). Soil surface is grass with 20% reflectivity.

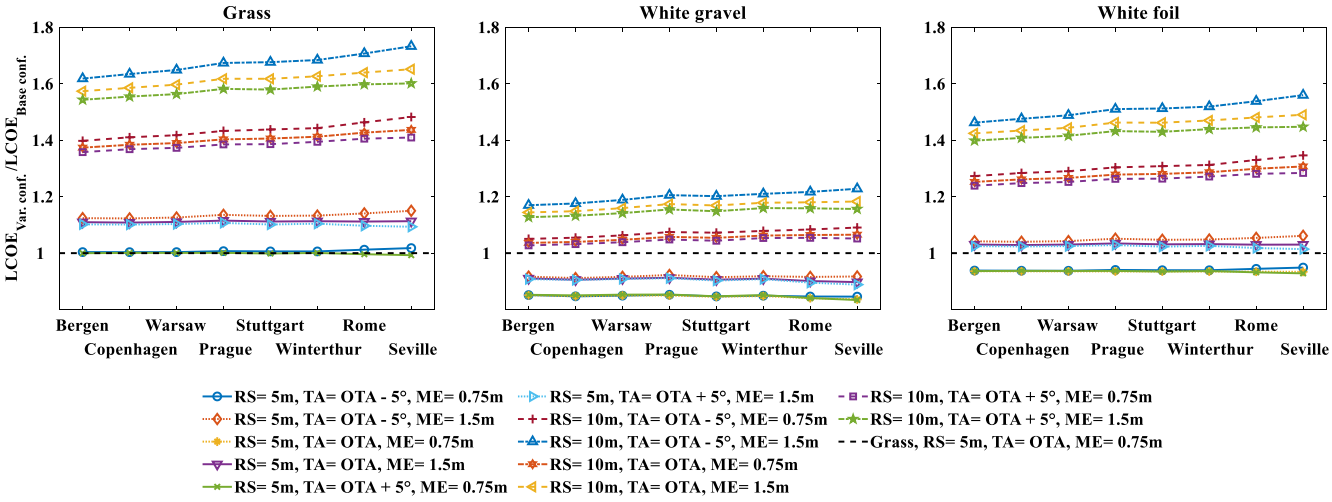

Fig. 9. Effects of varying installation parameters and soil brightening measures on the LCOE for FT. In all three plots, the LCOE of a varied configuration was related to the LCOE of the base configuration with the ground surface grass (black dashed line). RS: Row spacing, TA: Tilt angle, OTA: Optimal tilt angle, ME: Module elevation.

neither module elevation nor row spacing is increased. In general, a soil brightening measure changes the LCOE uniformly at all locations. The course over the locations, however, remains the same.

The results of the sensitivity analysis for single-axis tracked B-PV are shown in Fig. 10. The upper plots show the results for ET, the lower plots for AT. If the ground surface is grass, the LCOE can only be lowered marginally with a larger module elevation (orange cross). If the soil is covered with white gravel or white foil, a lower LCOE can be achieved by using either the base configuration (blue circle) or by doubling the module elevation (red cross). At all locations and for both ET and AT and for all three soil coverages, the higher amount of generated electricity obtained by doubling the inner zone cannot compensate for the additional cost of land lease, resulting in a higher LCOE. It can be observed that an increase in module elevation always leads to lower LCOE, ceteris paribus. It was also shown that a larger module elevation increases the amount of generated electricity (Fig. 6). Therefore, from both an energetic and an economic perspective, the axis of rotation should therefore always be placed as high as possible with the cost assumptions made. This example shows that there may well be combinations of measures that can both increase the energy yield and reduce the LCOE at the same time.

The question arises how expensive the soil brightening measures may be at maximum without leading to an increase in the LCOE as compared to the base configuration and the soil surface grass. The calculated maximum costs for the soil brightening measures for the fixed-tilt design are shown in Fig. 11. One can see that for the soil surface white gravel and some configurations the costs would have to be negative. This means that under the assumptions made it is not possible to apply these measures without increasing the LCOE. The measures requiring negative values for all locations include a simultaneous doubling of the row spacing and module elevation. If only the row spacing is increased and the module elevation is not, negative cost

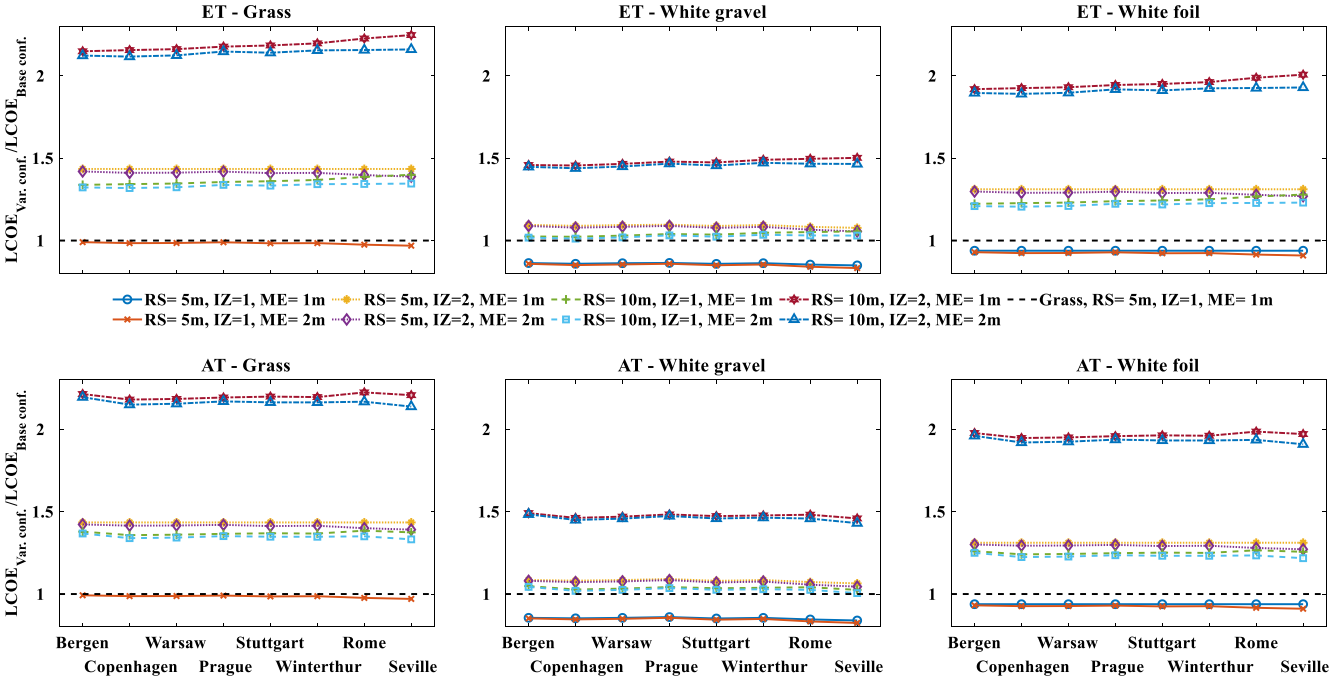

Fig. 10. Effects of varying installation parameters and soil brightening measures on the LCOE of ET and AT. The black dashed line marks identical LCOE of a varying configuration and the base configuration with the soil surface grass. RS: Row spacing, IZ: Inner zone factor (see Table 2), ME: Module elevation.

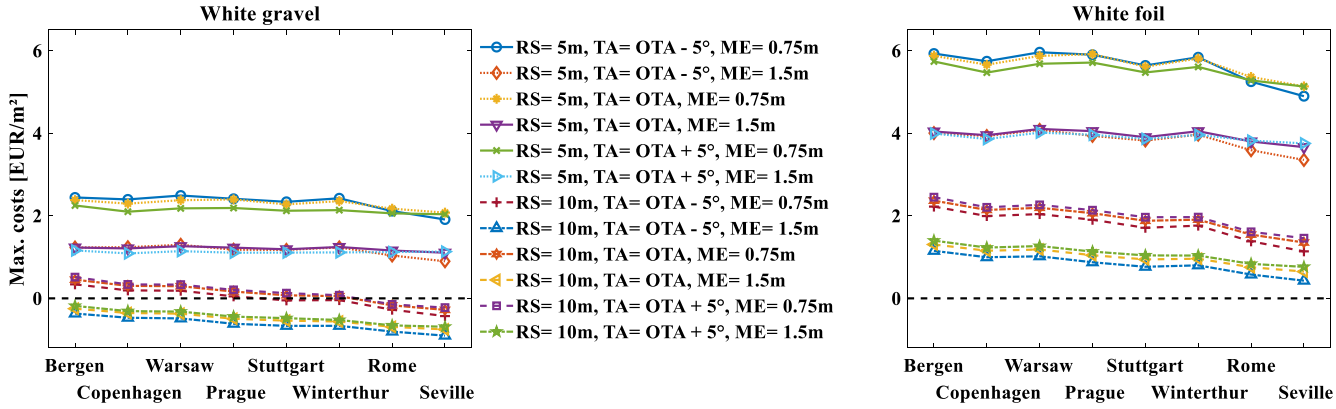

Fig. 11. Maximum permissible costs of soil brightening measures to achieve the same LCOE for FT as in the base configuration with the soil surface grass. Negative values mean that the costs for the brightening measure are not compensated through the additional energy yield and thus the LCOE is increased.

values are required only in the two southernmost locations while an unchanged LCOE can be achieved at the other six locations. If the row spacing is not increased, a constant LCOE can be achieved at all locations and for all configurations. If the soil is brightened with a white foil, constant LCOE can also be achieved at all locations and for all field configurations. Furthermore, a trend is noticeable for both soil surfaces that the better the radiation conditions at a site, the lower the maximum permissible costs for soil brightening measures are. Overall, it can be concluded that a high reflectivity of the soil and a lower solar potential at a given site favour the profitability of soil brightening measures.

Fig. 12 shows the corresponding maximum permissible costs for soil brightening measures for the ET and AT B-PV. It can be seen that soil brightening measures are more easily profitable with white foil than with white gravel. An interesting result is that for both designs and at almost all locations a constant LCOE cannot be achieved if the row spacing and the area of the inner zone are doubled (blue upward-pointing triangle, red six-pointed star). Hence, as a rule of thumb it can be concluded that if minimum LCOE is to be achieved, only the immediate ground surface under the PV field should be brightened. The brightening of the more distant soil surface leads to a higher LCOE. It is also noticeable that at all locations and for both tracking designs a constant LCOE in combination with ground brightening is always easier to achieve if the module elevation is doubled, although this entails additional costs. Therefore, from both an energetic and an economic perspective, it seems to be reasonable to increase the module elevation when soil brightening measures are applied.

In the last step of our analyses we take a closer look at the influence of row spacing and module elevation on the technical and economic characteristics of all three investigated plant designs. For this purpose, the number of considered values for the row spacing and module elevation was increased. For the sake of conciseness, only one single site, Winterthur, was considered. Fig. 13 shows the impact of row spacing and module elevation on the LCOE, on the amount of generated electricity in the first year of operation ($GE_{1st\ year}$) (i.e. without considering the degradation effects of the modules) and on the BG_{el}. The calculations were performed for the soil surface grass and the base configuration. A red plus marks the field configuration that leads to minimum

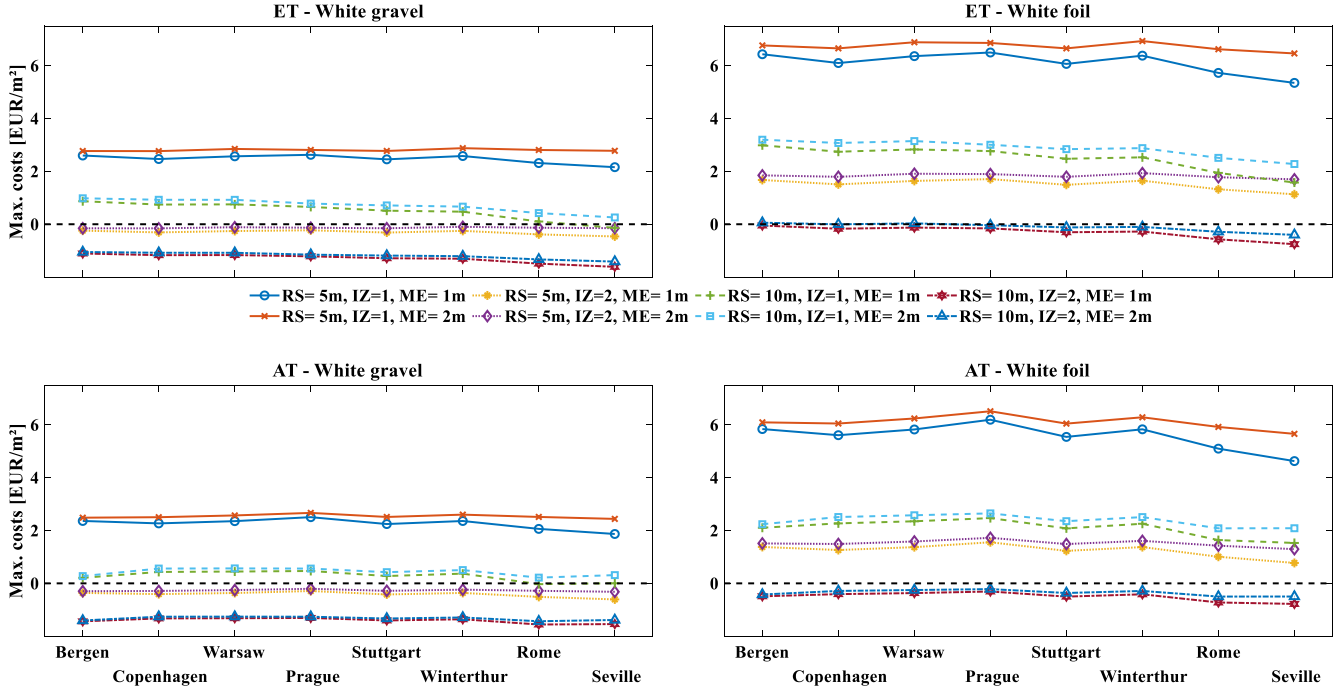

Fig. 12. Maximum permissible costs for soil brightening measures to achieve the same LCOE for ET and AT as in the base configuration with the soil surface grass. Negative values mean that the same LCOE cannot be achieved.

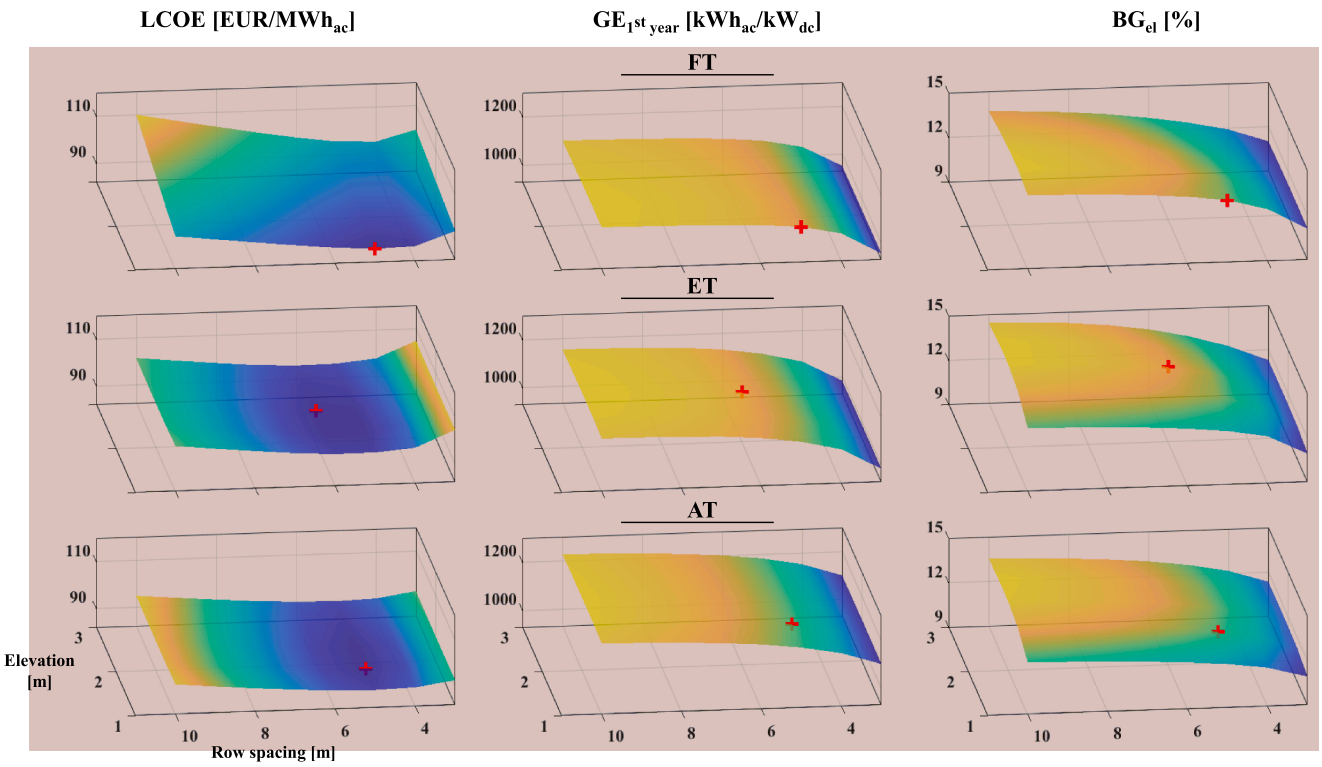

Fig. 13. Sensitivity analysis for all designs for Winterthur. The soil surface is grass and the field configurations correspond to the base configuration. The red cross marks the field configuration with minimum LCOE. (For interpretation of the references to colour in this figure legend, the reader is referred to the web version of this article.)

LCOE in all subplots.

If looking at the LCOE in the left column, it can be seen that an initial increase of the row spacing to 5 m leads to a decrease of the LCOE in all three field designs. It is noticeable that the initial reduction of the LCOE is much more pronounced in the case of ET, because a larger row spacing reduces the self-shading significantly. A further increase in row spacing then leads to a stronger increase in the LCOE for AT than for ET. Furthermore, it can be seen that in the case of FT an increase in module elevation always leads to higher LCOE. For ET and AT, on the other hand, a larger module elevation leads to almost unchanged LCOE, since the additional costs are compensated by the additional energy yield.

The middle column shows the changes in GE_1st_{year}. It is apparent that in all three designs an increase in row spacing leads to an asymptotic increase in GE_1st_{year}. As a result, the amount of GE_1st_{year} at the point of minimum LCOE is 98%, 98% and 96% of the maximum possible GE_1st_{year} for FT, ET and AT respectively. Regarding the influence of the module elevation, for ET and AT a larger module elevation leads to a slight increase of GE_1st_{year}, which is intuitive. For FT, however, an increase in module elevation from 1 m to 3 m (at a row spacing of 10 m) leads to a 0.1% lower GE_1st_{year}. This can be explained by the nature of the view factors, whose definition is given in Eq. (3) (VDI-Wärmeatlas, 2013). Let A_1 be the constant module area and A_2 the size of the view field. If the module elevation is increased, A_2 and the distance between the area elements s increase simultaneously. This means that both the numerator and denominator increase. Depending on the tilt angle of the modules, either the growth of the denominator or the numerator will prevail. From this it can be concluded that too large a module elevation can have a negative effect on the energy yield.

$$\varphi_{12} = \frac{1}{\pi A_1} \iint_{A_2 A_1} \frac{\cos(\beta_1)\cos(\beta_2)}{s^2} dA_1 dA_2 \tag{3}$$

The right column shows the influence of the row spacing and the module elevation on BG_{el}. Common to all system designs is that, as expected, the highest values are achieved with a row spacing of 10 m, because the generated electricity from the rear increases more than from the front side. The module elevations leading to maximum BG_{el} are 1 m, 2 m and 2.5 m for FT, ET and AT, respectively.

3.3. Validation of the energy yield simulation model

Three days in 2017 were considered for validation. The recorded data for GHI and DHI is shown in Fig. 14. October 15 was a very sunny day with a diffuse fraction of 18%. 2 and 8 November were cloudy days with a diffuse fraction of 72% and 99% respectively. It is important to mention that the recording of radiation data was deliberately made over a shorter interval than the actual day length in order to exclude the influence of shadows cast by neighbouring objects on the system.

A reference cell (model HOQ from Fraunhofer ISE) was used to determine the absorbed irradiation on the front side of module M2 (Frauenhofer ISE). The reference cell is mounted on the axis of rotation of the middle module row. To be able to compare the simulated absorbed irradiation on the module and the measured irradiation of the reference cell, the irradiation density in W/m^2 is considered. The simulated absorbed irradiation by the front side of a module includes four contributions: DNI_{front}, DHI_{front} as well as the ground-reflected irradiation (GRI) DNI_{front} ($GRI_{DNI\text{-}front}$) and DHI_{front} ($GRI_{DHI\text{-}front}$). A value of 0.9 was used in the simulation model for the effective transmittance-absorptance product $\tau\alpha$ (Duffie and Beckman, 2013). By contacting the manufacturer, it was found out that the ISE cell used has an average $\tau\alpha$ of 0.93 in the wavelength range from 250 nm to 1100 nm (Köhler, 2020). When simulating the absorbed irradiation, it was considered that the 60 PV cells take up about 89% of the surface of the entire module. Fig. 15 shows the measured and simulated absorbed irradiance by the front side of the module M2 at a tilt angle of 30°. On 15 October, the agreement between the simulated and measured values is consistently good. On 2 and 8 November, the temporal course is also well met, although it is noticeable that at low sun elevations in the morning

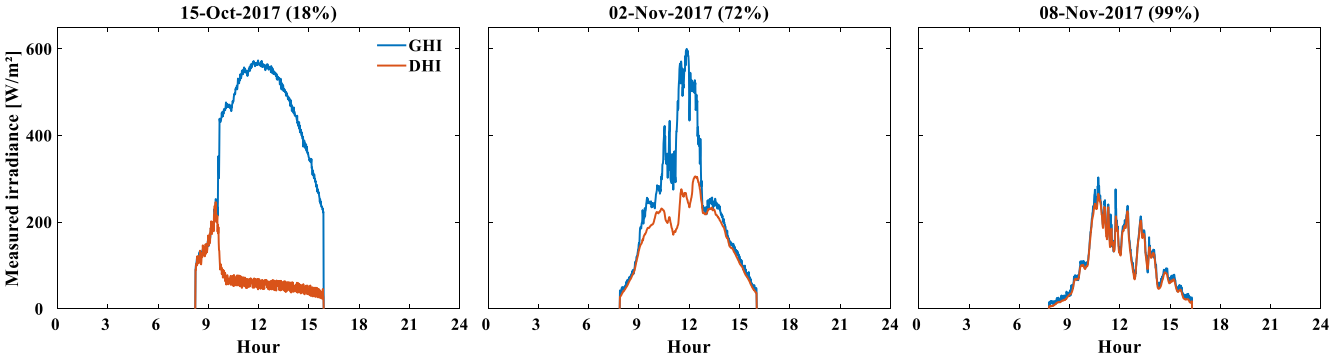

Fig. 14. From the recorded data at the BIFOROT test facility, three characteristic days were selected for validation. The values in brackets in the heading indicate the diffuse fraction.

and afternoon the simulation model overestimates the absorbed irradiance. Overall, it can be seen that by considering the four irradiance contributions on the front (DNI_{front}, DHI_{front}, $GRI_{DNI\text{-}front}$, $GRI_{DHI\text{-}front}$) a good prediction of the absorbed irradiation is achievable.

Fig. 16 shows the measured and simulated power of module M2 on the three reference days for a tilt angle of 30°. The simulation results shown are based on the values measured by the ZHAW (see Table 3). It can be seen that the simulated module power is almost always lower than the measured module power, whereby the deviations become smaller with increasing diffuse fraction. One possible reason for the observed deviations is that the model used for the temperature- and radiation-dependent electrical efficiency originally comes from the area of monofacial modules (Dubey et al., 2013). Another plausible explanation for this observation is that in the simulation model the modules are assumed to be completely opaque. This assumption implies that the shadows cast by the modules are not hit by any DNI. Under a completely cloudy sky, this simplification doesn't produce larger errors, but under a clear sky, significant deviations occur.

Finally, the ratio of the simulated and measured absorbed irradiation on the front side and generated electricity (direct current) on both sides of the module M2 for all available tilt angles is shown in Fig. 17 on a daily basis. The upper two plots show the results based on the measured values given in Table 3 (MV). The upper left plot reveals that at a tilt angle of 0°, the ratios are almost identical on all three days. As the tilt angle increases, the deviation on cloudier days is between −10% and +10%. On 15 October (sunny day) the deviation is between 2% and 7%. It turns out that the deviations are much more pronounced on the two cloudier days than on the sunny day. One reason for this is that due to the cloud cover, the absolute measured values were smaller than on the sunny day. As the measured values are in the denominator of the chosen metric, smaller measured values lead to higher ratios. Larger deviations of the measured and simulated values with increasing degree of cloud cover at the BIFOROT test site were also reported in (Nussbaumer et al., 2020).

The upper right diagram shows the ratios of simulated and measured generated electricity. On the cloudiest day the model overestimates the generated electricity by about 5% at all tilt angles except 0°. On the other two days, however, the model underestimates the generated electricity by between 8 and 19%. It can be noted that although the simulation model either overestimates or underestimates the amount of electricity generated, the angular dependence of the power output is well captured in the model. Only at a tilt angle of 0° (all three days) and 90° (8 November) does a change in tilt angle dependency become apparent.

The question arises what the results would look like if the literature values (LV) had been used instead of the measured values. The lower two plots visualize the results based on measured values (MV) and literature values and the potential range of deviation. In the case of absorbed irradiation (lower left plot), the LV would have always led to higher results, with the deviation being greatest on 8 November (completely cloudy day) when the module is oriented vertically. The qualitative trends between the individual days are maintained when using LV. It should be noted that in the case of absorbed irradiation, only the different reflectivity of the white foil led to different results.

Looking at the amount of electricity generated (lower right plot), it can be seen that the range of deviation on 8 November shows an opposite behaviour to that of the absorbed radiation. Here, the range of deviation is largest at 0° tilt angle and smallest at 90°. The other two days show that the range of deviation is largest on 15 October (sunny day) and increases slightly as the tilt angle increases. The differences in the amount of generated electricity can be attributed to all three parameters (reflectivity of the white foil, electrical efficiency and bifaciality). Thereby the differences in electrical efficiency and bifaciality partly cancel each other out and amount to about 10% in total (Eq. (4)).

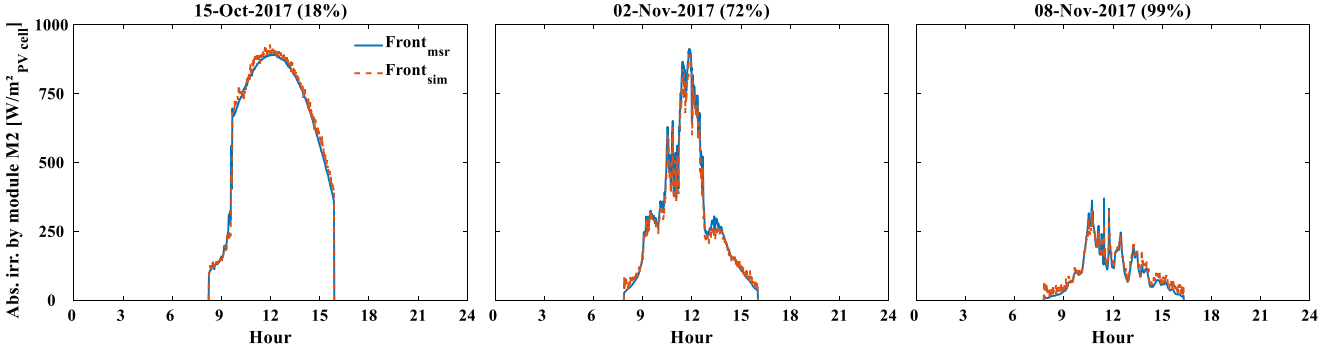

Fig. 15. Measured (msr) irradiance by the reference cell and simulated (sim) absorbed irradiance by the front side of module M2 for a tilt angle of 30°. The values in brackets in the heading indicate the diffuse fraction. With increasing diffuse fraction, the simulation model slightly overestimates the absorbed irradiance at times when the sun is low.

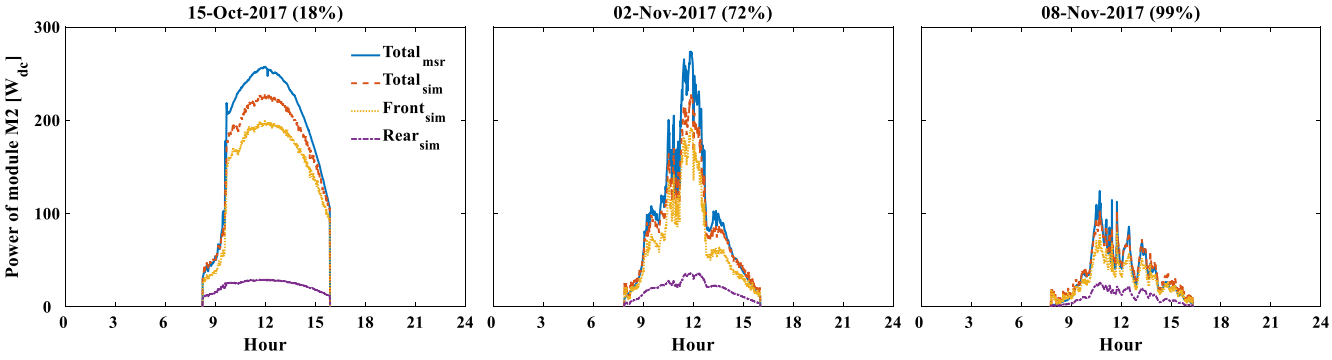

Fig. 16. Measured (msr) and simulated (sim) electrical power of module M2 on the three reference days for a tilt angle of 30°. The values in brackets in the heading indicate the diffuse ratio. The deviation of the measured and simulated values is smaller with higher diffuse fraction.

$$\frac{Totalel.\ efficiency_{MV}}{Totalel.\ efficiency_{LV}} = \frac{\eta_{el,front,MV} + \eta_{el,rear,MV}}{\eta_{el,front,LV} + \eta_{el,rear,LV}} = \frac{\eta_{el,front,MV}\cdot(1 + bifaciality_{MV})}{\eta_{el,front,LV}\cdot(1 + bifaciality_{LV})} = \frac{0.187\cdot(1 + 0.78)}{0.163\cdot(1 + 0.85)} = 1.104 \quad (4)$$

The range of the deviation illustrates how important it is for the quality of the simulation results to use solid input parameters. Although the presented results show that both MV and LV lead to the same qualitative patterns, significant quantitative deviations may occur.

3.4. Recommendations for energy yield simulations

Finally, based on years of experience with the simulation model used, Table 4 provides recommendations and lessons for the development of future energy yield simulation models for bifacial PV systems.

4. Conclusions

The current state of knowledge does not yet provide a comprehensive understanding of how the PV field of fixed-tilt and single-axis tracked bifacial PV power plants (B-PV) should be designed to find the best compromise between energy yield and levelized cost of electricity (LCOE). This is because the simultaneous effects of altered installation parameters like row spacing, module elevation, tilt angle and soil reflectivity on the energy yield and LCOE are complex and their representation in simulation models is challenging.

The present work shall contribute to close this research gap by analysing the influence of installation parameters on the energy yield and the LCOE of fixed-tilt (FT) and singles-axis tracked systems with an east–west and north–south axis. Since the modules of a system with an east–west axis follow the elevation angle of the sun and those of a system with a north–south axis follow the azimuth angle of the sun, in this work both systems are called ”elevation-tracked” (ET) and ”azimuth-tracked” (AT). To investigate the influence of the location, the analyses were carried out for eight European cities, covering a meridian range of 23°.

It has been found that AT has the highest energy yields at all sites, followed by ET and FT. By doubling the row distance from 5 m to 10 m and increasing the module elevation from 0.75 m to 1.5 m, FT can achieve an additional energy yield of approx. 5% at all locations, whereby the additional energy yield decreases with decreasing latitude. With ET and AT, additional yields of up to 6% can be achieved by simultaneously increasing the row spacing and module elevation. In the case of ET, the additional energy gain due to a larger row spacing decreases with decreasing latitude. In the case of FT, it was shown that if the tilt angle is chosen 5° smaller than the recommended latitude-

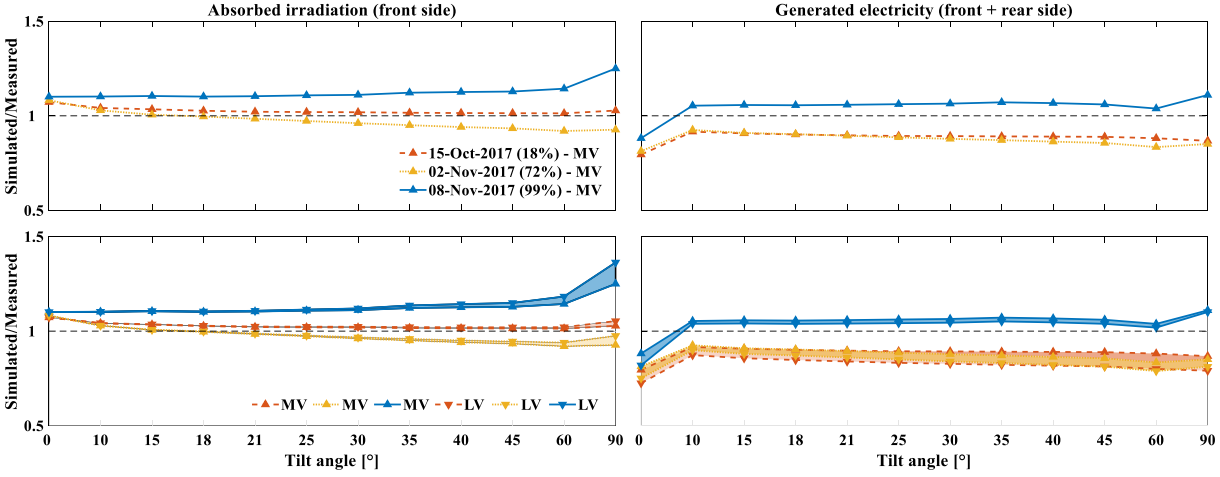

Fig. 17. Comparison of the measured and simulated absorbed irradiation (front side) and generated electricity (front + rear side) of module M2. Both measured values (MV) and literature values (LV) were used for the simulation. MV-based results are marked with an upward-pointing triangle, LV-based results with a downward-pointing triangle.

Table 4
Recommendations for energy yield simulation models for bifacial PV systems.

Topic	Applied technique in the model used	Recommendation
Calculation of the ground-reflected irradiance (GRI) using 3D view factors.	3D view factors are calculated numerically from the relevant areas of the ground to each cell string (front and rear side). This allows the effect of cast ground shadows to be considered.	The calculation of 3D view factors is very time consuming and the number of calculations should be reduced as much as possible. Especially for commercial simulation software very short simulation times are essential. By cleverly utilizing the symmetries in the PV field and considering representative cell strings, the computing time can be reduced significantly, while the quality of the results would probably be preserved.
Checking if a cell string is shaded.	For each cell string it is checked in each time step if there is shadowing on the front or back side (emulation of a bypass diode).	The emulation of a bypass diode is important and should be maintained. To reduce the computational effort, symmetries of the PV field can be used, considering only some representative cell strings.
Consideration of further objects belonging to the PV system (e.g. frame and mounting structure. In the case of tracked systems, the torque tube).	Not considered.	The presence of other objects would in all likelihood always reduce the energy yield, so it seems reasonable to take this into account (Ayala Pelaez et al., 2019). This could be done either by direct modelling or by exogenously determined loss factors.
Consideration of the fact that bifacial modules are not opaque.	The modules are considered to be completely opaque.	The assumption made so far leads to an underestimation of the irradiance that reaches the ground and is reflected by the ground. This should be corrected by considering the partial transparency of the modules.
Consideration of the spatial distribution of ground-reflected irradiance depending on the surface texture.	It was assumed that the ground-reflected irradiance propagates isotropically.	For example, the irradiance reflected by a smooth snow surface would probably have a more pronounced anisotropy than if it were reflected by a rougher surface as grass. Probably this effect is rather small, but it would be interesting to investigate how the roughness of a surface affects its reflective properties and how this is manifested in the energy yield.
Electrical model.	Using a model originally developed for monofacial modules (Dubey et al., 2013).	The model applied originally comes from the field of monofacial modules and should be updated with a more suitable model tailored to the characteristics of bifacial modules. The influence of the wind on the module temperature should also be considered.
Modelling of diffuse solar irradiation.	The model used applied the isotropic sky diffuse model. It is likely that the diffuse irradiation absorbed from the back is more overestimated in systems oriented towards the equator and installed at high latitudes than in systems near the equator.	The applied technique is easy to use, but there are more advanced models (Loutzenhiser et al., 2007). Their application would very likely improve the quality of the results.
Number of irradiation contributions considered	Consideration of each irradiation contributions for each cell string: DNI_{front}, DNI_{rear}, DHI_{front}, DHI_{rear}, $GRI_{DNI\text{-}front}$, $GRI_{DNI\text{-}rear}$, $GRI_{DHI\text{-}front}$, $GRI_{DHI\text{-}rear}$.	The consideration of the eight radiation contributions for both sides of a cell string seems reasonable and should be continued.
The light reflected by the modules partially hits the modules in front or behind.	Not considered.	Although the modules are coated with an anti-reflection layer, it would be interesting to investigate this effect and quantify its influence on the energy yield.

dependent tilt angle for monofacial systems, the energy yield could be increased at all locations.

The most effective measure to increase the energy yield, which is associated with additional investments, is an enhancement of the soil reflectivity through the use of white gravel or white foil. This can increase the energy yield at all locations and for all plant designs by 8–20%.

The LCOE analysis showed that FT achieves the lowest LCOE in the six northernmost locations, followed by AT and ET. If the reflectivity of the soil is not increased and corresponds to that of grass, almost any change in installation parameters for FT leads to higher LCOE. However, if the soil is lightened, several combined measures will result in lower LCOE than in the base configuration. Similar observations were made for ET and AT: A brightening of the soil in combination with different installation parameters can lead to a reduction in LCOE.

It was also found that if the row spacing is increased (leading to more land demand and higher land lease), the relative increase in LCOE of FT and ET is higher at low latitudes than at high latitudes. This leads to the conclusion that an investment in certain field configurations is more likely to pay off in higher latitudes i.e. less sunny locations. This was not found to be the case for AT.

Furthermore, it was calculated how expensive soil brightening measures may be at maximum in order not to increase the LCOE compared to the base configuration with the soil surface grass. It has been shown that constant LCOE is easier to achieve the smaller the row spacing and the higher the reflectivity of the brightened soil. Here it turned out that the additional investment in field configurations with a larger land requirement for all three investigated plant designs would be more economical at higher latitudes.

It has also been found that a too large module elevation can reduce the energy yield marginally. This is due to the nature of view factors where, depending on the system configuration, the greater distance between the modules and the ground has a stronger yield-reducing effect than the growth of the ground area ”seen” by the modules, which has a yield-increasing effect.

In the last step, the simulation model used was validated using the BIFOROT test site located in Zurich. It could be shown that the simulation model represents the angular dependence of the energy yield well. On a sunny day the deviation between the calculated and measured power was around 5%, but on cloudy days the relative deviation increased.

In summary, the results show that site-specific energy yield simulations and LCOE calculations must always be carried out carefully and holistically due to the complex interactions of the installation parameters.

CRediT authorship contribution statement

Dimitrij Chudinzow: Supervision, Project administration, Conceptualization, Methodology, Writing - original draft, Data curation, Formal analysis, Visualization. **Markus Klenk:** Resources, Data curation, Validation, Writing - review & editing. **Ludger Eltrop:** Writing - review & editing.

Declaration of Competing Interest

The authors declare that they have no known competing financial interests or personal relationships that could have appeared to influence the work reported in this paper.

Acknowledgement

The authors would like to thank the anonymous reviewers and editors for their useful comments during the review process.

Funding

This work was supported by the German Federal Ministry of Education and Research (BMBF).

Data statement

The energy yield simulation model is part of a doctoral thesis and can therefore not be shared at present. The measurement data of the BIFOROT test facility are the property of the ZHAW. All other data are freely available and were cited accordingly.

Appendix A

A.1. Glossary

(See Table 5).

Table 5
Abbreviations and technical terms.

Abbreviation	Full Term
AT	A single-axis tracked PV system with a north–south axis, whose modules follow the azimuth angle of the sun (azimuth-tracked, AT).
BG_{el}	Bifacial gain in generated electricity ($BG_{el} = \frac{GE_{rear}}{GE_{front}}$)
Bifaciality	Ratio of the back and front efficiency of a bifacial module.
BIFOROT	Bifacial Outdoor Rotor Tester.
B-PV	Bifacial PV power plant.
C-PV	Conventional PV power plant (monofacial, equator-oriented, optimally tilted).
DHI	Diffuse horizontal irradiance.
DNI	Direct normal irradiance.
EG	Electricity generation.
EPC	Engineering, procurement and construction.
ET	A single-axis tracked PV system with an east–west axis, whose modules follow the elevation angle of the sun (elevation-tracked, ET).
GE	Generated electricity.
GHI	Global horizontal irradiance.
GRI	Ground-reflected irradiance.
LCOE	Levelized cost of electricity.
ME	Module elevation.
NOCT	Nominal operating cell temperature.
O&M	Expenditures for operation & maintenance.
OTA	Location-dependent optimal module tilt angle for a monofacial PV system (Jacobson and Jadhav, 2018).
PV	Photovoltaics.
RS	Row spacing.
TA	Tilt angle.
TMY	Typical meteorological year.
ϑ_Z	Zenith angle of the sun.
$\tau\alpha$	Effective transmittance-absorptance product.

A.2. Technical and financial values

Where necessary, the US dollar was converted into Euros at an average exchange rate over one year (June 2018 - June 2019) of 1.1423 USD/EUR (European Central Bank) (See Table 6).

Table 6
Technical and financial values.

Parameter	Value	Reference
Annual degradation rate of modules.	0.3%/year	(Megacell, 2015)
Annual land lease.	0.18 EUR/(m^2·year) with an annual increase of 2%.	(Leipe and Zill, 2011)
Annual operation and maintenance.	15.8 EUR/(kW_{dc}·year) with an annual increase of 2%.	(Fu et al., 2018)
Costs for soil brightening measures.	White gravel: 6.7 EUR/m^2. This value is based on an online shop selling crushed stone, type "Carrara", and an assumed volume discount of 25%.	(Beckmann, 2018)
	White foil: 14.6 EUR/m^2. This value is based on personal communication and an assumed volume discount of 25%.	(Sika, 2020)
Engineering, procurement and construction.	13% of equipment costs	(Rodríguez-Gallegos et al., 2018)
Installation labour for PV power plant.	136 EUR/kW_{dc}	(Fu et al., 2018)
Interest rate.	5%	Own assumption
Inverter oversize for B-PV system.	20% additional inverter capacity in relation to the total front-side capacity.	(Rodríguez-Gallegos et al., 2018)
Investment bifacial module.	432 EUR/kW_{dc}	(Rodríguez-Gallegos et al., 2018)
Investment electrical components.	131 EUR/kW_{dc}	(Fu et al., 2018)
Investment inverter fixed-tilt design.	42 EUR/kW_{dc}	(Fu et al., 2018; Rodríguez-Gallegos et al., 2018)
Investment inverter tracked design.	52.5 EUR/kW_{dc}	(Fu et al., 2018; Rodríguez-Gallegos et al., 2018)
Lifetime of B-PV system.	30 years	(Fu et al., 2018)
Power consumption of tracking system.	5.2 W_{dc}/Module	(DEGER S100-DR Datasheet, 2018)

Appendix B. Supplementary material

Supplementary data to this article can be found online at https://doi.org/10.1016/j.solener.2020.06.096.

References

ABB, n.d. ABB string invertersTRIO-20.0/27.6-TL-OUTD20 to 27.6 kW. Available online at https://search-ext.abb.com/library/Download.aspx?DocumentID=BCD.00379&LanguageCode=en&DocumentPartId=&Action=Launch, checked on 4/9/2020.

Asgharzadeh, A., Marion, B., Deline, C., Hansen, C., Stein, J.S., Toor, F., 2018. A sensitivity study of the impact of installation parameters and system configuration on the performance of bifacial PV arrays. IEEE J. Photovoltaics 8 (3), 798–805. https://doi.org/10.1109/JPHOTOV.2018.2819676.

Ayala Pelaez Silvana, Deline Chris, Stein Joshua, Marion Bill, Anderson Kevin, Muller Matthew, 2019. Effect of Torque-Tube Parameters on Rear-Irradiance and Rear-Shading Loss for Bifacial PV Performance on Single-Axis Tracking Systems. Preprint. Available online at https://www.nrel.gov/docs/fy20osti/73203.pdf, checked on 6/25/2020.

Bahrami, A., Okoye, C.O., 2018. The performance and ranking pattern of PV systems incorporated with solar trackers in the northern hemisphere. Renew. Sustain. Energy Rev. 97, 138–151. https://doi.org/10.1016/j.rser.2018.08.035.

Bahrami Arian, Okoye Chiemeka Onyeka, Atikol Ugur, 2016. The effect of latitude on the performance of different solar trackers in Europe and Africa. Appl. Energy 177, 896–906. doi:10.1016/j.apenergy.2016.05.103.

Bauzentrum Beckmann (2018). Available online at https://www.beckmann-bauzentrum.de/naturstein-gartendeko/kiessplitt/zierkies.html, checked on 7/20/2018.

Bretz, Sarah, Akbari, Hashem, Rosenfeld, Arthur, 1998. Practical issues for using solar-reflective materials to mitigate urban heat islands. Atmos. Environ. 32 (1), 95–101. https://doi.org/10.1016/S1352-2310(97)00182-9.

Chiodetti Matthieu, Guédez Rafale, Lindsay Amy, 2015. Bifacial PV plants: performance model development and optimization of their configuration. KTH Royal Institute of Technology. Available online at http://kth.diva-portal.org/smash/get/diva2:848584/FULLTEXT01.pdf, checked on 2/15/2017.

Chudinzow, Dimitrij, Haas, Jannik, Díaz-Ferrán, Gustavo, Moreno-Leiva, Simón, Eltrop, Ludger, 2019. Simulating the energy yield of a bifacial photovoltaic power plant. Sol. Energy 183, 812–822. https://doi.org/10.1016/j.solener.2019.03.071.

Chudinzow, Dimitrij, Nagel, Sylvio, Güsewell, Joshua, Eltrop, Ludger, 2020. Vertical bifacial photovoltaics – A complementary technology for the European electricity supply? Appl. Energy 264, 114782. https://doi.org/10.1016/j.apenergy.2020.114782.

DEGER S100-DR Datasheet, 2018. Available online at https://www.degerenergie.de/files/pdf/Datenblaetter%20DEGERtracker/Deutsch/DEGER_S100-DR_Datenblatt_DE_2018-12.pdf, checked on 2/24/2020.

Dubey Swapnil, Sarvaiya Jatin Narotam, Seshadri Bharath, 2013. Temperature dependent photovoltaic (PV) efficiency and its effect on PV production in the world – A review. Energy Procedia 33, 311–321. doi:10.1016/j.egypro.2013.05.072.

Duffie, John A., Beckman, William A., 2013. Solar Engineering of Thermal Processes. 4th ed.

European Central Bank: ECB euro reference exchange rate. Available online at https://www.ecb.europa.eu/stats/policy_and_exchange_rates/euro_reference_exchange_rates/html/eurofxref-graph-usd.en.html, checked on 6/27/2019.

Frauenhofer ISE: Outdoor Reference Cells. Available online at https://www.ise.fraunhofer.de/en/rd-infrastructure/accredited-labs/callab/outdoor-reference-cells.html, checked on 3/16/2020.

Fu Ran, Feldman David, Margolis Robert, 2018. U.S. Solar Photovoltaic System Cost Benchmark: Q1 2018. NREL. Available online at https://www.nrel.gov/docs/fy19osti/72399.pdf, checked on 2/13/2019.

International Finance Corporation, 2015. Utility-Scale Solar Photovoltaic Power Plants. A project developer's guide. Washington, D.C.

Jacobson, Mark Z., Jadhav, Vijaysinh, 2018. World estimates of PV optimal tilt angles and ratios of sunlight incident upon tilted and tracked PV panels relative to horizontal panels. Sol. Energy 169, 55–66. https://doi.org/10.1016/j.solener.2018.04.030.

Joint Research Centre, 2019. Photovoltaic geographical information system. Available online at http://re.jrc.ec.europa.eu/pvg_tools/en/tools.html, checked on 2/21/2020.

Köhler Manuela, 2020. Reflectivity of ISE cell. E-Mail to Dimitrij Chudinzow, 2020.

Leipe Frank, Zill Thomas, 2011. Ein Leitfaden für Kommunen. Solarparks auf Brachflächen in Thüringen. Available online at http://www.thega.de/fileadmin/thega/pdf/projekte/solarparks/Leitfaden_Solarparks_gesamt.pdf, checked on 7/18/2018.

Loutzenhiser, P.G., Manz, H., Felsmann, C., Strachan, P.A., Frank, T., Maxwell, G.M., 2007. Empirical validation of models to compute solar irradiance on inclined surfaces for building energy simulation. Sol. Energy 81 (2), 254–267. https://doi.org/10.1016/j.solener.2006.03.009.

Megacell, 2015. Datasheet BiSoN MBA-GG60 series 270-280Wp. Available online at http://www.mega-group.it/wp-content/uploads/MBA-GG60-270_280B_rev3.pdf, checked on 4/5/2018.

NREL, 2018. System Advisor Model Manual. Available online at https://sam.nrel.gov/images/web_page_files/sam-help-2018-11-11-r4.pdf, checked on 2/23/2020.

Nussbaumer, Hartmut, Janssen, Gaby, Berrian, Djaber, Wittmer, Bruno, Klenk, Markus, Baumann, Thomas, et al., 2020. Accuracy of simulated data for bifacial systems with varying tilt angles and share of diffuse radiation. Sol. Energy 197, 6–21. https://doi.org/10.1016/j.solener.2019.12.071.

PVsyst, n.d. Albedo coefficient. Available online at http://files.pvsyst.com/help/albedo.htm, checked on 10/8/2018.

Rodríguez-Gallegos, Carlos D., Bieri Monika, Gandhi Oktoviano, Singh Jai Prakash, Reindl Thomas, Panda, S.K., 2018. Monofacial vs bifacial Si-based PV modules: Which one is more cost-effective? Sol. Energy 176, 412–438. doi:10.1016/j.solener.2018.10.012.

Sika, 2020. Available online at http://deu.sika.com, checked on 4/2/2020.

Stahlshop, 2018. Available online at https://stahlshop.de/stabstahl-verzinkt/u-stahl-verzinkt, checked on 7/16/2018.

Sun Xingshu, Khan Mohammad Ryyan, Deline Chris, Alam Muhammad Ashraful, 2018. Optimization and performance of bifacial solar modules: A global perspective. Appl. Energy 212, 1601–1610. doi:10.1016/j.apenergy.2017.12.041.

Tillmann, Peter, Jäger, Klaus, Becker, Christiane, 2020. Minimising the levelised cost of electricity for bifacial solar panel arrays using Bayesian optimisation. Sustainable Energy Fuels 4 (1), 254–264. https://doi.org/10.1039/C9SE00750D.

VDI-Wärmeatlas, 2013. 11., bearb. und erw. Aufl. Berlin, Heidelberg: Springer (VDI-Buch).

3.3 Supplement 1: Site-dependent energy yield

The model validation presented in the second paper was carried out for a single bifacial PV module placed within a bifacial PV test site for 12 different inclination angles for a single site (Winterthur, Switzerland). Since in this work much emphasis was put on the elaboration of the **site-specific differences in energy yield** of fixed-tilt and single-axis tracked B-PV systems, it is important to examine whether the developed energy yield model also captures site-specific differences in the energy yield well. To investigate this, another energy yield model was used as a benchmark, namely the System Advisor Model (SAM, version 2020.2.29, revision 3) [20]. SAM is a free simulation software with a graphical user interface that allows technical and economic analyses of different renewable technologies and that is able to simulate bifacial PV systems since the year 2018 [9]. To compare the results of the developed model and of SAM, the same weather data was used for the eight European sites [21]. All other parameters to be adjusted in SAM (module type, inverter, field geometry, ground reflectivity) were selected in such a way as to reproduce the investigated bifacial PV systems as accurately as possible. The annual specific energy yield (front +rear) calculated by SAM for the three plant designs is plotted on the left axis in Figure 37. This representation is the direct counterpart to Figure 23, which is also duplicated below for better comparability (Figure 38). The right axis in Figure 37 shows the ratio of the annual energy yield of the presented energy yield model and SAM. It is plain to see that the **trend in the site-specific energy yield is determined by both models in a similar way**, with the ratio of model results ranging from 85 % for the fixed-tilt design (FT) in Bergen to 108 % for the azimuth-tracking design (AT) in Stuttgart.

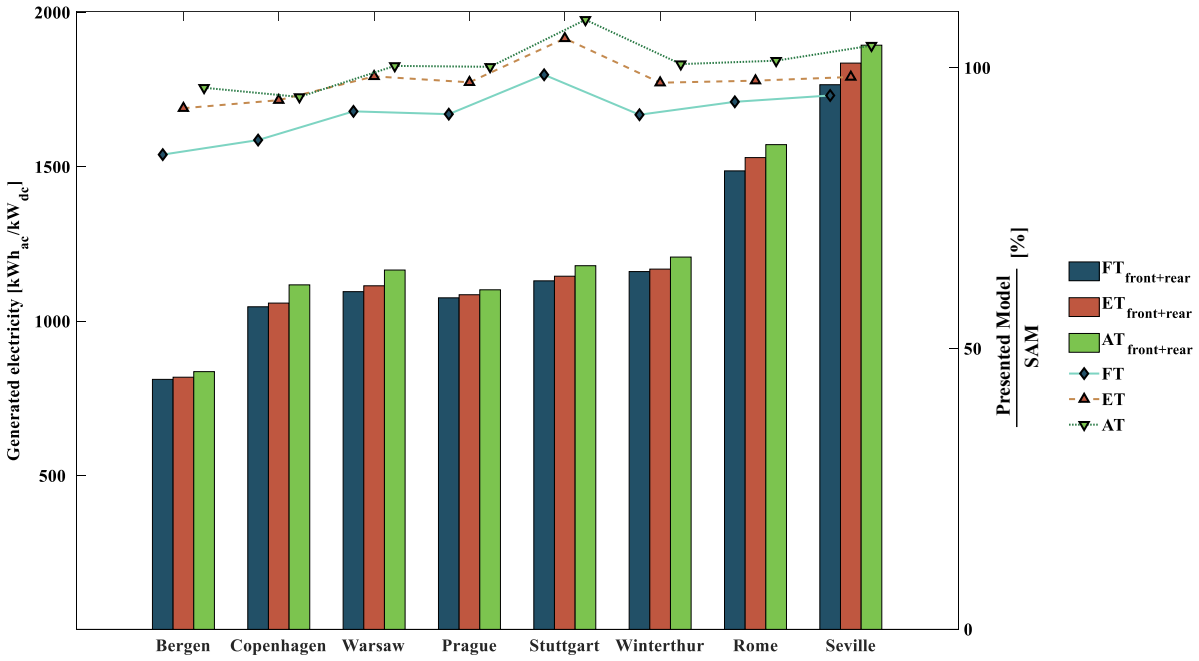

Figure 37: Comparison of the annual generated electricity (bar plot) at the eight locations, calculated with the presented energy yield model and the System Advisor Model.

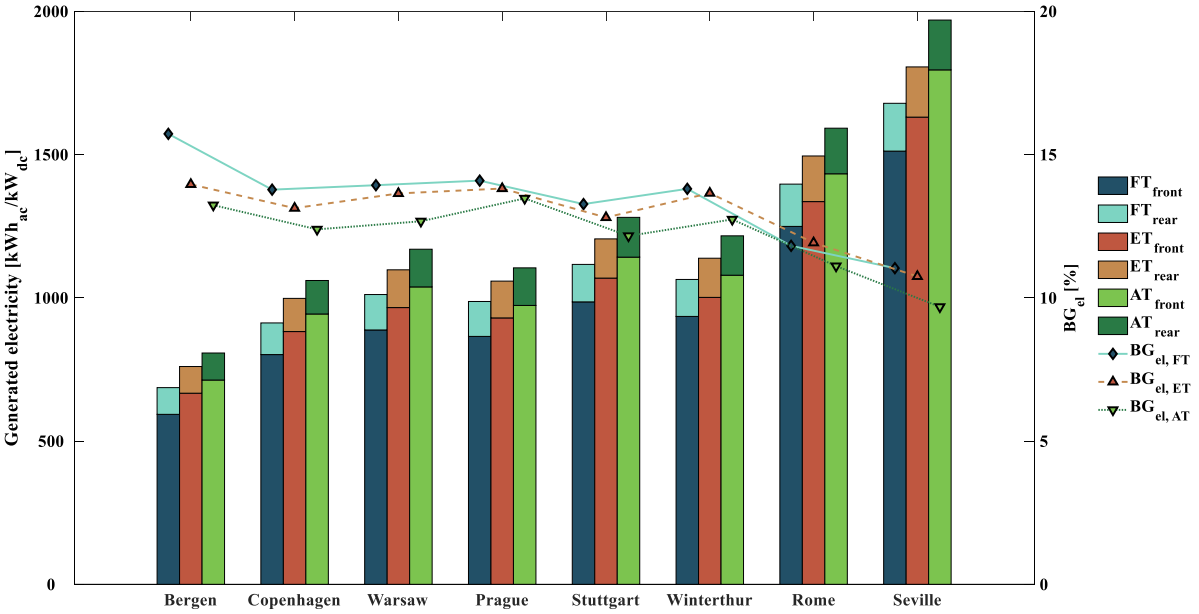

Figure 38: Generated electricity (bar plot) by the three PV system designs, calculated with the developed energy yield model. Figure 38 is a copy of Figure 23.

The reasons for the observed differences are due to the different optical, thermal and electrical submodels of both energy yield models. Nevertheless, the comparison shows that the statements made in this thesis regarding the site-specific energy yield differences of bifacial PV systems can be considered valid and meaningful.

3.4 Supplement 2: International model benchmark

In 2021, a report was published by the IEA PVPS (International Energy Agency - Photovoltaic Power Systems Programme), in which 13 energy yield models for B-PV were compared with each other. The model presented here was part of this benchmark [22]. It has been shown that the variation of the simulation results of the 13 models significantly depends on the plant design, location and weather conditions. The simulated energy yields of the model presented here fit in well with the results of the other models, although depending on the scenario, the model tends to underestimate the frontal energy yield. This could be due to the finite and relatively small size of the view fields and the approach used to take diffuse irradiation into account (isotropic sky diffuse model), which presumably underestimates the absorbed diffuse irradiation. For the calculation of diffuse irradiation, more advanced and more accurate methods exist than the one chosen here [23], but during the conceptualisation of the model, the choice fell on the method of the isotropic sky diffuse model because of its simplicity and because the focus of the developed energy yield model was a better representation of ground-reflected irradiance.

4 Chapter III – Analysis of vertical bifacial PV systems

4.1 Summary of Paper 3

PV systems are becoming increasingly important for the energy transition in many national power supply systems. Germany, for example, had the highest share of installed PV capacity in Europe in 2018 [24], which means that it is a role model for other countries with regard to expansion and financing mechanisms. As with all non-dispatchable renewable technologies, the system integration of PV systems is challenging. A steadily increasing share of PV capacity in the system leads to technical challenges, because fixed-tilt PV systems with the same orientation (usually towards the equator) have a nearly synchronous feed-in profile, which is only influenced by regional differences in weather conditions. In the case of Germany, there are only about 30 minutes between solar noon in the far east and far west. This means that in principle there is a single feed-in peak at noon, especially in sunny weather, which can, however, drop off quickly due to passing clouds. To ensure frequency stability in the system, more ancillary services are required, which leads to higher overall system costs.

A further challenge for PV systems that do not have an electricity storage and therefore cannot control the timing of electricity sales is that their market value factor (VF) decreases as the amount of installed PV capacity increases [7]. This means that for the same amount of electricity sold, the absolute market revenue decreases. If one considers that renewable technologies shall become competitive in the medium term without support mechanisms and that their capacities are to be expanded, a dilemma unfolds.

In contrast to conventional PV systems (C-PV) (monofacial, optimally inclined, oriented towards the equator), vertical bifacial PV systems (VBPV) with a north-south axis have a feed-in profile with a peak in the morning and afternoon (see Figure 3). Consequently, the question arises in the described context whether VBPV can reduce integration costs on the one hand and increase market-based revenues on the other.

In order to be able to carry out an impartial evaluation of VBPV, the characteristics of VBPV were always compared with those of C-PV in the analyses carried out. To evaluate the effect of latitude on the energy yield and the effect of the electricity market on the VF, twelve sites in four European countries were considered (Norway, Denmark, Germany, Spain).

The analysis of the simulated annual energy yield at the twelve investigated sites led to the important finding that above a latitude of about 50° (corresponds to the latitude of the city of Frankfurt am Main) VBPV has a higher annual energy yield than a corresponding C-PV system with the same front-side capacity. This can be explained by the fact that with increasing distance

from the equator the duration of sunrise and sunset increases, which favours the energy yield of VBPV.

When installing VPBV, it must be thoroughly checked in which compass direction the more efficient side should be oriented. Both the diurnal electricity price curve and local weather conditions must be taken into account. Of the eight sites investigated here, it was advantageous for seven sites to orient the more efficient side towards the east, because more electricity was produced in the first half than in the second half of the day.

Furthermore, the calculated VF, which are based on simulated power generation and historical market prices, were analysed. Markets with different levels of penetration of PV systems were compared. For example, the share of installed PV capacity in Norway, Denmark, Germany and Spain was ≈0 %, 5.9 %, 19.6 % and 4.7 % in 2016, respectively. It was found that in countries with little installed PV capacity (Norway, Denmark, Spain) the VF of C-PV is higher than that of VBPV throughout the period considered. However, a different picture has emerged for Germany: while from 2006 - 2011 C-PV had higher VF than VBPV, from 2012 - 2018 VBPV always achieved higher VF than C-PV. The share of installed PV capacity in Germany was around 20 % in the tipping year 2012. These results illustrate that with a high proportion of installed PV capacity, higher VF can be achieved with VBPV. Below a latitude of approx. 50°, however, the higher VF would be associated with a lower annual electricity yield compared to C-PV; above 50° with a higher absolute annual electricity yield.

In order to compare the profitability of C-PV and VBPV, which depends on both income and expenditures, the net present value of both systems was calculated for three German sites and for three historical years for the first year of operation. The years 2008, 2012 and 2016 were chosen to consider high, medium and low VF of both PV technologies. The comparison of the net present values showed that although C-PV always had a higher net present value, the corresponding difference between C-PV and VBPV decreased steadily over the years. This shows that if installed PV capacity in Germany continues to increase in the future, the tipping point will probably be reached where the profitability of VBPV will be higher than that of C-PV, which would favour the expansion of VBPV.

The influence of VBPV on the overall system costs of a national electricity system was investigated using the cost-minimizing electricity market model E2M2 with Germany as an example [25]. The aim of this investigation was to find out under which boundary conditions the electricity market model would choose the currently more expensive VBPV instead of the cheaper C-PV; or in other words, under which boundary conditions system costs can be reduced by using VBPV. Three scenarios were considered for the analysis. In the first scenario, 50 %

renewable electricity and 50 % $CO_{2\text{-eq}}$ reduction compared to 1990 had to be achieved. In the second scenario both barriers were set to 70 %, in the third scenario to 90 %[5]. In addition, the ratio of the investment of VBPV and C-PV was varied. In order to identify the effects caused by VBPV, the results of two calculation runs were compared in all scenarios: in one calculation run the optimization model can build VBPV, in the other calculation run it cannot, ceteris paribus. All calculation runs were calculated using a "greenfield approach", i.e. at the beginning of a calculation the installed capacity of all technologies was 0 MW.

Regardless of the ratio of the investment of VBPV and C-PV, no VBPV was built in the first scenario (Figure 51). In the second scenario VBPV was built, whereby the share of installed VBPV capacity in the total PV capacity decreased with a higher investment ratio. If the investment of VBPV is approximately 6 % higher than that of C-PV, no more VBPV was built in the second scenario. In the third scenario, from an environmental point of view the most ambitious one, the share of installed VBPV capacity in relation to total PV capacity was over 80 % for equal investments and fell to around 15 % with a 25 % higher investment of VBPV. At the same time, it was possible to save approx. 1 % of overall annual system costs for equal investments compared to a system that has no possibility to build VBPV. Based on these results, it can be concluded that if high shares of renewable electricity and high $CO_{2\text{-eq}}$ reductions are to be achieved, VBPV can contribute to reducing costs in the power supply system.

In summary, the most important contributions to the state of knowledge described in Chapter III can be summarised as follows:

1. Above a latitude of approx. 50° a higher energy yield can be achieved with VBPV than with a comparable C-PV system.
2. When installing VPBV, it must be thoroughly checked in which compass direction the more efficient side should be oriented. Both the diurnal electricity price curve and local weather conditions must be taken into account.
3. In electricity markets with increasing shares of installed PV capacity, higher VF can be achieved with VBPV. In the case of Germany this occurred at a share of around 20 % of the overall installed power capacities.
4. With increasing shares of installed PV capacity in Germany, the market revenue-based profitability of VBPV would decline less than that of C-PV.
5. VBPV can help to reduce the overall costs in the electricity system if very high shares of renewable electricity and $CO_{2\text{-eq}}$ reduction goals are to be achieved.

[5] The scenarios contained more technical boundary conditions than the two described, which, however, do not play a major role for this work.

4.2 Paper 3

VERTICAL BIFACIAL PHOTOVOLTAICS – A COMPLEMENTARY TECHNOLOGY FOR THE EUROPEAN ELECTRICITY SUPPLY?

Authors: Dimitrij Chudinzow[6], Sylvio Nagel, Joshua Güsewell, Ludger Eltrop

Published in: Applied Energy, Volume 264, 15 April 2020, 114782

DOI: https://doi.org/10.1016/j.apenergy.2020.114782

4.2.1 Author contributions for the third paper

The following Figure 39 shows the contributions of the co-authors to the third paper, using the "CRediT author statement" system [14]. Sylvio Nagel was responsible for the calculations in E2M2; Joshua Güsewell assisted in the data processing of historical stock exchange electricity prices and creation of figures. Ludger Eltrop reviewed the submitted manuscript.

	Vertical bifacial photovoltaics – A complementary technology for the European electricity supply?			
	Dimitrij Chudinzow	Sylvio Nagel	Joshua Güsewell	Ludger Eltrop
Conceptualization	✓	✓	✓	
Methodology	✓	✓	✓	
Software				
Validation				
Formal analysis	✓	✓	✓	
Investigation	✓			
Resources				
Data Curation	✓	✓	✓	
Writing - Original Draft	✓	✓		
Writing - Review & Editing				✓
Visualization	✓		✓	
Project administration	✓			

Figure 39: Author contributions for the third paper.

[6] Main author

Applied Energy 264 (2020) 114782

Contents lists available at ScienceDirect

Applied Energy

journal homepage: www.elsevier.com/locate/apenergy

Vertical bifacial photovoltaics – A complementary technology for the European electricity supply?

Dimitrij Chudinzow*, Sylvio Nagel, Joshua Güsewell, Ludger Eltrop

Institute of Energy Economics and Rational Energy Use (IER), University of Stuttgart, Heßbrühlstraße 49a, 70565 Stuttgart, Germany

HIGHLIGHTS

- Energy yield simulation of vertical bifacial PV array in 12 European locations.
- Comparison with a conventional PV array (monofacial, equator-oriented, tilted).
- Evaluation of market revenues based on historic day-ahead market prices.
- Evaluation of LCOE and net present value.
- Evaluation of system cost reduction from a macroeconomic perspective for Germany.

GRAPHICAL ABSTRACT

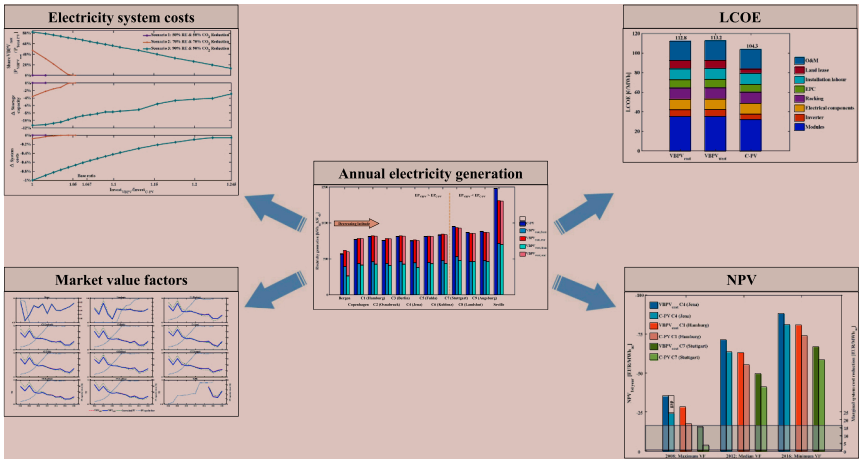

ARTICLE INFO

Keywords:
Market value
Electricity market
Electricity system costs
System-friendly renewables
Energy transition
PV

ABSTRACT

Thanks to the two diurnal generation peaks, vertical bifacial photovoltaic power plants (VBPV) with a north-south axis represent an option to meet the challenges of a mismatch between electricity demand and the generation profile of conventional photovoltaic systems (C-PV). Despite this promising characteristic, it is hardly possible to assess the technical and economic properties of VBPV on the basis of existing studies. The present work is a contribution to close this gap. Among other things, the conducted analyses included electricity generation, market revenues, levelized costs of electricity (LCOE) and the cost-reducing effect of VBPV in a national electricity system. C-PV was used as a benchmark in all analyses. Electricity generation was simulated at twelve European sites in four countries.

It has been found that above a latitude of 50° VBPV generates more electricity than C-PV. Due to the higher investments, VBPV had higher LCOE at all locations investigated. The results also showed that VBPV can generate higher revenues in electricity markets with a high share of C-PV capacity, but that these additional revenues are not yet sufficient to compensate for the higher investments. With an optimising electricity market model, it was also found that VBPV can contribute to reducing system costs in an electricity system with high shares of C-PV capacity. Against the background of the increasing importance of PV for the electricity supply of most European countries, these findings are of particular importance. In summary, it can be said that VBPV has significant potential at both the business and macroeconomic level and that decision makers should promote the market entry of this technology.

* Corresponding author.
E-mail address: dimitrij.chudinzow@ier.uni-stuttgart.de (D. Chudinzow).

https://doi.org/10.1016/j.apenergy.2020.114782
Received 13 December 2019; Received in revised form 12 February 2020; Accepted 28 February 2020
Available online 06 March 2020

1. Introduction

In the past decade, PV systems have experienced a rapid rise within the European power supply. In 2016, PV accounted for more than 10% of total installed capacity in the EU [1]. From 2010 to 2016, the annual average expansion of PV capacity in the EU was 12.4 GW/a [2]. Today, PV is a key technology for European countries to meet their carbon reduction targets and reduce their dependence on fossil fuels [3]. The photovoltaic technology dominating the market is monofacial, but the importance of bifacial photovoltaics is constantly increasing. A special variant of bifacial systems are vertically installed module rows with a north-south axis (VBPV) (A glossary is provided in the Appendix A.1). Although some commercial VBPV systems have been realized (e.g. by the German company Next2Sun [4]), there are very few studies in the scientific literature dedicated to the techno-economic evaluation of VBPV.

A global comparison of the energy yield of vertical bifacial and conventionally installed monofacial modules is given in [5]. Although this study provides a good global overview of the energy yields of the two module types, the findings of individual modules cannot easily be transferred to a PV field, since shading effects in a PV field play a major role. It was also assumed that the return on investment depends only on the absolute amount of electricity generated, but not on the generation profile. This assumption is not appropriate for PV systems that generate their revenues on electricity markets, as the diurnal electricity prices are usually not flat. Another global assessment of the energy yield of vertical bifacial PV systems was presented in [6]. The authors provided a sound technical yield analysis, but economic aspects were not part of their work. The comparison of the energy yield of vertically and south inclined bifacial systems in Tel Aviv was carried out by [7]. However, this work did not include economic aspects either.

Against this background, this work aims to provide a comprehensive techno-economic analysis of VBPV. For the concept of this work it is of great importance to describe the challenging nexus between renewable energy technologies (RET) and electricity markets with increasing shares of RET. For this reason, in the remainder of this section we focus on studies that examine the specific challenges associated with RET and electricity systems. In terms of content, the overview is divided into two parts.

1.1. The impact of RET on electricity prices

The merit order effect (MOE) of RET on German market pricing was analysed qualitatively and quantitatively in [8]. Using a model-based approach, it was found that average market prices were reduced by 7% due to the presence of solar electricity generation in the period 07/2010–07/2011. This would correspond to a price drop caused by the MOE of 0.3 €/MWh per generated TWh of solar electricity. This means that with increasing installed PV capacity, the market revenues of all market participants decrease.

Further effects of increasing RET market shares on policy and market behaviour in the German electricity market were investigated in [9]. The authors emphasized that the current German electricity market design is based on short-term marginal costs of generation, which are usually set at zero for wind and solar plants, while long-term costs are not considered. This leads to the remarkable situation that short-term zero costs lower market prices, making profitable and unsubsidized operation even more difficult to achieve. Consequently, this would hinder new investment in RET if investors did not have confidence in covering their cost of capital and generating profits.

The impact of RET on market price setting was also assessed by [10]. The value factor (VF) was chosen as a measure, which is defined as the ratio of the specific day-ahead sales of a technology in €/MWh and the average day-ahead market price in €/MWh (see also Eq. (1)). In the simplest case, a power plant would have a VF of one if the electricity it produces had a perfectly flat (i.e. time-invariant) profile throughout the year. A VF greater than one indicates that the generation profile allows to benefit from higher prices than to choke on lower prices. Consequently, generators with an unfavourable profile would have a VF less than 1. The analysis of the German data (2006–2012) showed that the VF of PV power plants decreased steadily as the market share of PV increased. In detail, the VF decreased from 1.33 in 2006 to 1.05 in 2012 (−21%), while the share of solar electricity increased from 0.4% to 4.5%. This can also be explained by the MOE on a daily basis: To maximise energy yield, most German ground-mounted PV power plants are south-facing and have a fixed slope. Therefore, if one disregards local weather effects and considers that the solar time differs by about 30 min at the western and eastern border of Germany, their production profiles are almost identical. This leads to a shift in the merit order curve, which results in significantly reduced market prices.

A similar finding was made by [11], who analysed the effects of increased RET shares on VF. Using a liner optimization model for the German electricity system, it was shown that in a scenario with very high growth of installed PV capacity, the VF of PV would decrease by 14%. These results were further substantiated by [12] who calculated the VF of PV in different scenarios. They showed that a 50% increase in PV electricity would lead to an 8% decrease in VF.

1.2. Electricity system costs & system-friendly RET

The composition of system costs was described in [13]. The system costs were defined as the difference between the average electricity price and the market value of a given technology. In addition, the system costs include three basic contributions: profile costs related to the variability of electricity production, balancing costs related to the uncertainty of electricity production and network costs resulting from the distance between the place of electricity demand and the place of electricity generation. Based on this, options for reducing electricity system costs were presented. Among other things, the authors proposed the installation of east-west oriented PV systems. This would give the PV system a camel-shaped generation profile with two generation peaks: one in the morning and one in the afternoon. Further penetration of such systems would therefore help to smooth the aggregated generation profile of PV systems and stabilize the market value of PV. Furthermore, it was pointed out that with increasing variability of RET in the generation portfolio, storage requirements would also increase, which would raise system costs [14].

The need to facilitate the integration of the system-friendly RET into the German electricity system was discussed in [15]. In simplified terms, system-friendly RET generate electricity at times and places characterised by high electricity prices. The authors explicitly mention that VBPV is a system-friendly technology, as VBPV systems have a camel-shaped diurnal generation profile and offer the possibility to generate electricity in times of higher market prices.

1.3. Summary

The current and future role of RET for European electricity supply is both promising and challenging. Promising because RET are essential for achieving the European emission reduction targets and increasing the share of electricity from renewable energy sources, and therefore their market share is expected to grow further. In the case of PV, it is challenging because the interaction of the MOE and regionally simultaneous electricity generation leads to decreasing electricity market prices (especially around noon), which aggravates the financial situation of market-oriented PV systems. This requires new business models and technologies to ensure the long-term financial viability of PV systems. In order to achieve the goal of this thesis, the preparation of a sound techno-economic evaluation of VBPV, the following analyses were carried out:

1.3.1. Business perspective

1. The annual electricity generation of VBPV and C-PV was simulated for twelve European sites: Bergen (Norway), Copenhagen (Denmark), nine sites in Germany and Seville (Spain). A meridian area of about 23° was covered, which corresponds to a distance of about 2700 km.
2. In order to assess the potential market revenues, the VF were calculated on the basis of the available historical market data of the individual countries (Germany, Norway, Denmark: 2006–2018; Spain: 2015–2018) for VBPV and C-PV.
3. The net present value in the first year of operation ($NPV_{1st\ year}$) was calculated for Germany in order to compare the profitability of C-PV and VBPV.
4. Based on the simulated electricity generation and available cost data, LCOE were calculated for the sites.

1.3.2. Macroeconomic electricity system perspective

1. Using the "European Electricity Market Model" E2M2 [16,17], it was investigated whether VBPV is a system-friendly technology and can bring technical and economic benefits to the German electricity system as a whole, which is characterized by a high proportion of installed C-PV capacity.

The further work is structured as follows: Section 2 describes the methods used, which include the selection of the locations examined, the energy yield simulation of VBPV and C-PV, and the data basis for the evaluation of the value factors. Furthermore, the assumptions and data basis for E2M2 are presented. Section 3 contains the results and discussion, which serve for the conclusions in Section 4.

2. Methods

2.1. Selection of the investigated sites

The selection of sites was guided by two main hypotheses. The first hypothesis states that both the electricity generation and the profitability of VBPV depend largely on the latitude of the site. For sites further away from the equator, the duration of sunrise and sunset is longer than for sites near the equator. This would favour the east-west oriented VBPV, as the time when direct sunlight hits one of the two sides at a favourable angle increases. In order to quantify the influence of the latitude of a site, it is therefore desirable to evaluate sites that are distributed over a wide meridian range. For this purpose, a total of twelve sites were investigated (see Table 1 and Table 2), with Bergen (Norway) being the northernmost (60.3° latitude) and Seville (Spain) the southernmost (37.4° latitude).

The second hypothesis states that the integration of VBPV into a national electricity system characterised by a high share of renewable C-PV electricity and low carbon emissions can have cost-reducing effects. This assumption is based on the camel-shaped diurnal generation profile of VBPV, which is complementary to that of C-PV. To address the second hypothesis, the German electricity system was selected as a case study and examined with the fundamental, cost-minimizing "European Electricity Market Model" (E2M2). A detailed description of E2M2 is given in Section 2.6 and in [17]. Since Germany was modelled as a single node ("copper plate"), it was imperative to generate aggregated generation profiles for C-PV and VBPV from representative locations. The two aggregated generation profiles were created according to the following approach:

2.1.1. Geo-referencing of existing PV systems in Germany

Based on the 2017 system master data of the four transmission system operators (Amprion, 50Hertz, Tennet, TransnetBW) [18], the 1,636,857 PV systems listed were aggregated at postcode level. Fig. 1 (left) shows the geographical distribution of installed PV capacity in Germany as of 31st December 2017, with a total installed capacity of 40.25 GW.

2.1.2. Clustering of existing PV systems

The georeferenced PV systems were clustered into groups using the k-mean clustering algorithm [19]. In order to consider the climatic conditions in Germany and to limit the calculation effort, a group number of nine was chosen. K-means calculated the groups iteratively in such a way that the Euclidean distance of each group member to its centre of gravity was minimized. The latitudes and longitudes of each system served as observations, i.e. as input for the algorithm. The result contained both the centre of gravity of each group and the group membership of each PV system. Fig. 1 (right) shows the resulting cluster formation of German PV systems. After cluster formation, the share of each group in the total installed PV capacity was calculated (referred to as "weight"). The weights were used to create the representative generation profiles for both C-PV and VBPV and implemented in E2M2.

Tables 1 and 2 show an overview of the investigated sites, sorted by descending latitude, and the references for the cost and weather data used.

2.2. Electricity generation simulation of VBPV

The electricity generation of the VBPV power plants was simulated with the methodology described in [23]. The simulation was carried out in hourly resolution for one year. The 280 W_p BiSoN module was chosen as reference for the technical parameters bifaciality, efficiency, NOCT and module dimensions [24]. The electrical front-side efficiency at STC was 16.9%. The modelled power plant consisted of four rows with six modules each in landscape format along the long side and three modules along the short side of a row. Thus, the VBPV power plant consisted of 72 modules with a total of 20.16 kW_{dc} front-side capacity. For the DC-AC inverter efficiency, an EU weighted constant value of 0.98 was used for both C-PV and VBPV [25]. Based on the field design of Next2Sun's VBPV power plant, the row spacing for all locations was

Table 1
Investigated German sites.

Centroid	Centroid's coordinates [°] (Lat., Long.)	Neighbouring city (approx. distance from city to centroid)	Day-ahead spot market	Price data	Weather data source
C1	53.565, 10.126	Hamburg (0 km)	Epex Spot DE	2006–2017: [20]	[22]
C2	52.458, 8.271	Osnabruck (30 km)		2018: [21]	
C3	52.353, 13.455	Berlin (0 km)			
C4	50.518, 11.71	Jena (65 km)			
C5	50.394, 9.488	Fulda (30 km)			
C6	50.292, 7.331	Koblenz (25 km)			
C7	48.627, 8.656	Stuttgart (50 km)			
C8	48.567, 12.412	Landshut (20 km)			
C9	48.470, 10.553	Augsburg (35 km)			

Table 2
Investigated European sites outside Germany.

Site	Coordinates [°] (Lat., Long.)	Country	Day-ahead spot market	Price data	Weather data source
Bergen	60.3, 5.22	Norway	Nord Pool NO5	2006–2017: [20] 2018: [21]	[22]
Copenhagen	55.63, 12.67	Denmark	Nord Pool DK2	2006–2017: [20] 2018: [21]	
Seville	37.42, −5.9	Spain	Omie ES	2015–2017: [20] 2018: [21]	

kept constant at 10 m and the mounting height (distance from the ground to the lower edge of the lower module) at 1 m [4]. For both PV technologies and for all sites, the ground surface was assumed to be grass with a reflectance of 20% [26].

2.3. Electricity generation simulation of C-PV

One focus of the present work is the direct comparison of VBPV and C-PV. The use of different simulation tools for VBPV and C-PV was avoided. Therefore, the C-PV technology was simulated with the same simulation model as for VBPV, with some necessary adjustments. It was considered that the back of a conventional module absorbs the radiation with an absorption coefficient of about 0.2 [27]. This rear-absorbed radiation did not contribute to the electricity generated, but heated the module and attenuated the electrical efficiency. For the technical module properties, the 280 W_p Longi module was used as a reference [28]. The electrical efficiency on the front side was 17.1% at STC. Consequently, C-PV also consisted of 72 modules with a total capacity of 20.16 kW_{dc}. Furthermore, the optimal angle of inclination was determined depending on the geographical latitude of a location according to [29]. The row spacing was kept constant at 5 m for all locations and the installation height was always 1 m (distance from the ground to the lower edge of a module row).

2.4. Economic assessment using VF and LCOE

Two metrics were used for the economic analysis from a business perspective:

2.4.1. Value factors of day-ahead market prices

In order to be able to compare the market revenues from both VBPV and C-PV, value factors (VF) were calculated on the basis of simulated electricity generation and historical day-ahead price data for the market zones under consideration (information on price data in Table 1 and Table 2). The VF was defined according to Eq. (1) [30].

$$VF = \frac{Specific\ revenues\ of\ a\ power\ plant\ \left[\frac{€}{MWh}\right]}{Average\ market\ price\ \left[\frac{€}{MWh}\right]} \quad (1)$$

The shares of installed PV capacity in the four investigated countries are provided in Table 3 for the year 2016. As discussed in Section 1, the PV share has a large influence on the VF.

The following Fig. 2 (left) shows the hourly averaged day-ahead prices from all years in which market data was available in the four market zones examined. Obviously, the day-ahead price in electricity systems with a significant share of PV capacity has two distinct price peaks during the day: one around noon and one in the evening. This price pattern is not the only consequence of the generation profile of PV. Other factors such as electricity demand, trade, etc. also contribute

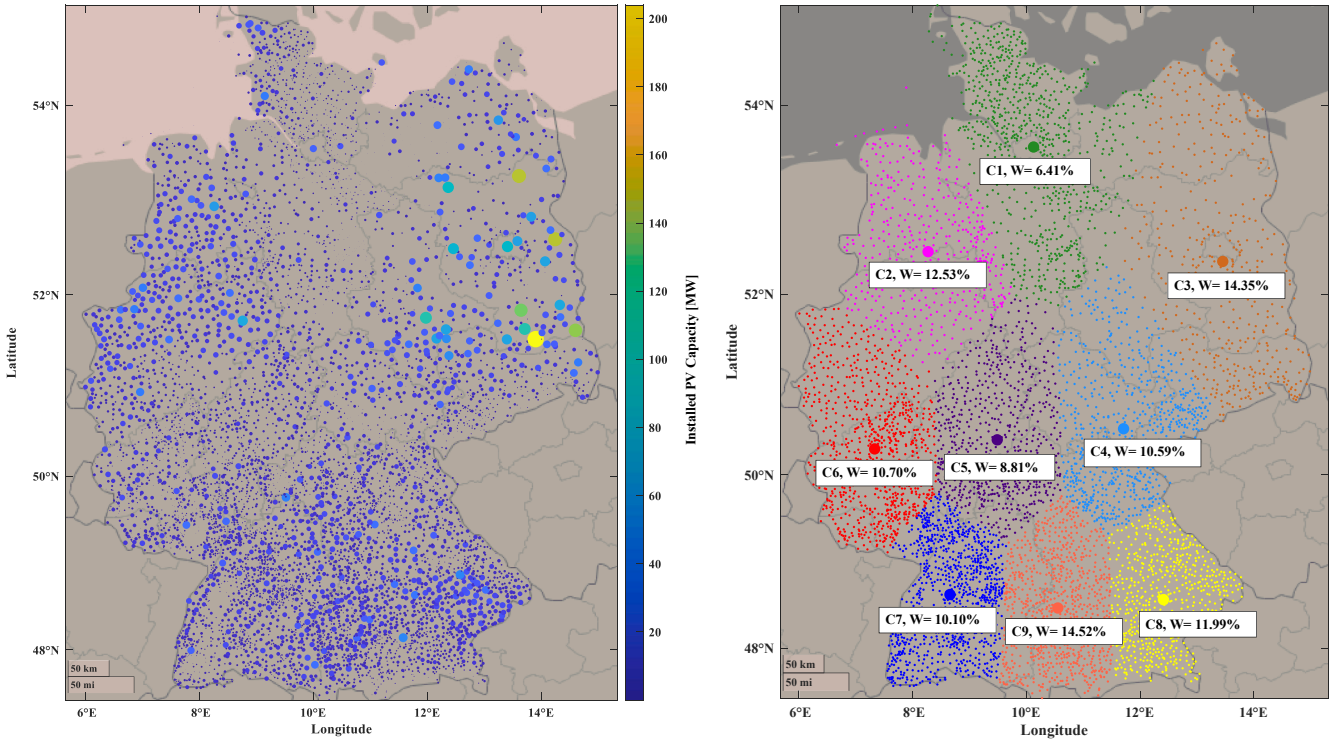

Fig. 1. Installed PV capacity in Germany in 2017, aggregated at postcode level (left) and clustered PV capacity in Germany using the k-means algorithm (right). The "C" indicates the geographic centroid of each group, the weights (W) represent the share of each group in total PV capacity.

Table 3
Share of PV capacity in 2016 in the countries studied [31].

Country	Share of PV capacity in 2016
Spain	4.7%
Germany	19.6%
Denmark	5.9%
Norway	0%

to the observation described. In contrast, the Norwegian power generation mix is mainly based on hydropower (98% of electricity was generated from hydropower in 2016, [32]), so that the daytime price pattern is rather flat. Fig. 2 (right) shows the integrals of the hourly averaged day-ahead market prices in the first and second half of the day. The areas A_1 (yellow) and A_2 (blue) illustrate that in all four markets higher revenues can be achieved in the second half of the day (because $A_2 > A_1$). In this context, it is important to note that 12 am local time (i.e. clock time), which represents the half of the day in Fig. 2 (right), usually does not coincide with the zenith time of the sun, which marks the actual midday. The local time "12 am" and the zenith time only coincide in places whose longitude is an integral multiple of 15° (including zero). This means that places that are located west of their reference longitude (e.g. most of Germany and Norway, Denmark, Spain) have a longer time span from 12 am to sunset than from sunrise to 12 am when referring to local time. Therefore, in the case of Germany, if one neglects local weather conditions, air temperature, etc., it seems reasonable to always orient the more efficient front side of VBPV towards the west, since the second half of the day has longer sunshine and the area A_2 in the market zone of Germany is larger than A_1.

2.4.2. Levelized cost of electricity (LCOE)

To analyse the influence of a site's latitude on the electricity generation costs of C-PV and VBPV, the LCOE for all twelve sites were calculated using the following Eq. (2) [34]:

$$LCOE = \frac{I_0 + \sum_{t=1}^{n} \frac{A_t}{(1+i)^t}}{\sum_{t=1}^{n} \frac{M_{t,el}}{(1+i)^t}} \quad (2)$$

where I_0 is the investment in year zero, A_t is the annual cost in year t, $M_{t,el}$ is the electricity generated (alternating current) in year t, n is the lifetime of the PV power plant and i is the interest rate. All economic and technical values used are given in Appendix A.2. Since the aim was not to calculate the exact site-specific LCOE, but to investigate the influence of the amount of electricity generated and the land area occupied, all cost items were kept constant for all countries. In addition, for the sake of brevity, only the LCOE for site C5 (Fulda), the most central German site among those investigated, was broken down. An average annual degradation rate of 0.3%/year was considered for both PV technologies [24].

2.5. The fundamental European electricity market model E2M2

The European electricity market model "E2M2", which is a proprietary model of the IER, was used to investigate the system cost effects induced by VBPV. Based on a fundamental analytical approach, E2M2 optimizes future investments and the use of power plants while ensuring a reliable electricity supply. E2M2 is written in the algebraic modeling language GAMS (General Algebraic Modeling System). The cost function to be minimized by the CPLEX solver includes capital costs, operating costs and costs for grid expansion. An overview of the most important mathematical formulations is given in Appendix A.5. Usually E2M2 is adapted to specific research questions. Therefore, the following specifications contain tailor-made adaptations to meet the focus of this work. The description of the model is divided into the spatial, temporal, energetic and economic dimensions.

2.5.1. Spatial dimension

Since the electricity system analysis was only carried out for Germany, E2M2 was spatially limited to the optimization of the German electricity system, with fixed amounts of imported and exported electricity to reduce the calculation time. In E2M2, Germany is represented by a single node. Spatial disparities were therefore not considered. The costs of grid expansion triggered by fluctuating renewable energies were calculated with a specific value (EUR/GW_{RET}) and allocated to the corresponding power plant [35].

The starting point for all model runs was a "greenfield" approach, i.e. E2M2 assumed that no energy plants exist in Germany. This helped to identify the effects of VBPV compared to a system without this technology by negating all non-optimal decisions in advance.

2.5.2. Temporal dimension

The temporal optimization horizon was a hypothetical year, whereby future aspects were considered by policy-related boundary conditions (e.g. binding share of renewable electricity and reduction of

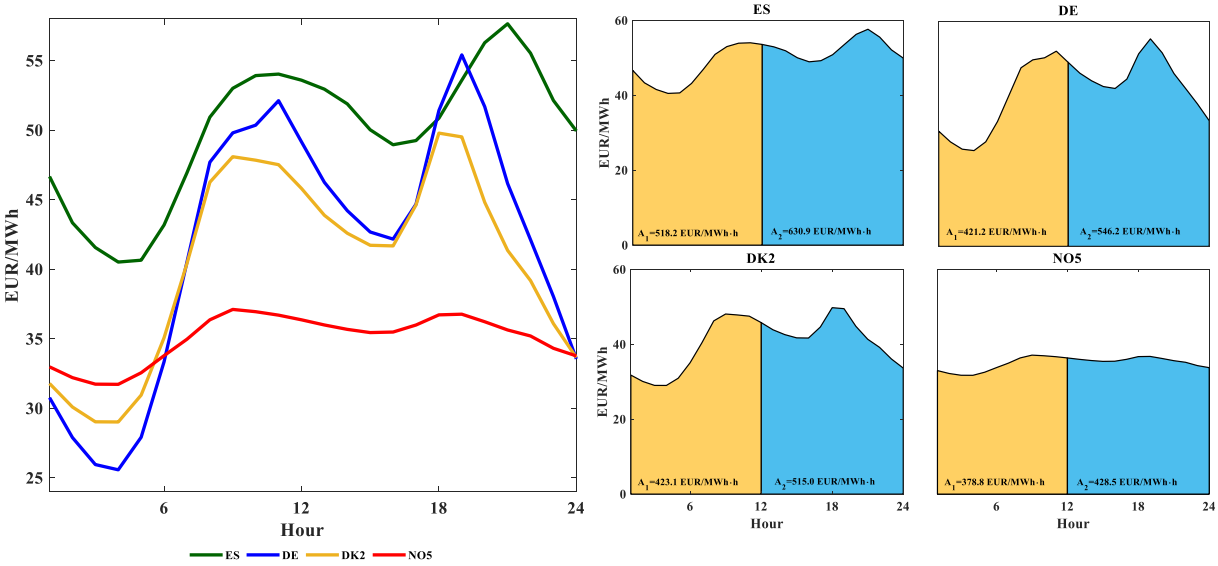

Fig. 2. Hourly averaged day-ahead prices from the four market zones examined (ES: 2015–2018, DE/DK2/NO5: 2006–2018) (left) and integrals of the hourly-averaged day-ahead price in the first and second half of a day (right). The price data refer to winter time, i.e. without taking summer time into account [33].

CO_2 emissions). At the same time, investment decisions and the dispatch of the power plant park were optimized. Power plant dispatch was regulated by calculating the residual load (total electrical load minus the feed-in from PV and wind power plants), which was then covered by more flexible generators. All costs incurred over several years were annuitized at an interest rate of 5% over the lifetime of each invested infrastructure component, so that the annuities were considered for the optimization calculations. Throughout the optimization process, the solver was aware of the states of all variables (e.g. costs, electricity generation of all technologies in every hour of the year). This behavior is called "perfect foresight". The hourly temporal resolution made it possible to quantify the required electrical storage capacities.

2.5.3. Energetic dimension

The endogenous decisions on investments and the operation of power plants were aimed at a reliable electricity supply. This included both the simultaneous coverage of the specified load and the provision of sufficient reserve capacities. The reserve power requirement calculated in the model depended on the composition of the entire power plant park. The dispatch determined the operating status and, if necessary, the generation capacity at any time for each generation unit. A distinction was also made between rotating and stationary states for the turbines. The power plants characterized by a rotating turbine (CHP (combined heat & power plant), district heating plants) could feed electricity into the grid and contribute to the provision of power reserves depending on the current generation capacity.

In order to cover the given heat demand, the model included the coupled generation of electricity and heat by CHP. Depending on the technical design of a CHP plant, a distinction was made between back-pressure and extraction condensation plants. While the former produced electricity and heat in a fixed ratio, the latter allowed a flexible production ratio of electricity and heat [36]. Another possibility to cover the heat demand were heat pumps, whose electricity consumption was added to the total electricity demand. The investment and operation of heat pumps was optimised endogenously. For reasons of comparability, the demand for electricity and grid-bound heat in Germany was set at the level of 2017 for all scenarios examined [37].

All fluctuating renewable energies (C-PV, VBPV, wind onshore & offshore) were integrated with representative feed-in curves. To ensure comparability of the results, the feed-in time series were not changed across the scenarios - they were therefore deterministic, not stochastic.

In order for the relatively expensive renewable energies to be used at all in a cost optimization model, boundary conditions were included that go beyond a strict cost perspective. In E2M2 two boundary conditions were included which served as distinguishing features for the scenarios investigated:

1. Share of RE: A fixed part of the electricity must be covered by renewable energies every year.
2. Maximum CO_2 emissions: All fossil-based technologies were characterized by a CO_2 emission factor per functional unit (e.g. kWh_{el}). Annual emissions were not allowed to exceed the specified threshold value, which was defined by a reduction rate, based on 366 Mt CO_2 emissions of the energy sector in Germany in 1990 [38]. Since only direct CO_2 emissions were considered, the associated values for renewable technologies were zero.

2.5.4. Economic dimension

In the objective function, all costs incurred were added and minimized. The system costs consisted of the annualized capital costs for the investment of the power plants and the variable costs for their operation as well as costs for system services and grid expansion due to fluctuating renewables. Costs for grid expansion were taken from [35]. All cost assumptions for fluctuating renewables are listed in Appendix A.6. Since the focus of this work is on the investigation of the cost-optimal electricity system design from a macroeconomic perspective, no subsidies were considered.

3. Results and discussion

3.1. Electricity generation of VBPV and C-PV

3.1.1. Impact of latitude on annual electricity generation

The following Fig. 3 shows the simulated annual specific power generation of C-PV, $VBPV_{east}$ and $VBPV_{west}$. On the right Y-axis, the ratio of generated electricity from C-PV and $VBPV_{east}$ is plotted. To visualize the influence of the latitude of a site, the sites were sorted by descending latitude. The site comparison yielded several results. First, $VBPV_{east}$ generated slightly more electricity than $VBPV_{west}$ at all sites. Second, there is a geographical threshold at the north-south transition where C-PV performs better than $VBPV_{east}$ and $VBPV_{west}$. For the sites studied, this threshold was between C6 (Koblenz) and C7 (Stuttgart), which corresponds to a latitude of about 50°. This finding is also supported by an empirical study of a VBPV system in Linköping (Sweden)

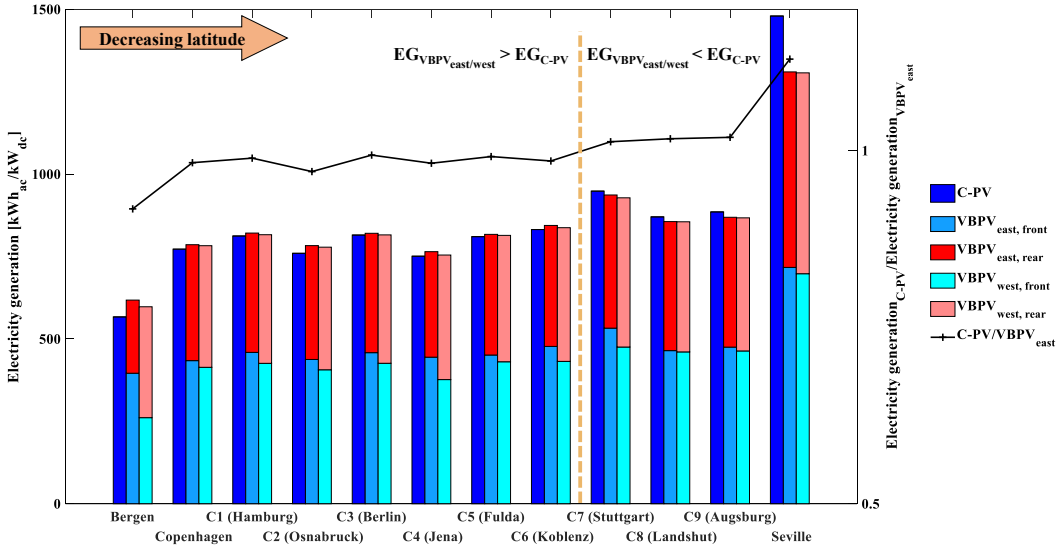

Fig. 3. Simulated annual specific electricity generation (left Y-axis) and ratio of generated electricity from C-PV and $VBPV_{east}$ (right Y-axis). In the legend, the first word in the index specifies, which direction the more efficient front side is facing; the second word indicates the side contributing to the electricity generation. EG: Electricity generation. In all sites from Bergen till C6 (Koblenz), VBPV generated more electricity than C-PV.

(58° latitude), which generated slightly more electricity than its C-PV counterpart [39]. Another study confirms that VBPV can generate more electricity at higher latitudes [40]. For the case of Germany, in C7 (Stuttgart), C8 (Landshut) and C9 (Augsburg) C-PV generated slightly more electricity than $VBPV_{east}$ and $VBPV_{west}$. For the three cities the additional electricity yields were 1.2%, 1.7% and 1.9% respectively. This observation became even clearer when comparing the three sites outside Germany. While in Bergen and Copenhagen the ratio of electricity generation of C-PV and $VBPV_{east}$ was 91.7% and 98.3% respectively, the picture changed drastically in Seville with a ratio of 113%. These results confirmed the first hypothesis, namely that the latitude of a site has a great influence on the electricity generation of VBPV and that sites closer to the equator are less suitable for VBPV due to the shorter times of sunrise and sunset. It is important to emphasize that bifaciality, defined as the ratio of $\eta_{el,back}$ and $\eta_{el,front}$, has a significant influence on these results. In this work, bifaciality was assumed to be 0.85 [24]. With the improvement of the bifacial PV technology, bifaciality will most likely increase. Consequently, at sites where VBPV already exceeds C-PV, the difference in electricity generation would increase further. At the other sites, VBPV could catch up and even exceed C-PV.

3.1.2. Impact of latitude on diurnal and seasonal electricity generation

To analyse the influence of the seasons and the latitude of a site on the diurnal generation profile, Fig. 4 shows the hourly averaged generation profiles for a northern (Bergen), central (C5 Fulda) and southern (Seville) site (The daily electricity generation is also available online as a supplementary video animation, see Appendix B). To improve readability, the profiles of $VBPV_{west}$ are not shown. One can clearly see the difference between C-PV and $VBPV_{east}$: while C-PV had its peak at noon, $VBPV_{east}$ had one peak in the morning and one in the afternoon. Usually the larger peak of $VBPV_{east}$ occurs before noon, the smaller one after noon. The different heights of the two peaks were caused by the bifaciality of the module and local weather conditions. It can also be observed that the generation profile of VBPV in Seville did not change much in shape throughout the year, while in Bergen and C5 (Fulda) the humps were most pronounced from April to June and were rather flat in the other periods. This can be explained by the fact that Seville is a dry region with much direct sunlight and less diffuse light, while the other two locations are characterised by a more humid climate (see Fig. 5). Therefore, dry regions encouraged the formation of humps and humid regions caused a flattening. Appendix A.3 contains the hourly averaged generation profiles of all sites.

Fig. 6 shows the monthly electricity generated (left) and the share of monthly electricity generated (right) by C-PV and $VBPV_{east}$ in Bergen, C5 (Fulda) and Seville. It can be seen that at high latitudes (Bergen) $VBPV_{east}$ performs significantly better than C-PV throughout the year, while the additional yields of $VBPV_{east}$ are greater in winter than in summer. In C5 (Fulda) $VBPV_{east}$ produced more electricity in winter, but significantly less in spring and autumn. In Seville, $VBPV_{east}$ produced less electricity all year round, while the surplus yields from C-PV were lowest in summer. This can be explained as follows: On the one hand, at higher latitudes the duration of sunrise and sunset is longer, which favours VBPV's electricity production, while lower latitudes are disadvantageous. On the other hand, when there is heavy cloud cover, the difference in performance between C-PV and VBPV is attenuated, since diffuse light is distributed fairly homogeneously over the celestial dome, while direct light is emitted by the sun, which is practically a point source. Therefore, the geometric arrangement of a PV system is less important under cloudy skies than under clear skies. The interaction of these two effects therefore led to the results outlined above. Other effects, such as air temperature, have also influenced energy production. When considering electricity systems, these results suggest that at higher latitudes VBPV could help to smooth the aggregated generation profile of PV power plants during the winter months.

3.1.3. Impact of latitude on electricity generation in the first and second half of a day

As discussed in Section 2.4, if the integrals of the diurnal market price structure were to be considered exclusively, it would make sense to orient the more efficient front side towards the west, i.e. to give preference to $VBPV_{west}$. However, in order to maximise market revenues, it is also necessary to consider the distribution of the generated electricity over the day. Fig. 7 shows the ratio of the annually generated electricity in the first and second half of the day, the ratio of the summed irradiance values DNI and DHI and the air temperature. It is noticeable that the sum of DNI and DHI in the first half of the day was higher at all sites except Seville. Seville falls out of the range, probably because it is the most western location, i.e. it has significantly more daylight after 12 am (local time). In addition, the average air temperature in the first half of the day is lower in all sites than in the second half of the day, and a lower air temperature is beneficial for PV power generation. Based on these observations, $VBPV_{east}$ would be the better choice.

3.2. Market revenues of VBPV and C-PV

In order to compare specific market revenues, VF were calculated for all 12 locations, based on historic market spot prices. For improved readability, Fig. 8 shows the results of Bergen, Copenhagen, C5 (Fulda) and Seville. The results for all sites are given in Appendix A.4. Based on these results, several deductions can be made.

3.2.1. Bergen, Norway

Firstly, C-PV and $VBPV_{east}$ and $VBPV_{west}$ achieved almost the same VF in Bergen. This can be explained by the relatively flat market price profile in the Norwegian market zone NO5 (Fig. 2), as 98% of Norwegian electricity supply is based on hydropower [32]. Considering that both VBPV orientations in Bergen generate more electricity than C-PV and achieve almost the same VF, the use of VBPV could generate higher market revenues compared to C-PV.

3.2.2. Copenhagen, Denmark

In the period 2006–2014, the $VF_{C\text{-}PV}$ was higher than that of both VBPV orientations, while the gap was always rather small: in 2006, the $VF_{C\text{-}PV}$ was 1.5% higher than the VF of both VBPV orientations. From 2015, the $VF_{C\text{-}PV}$ and $VBPV_{east}$ alternated, with differences of less than 1%. In 2018 the VF of $VBPV_{east}$ was 0.27‰ higher than the $VF_{C\text{-}PV}$, which can be considered negligible. Considering that both VBPV orientations generate more electricity in Copenhagen (Fig. 3), the use of VBPV would generate more revenues.

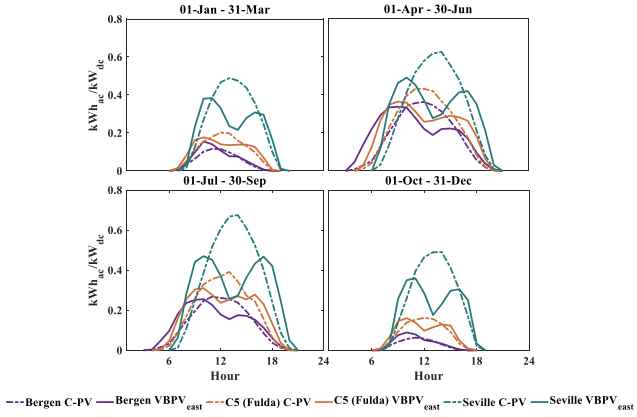

Fig. 4. Hourly averaged specific electricity generation in four quarters of a year at a northern, central and southern European location. In dry regions such as Seville, the humps of VBPV are more pronounced than in humid regions like Bergen.

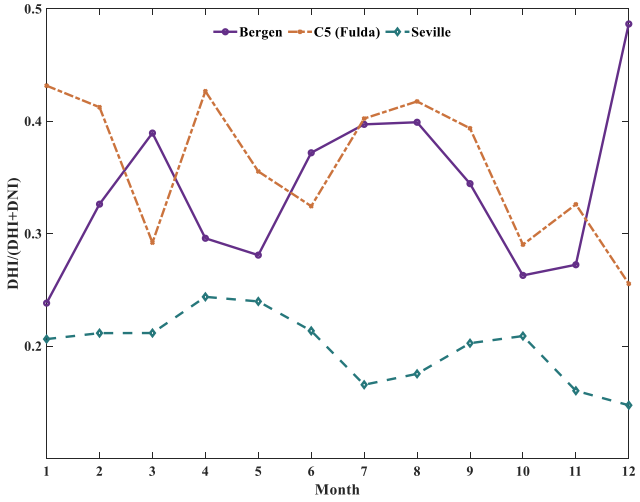

Fig. 5. Characterization of the local climate of three selected sites by comparing the monthly ratios of DHI/(DHI + DNI). Smaller values indicate a dry and less cloudy month.

3.2.3. C5 (Fulda), Germany

While C-PV achieved a higher VF than $VBPV_{east}$ and $VBPV_{west}$ in the years 2006–2011, the situation changed from 2012 onwards, when the share of installed PV capacity reached around 20%. From that year on both VBPV orientations reached higher VF than C-PV. This observation is consistent with the results of other studies, as described in Section 1. As discussed in Section 2.4, the second half of the day offered higher market returns. However, since the greater proportion of electricity was generated on average in the first half of the day in all German locations, $VBPV_{east}$ always achieved a slightly higher VF than $VBPV_{west}$. These results illustrate that in order to maximize market returns, it is crucial to carefully analyse electricity generation and the market price structure in order to make an informed decision on the orientation of VBPV.

3.2.4. Seville, Spain

In the case of Spain, all VF showed marginal differences well below 1%. In view of the fact that C-PV has a significantly higher energy yield (Fig. 3), the use of VBPV is not advisable from a purely revenue-based perspective.

3.3. LCOE of VBPV and C-PV

3.3.1. Breakdown of LCOE for C5 (Fulda)

In order to analyse the composition of the LCOE, they were disaggregated exemplarily for the site C5 (Fulda) and are shown in Fig. 9. Several conclusions can be drawn from this. First of all, the LCOE of $VBPV_{east}$ were about 8% higher than those of C-PV. Although $VBPV_{east}$ generated slightly more electricity, this could not offset the additional costs caused by higher module costs, higher land rental due to the double row spacing of C-PV and increased inverter capacity. Since bifacial modules can generate significantly more power than their monofacial counterparts, the inverter was oversized by 20% [41]. The higher equipment costs also led to higher engineering, procurement and construction costs (EPC), as these were defined as a fixed proportion (13%) of the total equipment costs [41].

3.3.2. Impact of latitude on the LCOE

In analogy to the procedure described in Section 3.1, the calculated LCOE for all sites were sorted by decreasing latitude from north to south and are shown in Fig. 10. It is important to note that the aim was not to determine the exact site-specific LCOE, but to derive general conclusions. Therefore, the same equipment, labour and land lease costs were assumed for all sites. The variations in LCOE values were thus due to different amounts of electricity produced and rather small variations in the land area occupied by C-PV at the individual sites. The differences in the occupied land area by C-PV were a consequence of the different slope angles at the individual sites, which served as input for determining the required land area, whereby a higher slope angle led to less occupied land area [23]. VBPV occupied the same area at all locations. Against this background, the results show that, at current costs, $VBPV_{east}$ is able to achieve cost parity in electricity generation with C-PV only in northern regions. At all other locations, C-PV has significantly lower LCOE values.

3.3.3. Sensitivity analysis for LCOE

The question arises which LCOE can be achieved under different economic conditions. Therefore, Fig. 11 shows a sensitivity analysis for the site C5 (Fulda). It becomes clear that for all three PV configurations the interest rate is the biggest lever for reducing the LCOE. By lowering the initial interest rate from 5% to 1.25% the LCOE of $VBPV_{east}$ were reduced by almost 30%. Furthermore, it should be noted that although land lease expenditure represented the smallest contribution in the case of C-PV, it became more important for vertical bifacial PV due to the

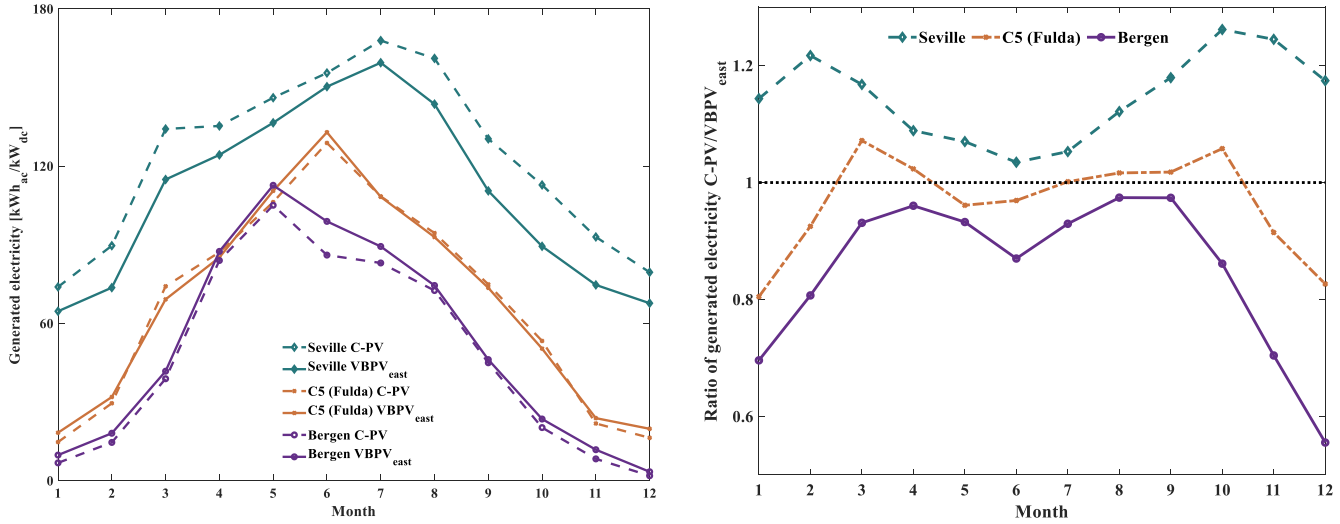

Fig. 6. Monthly generated electricity (left) and the share of monthly generated electricity from C-PV and $VBPV_{east}$ in Seville, C5 (Fulda) and Bergen (right). In Bergen, $VBPV_{east}$ exceeds C-PV in every month, while in Seville the opposite is true.

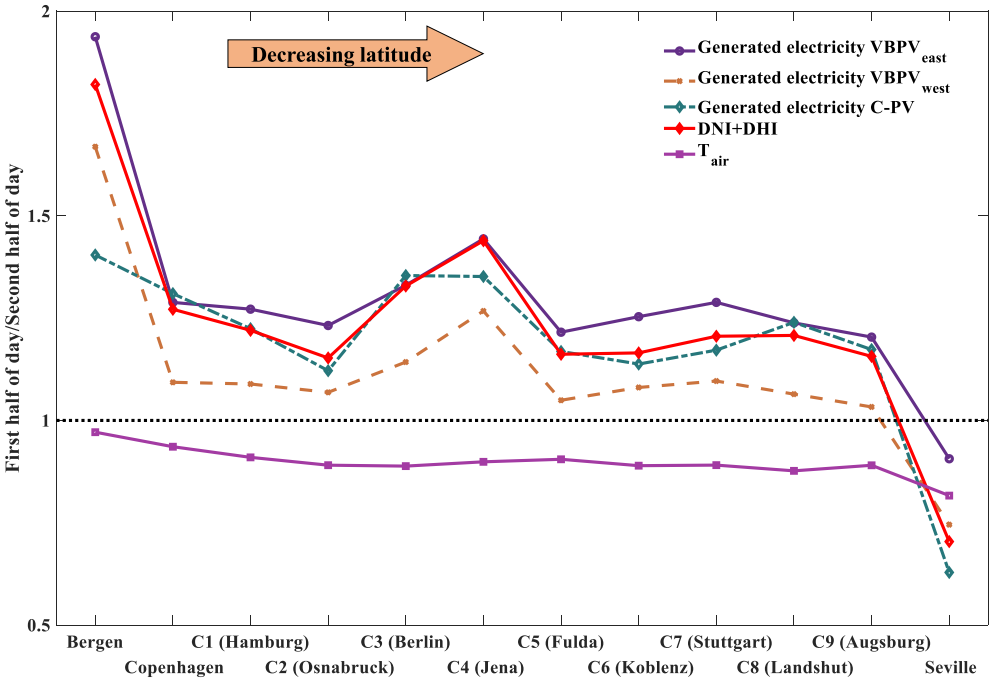

Fig. 7. Comparison of the electricity generated, the sum of DNI and DNI and the air temperature in the first and second half of the day on an annual basis. Orientation of the front side to the east is recommended because of the lower air temperature and the higher irradiation in the first half of the day. Only in Seville does the second half of the day show a higher irradiation intensity due to the high discrepancy between local and solar time.

much higher row spacing. However, since the large area between two vertical module rows can be used for other purposes, e.g. for agriculture [42–44], there is potential to reduce the land lease for VBPV.

3.4. Effects of VBPV on the German electricity system

The effects of VBPV on a national electricity supply system were examined using the case study of Germany. While the optimization model E2M2 minimized the overall system costs and covered the entire power demand, three different boundary conditions (scenarios) were to be fulfilled. Table 4 shows the definition of the scenarios.

In all scenarios, the ratio of the investment of VBPV and C-PV was varied. In all three scenarios, the use of $VBPV_{east}$ was more economical than $VBPV_{west}$ due to slightly higher electricity generation at all investigated sites. $VBPV_{west}$ was not built in any scenario.

Fig. 12 (above) shows the share of $VBPV_{east}$ in the total built PV capacity in all three scenarios. To improve the readability of the figure, most of the zero values have been hidden. In the first scenario $VBPV_{east}$ was not built at all and C-PV was the only PV technology. This was because even with the same investment ($Invest_{VBPV}/Invest_{C\text{-}PV} = 1$), the annual O&M costs were not the same, as $VBPV_{east}$ required more area than C-PV due to larger row spacing, which resulted in a higher land lease (see Section 3.3). The target RE share in the first scenario was achieved with C-PV and other RET (wind, dispatchable biogas plants).

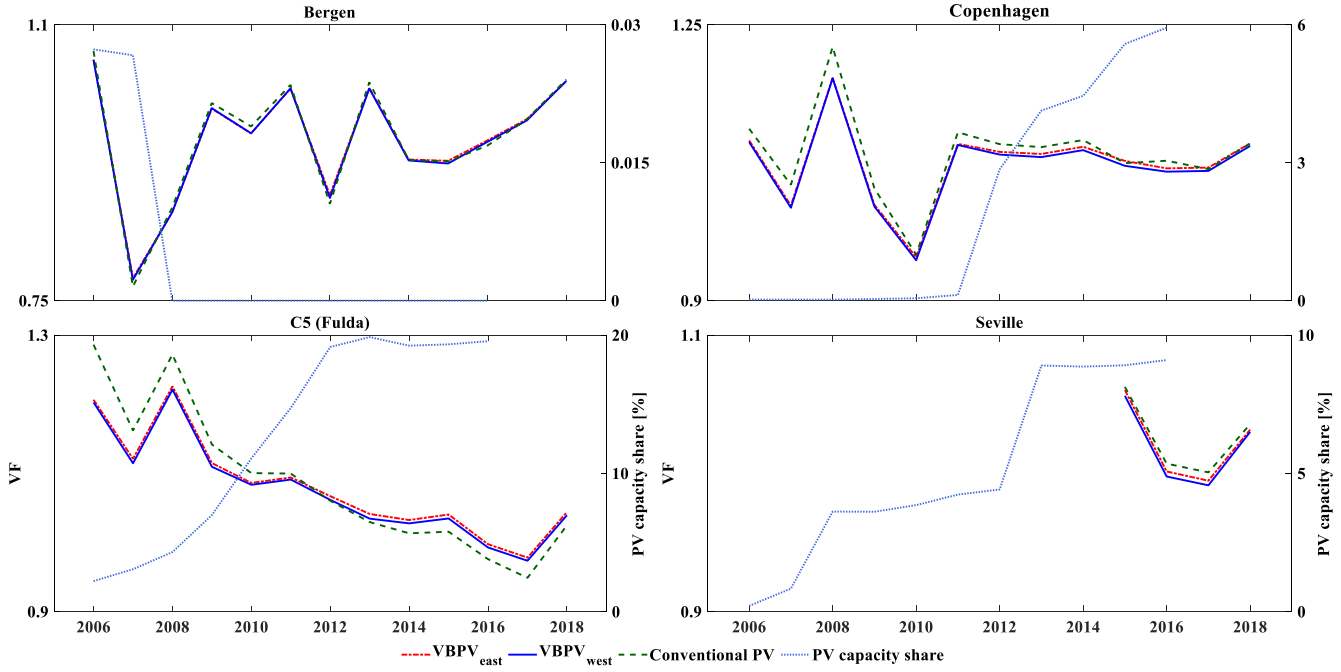

Fig. 8. Calculated market value factors (VF) and historical PV capacity shares. In markets with almost no PV capacity (Bergen, Norway), all PV technologies achieved nearly the same VF. In contrast, in Germany, a country with a significant amount of installed PV capacity, VBPV reached higher VF from 2012 onwards.

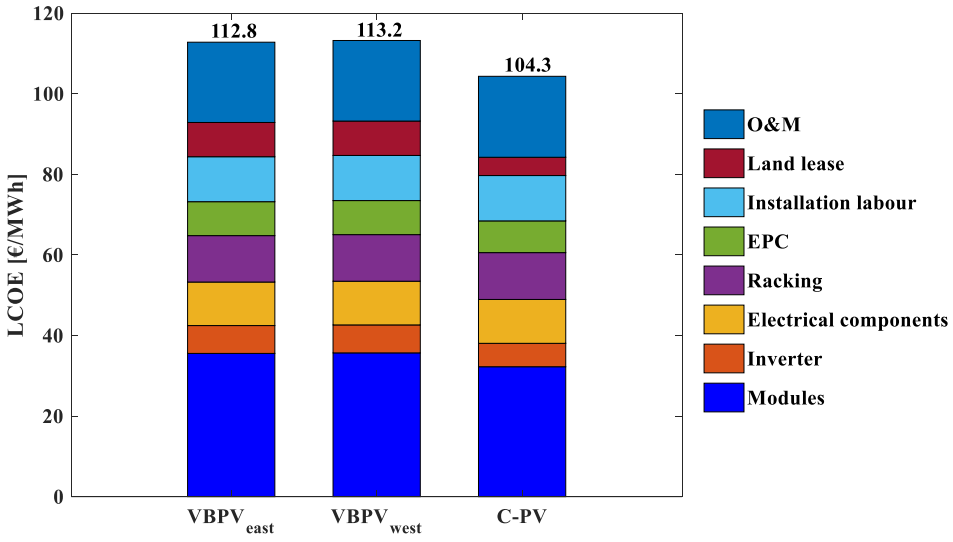

Fig. 9. Breakdown of the LCOE for C5 (Fulda), the central investigated German location. On the basis of the available cost data and simulated electricity generation, VBPV has about 8% higher LCOE values compared to C-PV.

The more expensive VBPV technology was not able to generate cost savings. This picture changed completely in the other two scenarios: In the second scenario, $VBPV_{east}$ accounted for almost 50% of the total installed PV capacity at the same investment and dropped to almost 0% capacity share at 5.3% higher investment. In the third scenario, when the most ambitious targets were to be achieved, $VBPV_{east}$ accounted for over 80% of total PV capacity at the same investment and fell to 13% at an investment ratio of 1.245.

In the middle of Fig. 12, the reduction in capacity (measured in GW) of the electrical storage devices is shown in comparison to a system without the possibility to build VBPV This illustration shows that with the construction of VBPV the required storage capacity could be reduced significantly. With the same investment, 3.6% and 11.3% less storage capacity was required in the second and third scenarios, respectively.

Finally, Fig. 12 (below) shows the overall reduction in system costs. For the same investment, the costs of the entire electricity system were reduced by 0.08% and 1% in the second and third scenarios. These results show that $VBPV_{east}$ can help to achieve ambitious climate targets at lower costs and should play a prominent role in future low-carbon electricity systems.

3.4.1. *The marginal system cost reduction*

Since the reduction in system costs is not proportional to the installed capacity of $VBPV_{east}$, the total system costs and the marginal system cost reduction as a function of the installed capacity of $VBPV_{east}$ are shown in Fig. 13 in the third scenario. The share of investment was kept constant (1.067). This ratio corresponded to about 11% more expensive bifacial modules compared to monofacial modules [41]. The cost-reducing effect of $VBPV_{east}$ on the overall system was determined

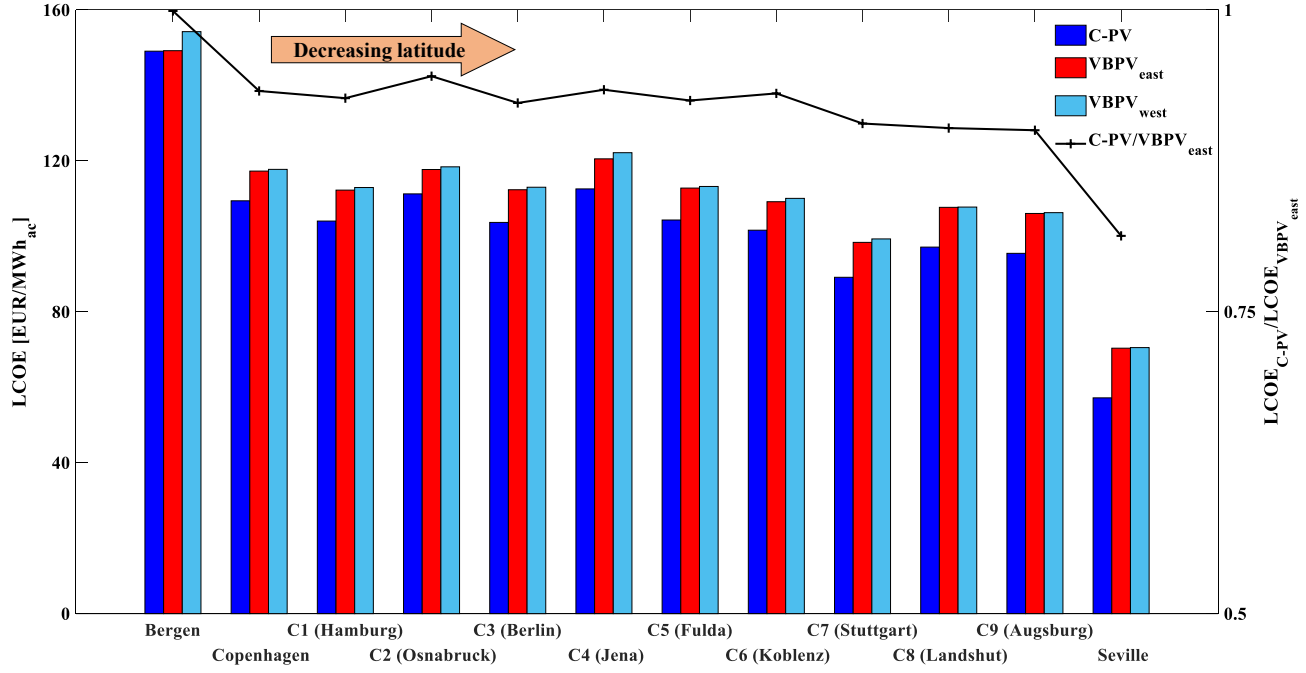

Fig. 10. Calculated LCOE in the investigated sites. The right Y-axis shows the ratio of the LCOE of C-PV and $VBPV_{east}$. Assuming the same investment and land costs, $VBPV_{east}$ achieves LCOE parity with C-PV only in Bergen.

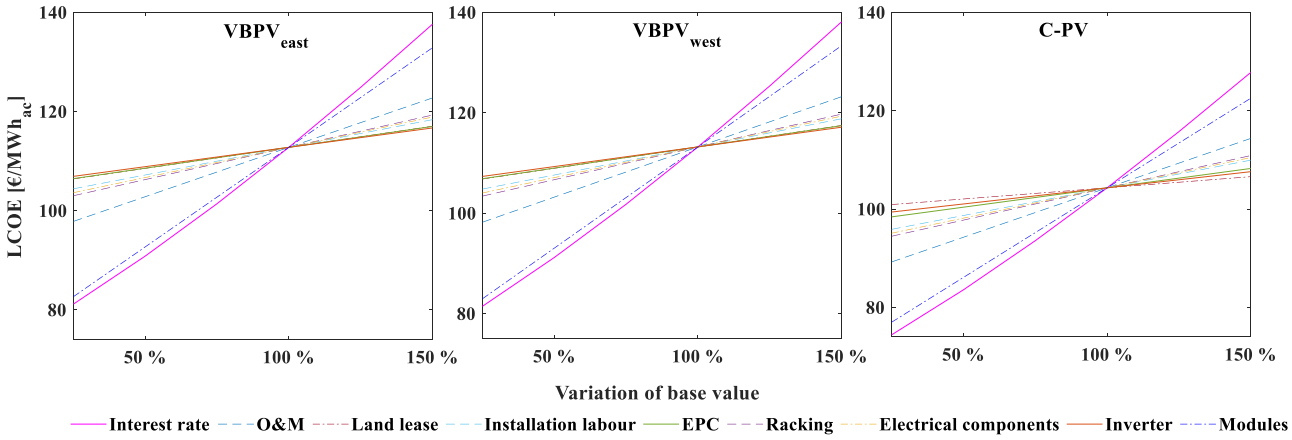

Fig. 11. Sensitivity analysis of the LCOE for the site C5 (Fulda). The interest rate represents the greatest leverage for reducing the LCOE.

Table 4
Definition of scenarios for the macroeconomic electricity system perspective.

	Scenario 1	Scenario 2	Scenario 3
Minimum share of renewable electricity (RE) generation	50%	70%	90%
Minimum CO_2 emission reduction compared to 1990	50%	70%	90%

by a gradual reduction of the capacity-related upper bound from 83.75 GW to 1 GW, whereby the 83.75 GW corresponded to the unrestricted installed $VBPV_{east}$ capacity in the third scenario. The marginal system cost reduction (right Y-axis) corresponds to the first derivation of the total system costs (left Y-axis). It can be clearly seen that the marginal system cost reduction decreases with increasing installed capacity. This effect is known as the *Law of diminishing marginal utility* and is a concept originally described in economics, but which is also observed in many other areas, including energy supply systems [45]. In a system with cardinal utility characteristics, this law states that the first quantity of a good or service generates more utility than the subsequent quantities. In the context of this work, this means that the first GW of $VBPV_{east}$ capacity generates more system cost savings than subsequent GW. This is a consequence of the merit order, which is a step function that describes the marginal costs of electricity generation and the total generation capacity with "steps" of varying height and width. If $VBPV_{east}$ is chosen by the cost-minimizing E2M2, then the most expensive generators are replaced first, the second most expensive generators are displaced second, and so on.

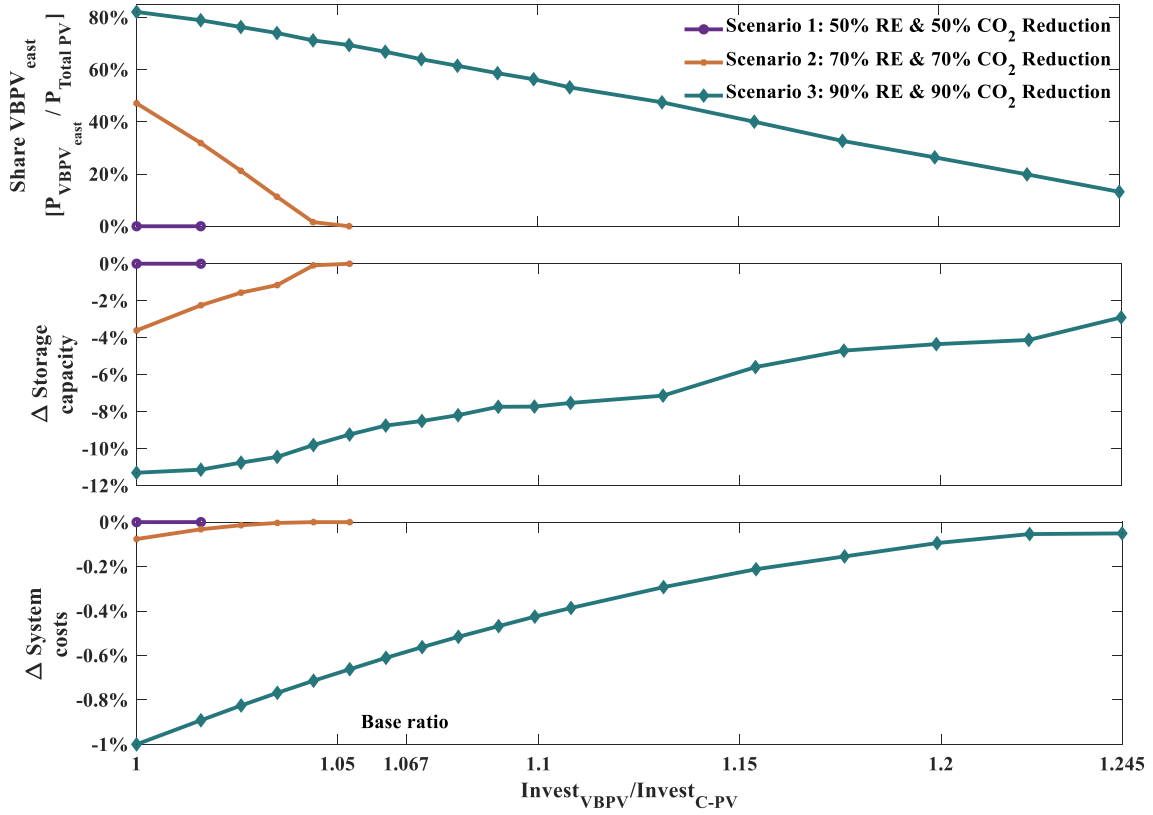

Fig. 12. Results from E2M2: Share of $VBPV_{east}$ in total installed PV capacity (above); reduction of required storage capacity (middle) and reduction of overall system costs compared to a system without VBPV (bottom). The Δ-values refer to a system without the possibility to build VBPV (cet. par.). The basic investment ratio was 1.067.

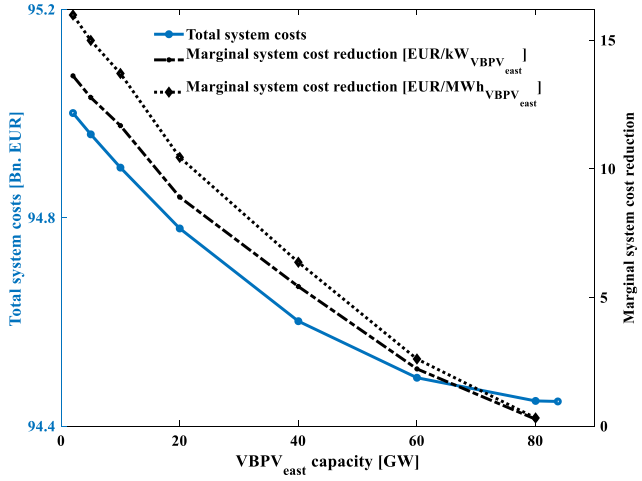

Fig. 13. Total annual cost of the system and marginal system cost reduction in the third scenario. According to the Law of diminishing marginal utility, the marginal system cost reduction decreases as the capacity of $VBPV_{east}$ increases.

3.5. Comparison of business and electricity system perspective

Based on previous analyses, this section brings together the economic and electricity system perspectives. The aim is to investigate how the system cost reduction and the economic viability of VBPV are related to each other. For this purpose, the net present value in the first year of operation ($NPV_{1st\ year}$) of C-PV and $VBPV_{east}$ was calculated for three German locations as well as for three historical years and the corresponding market prices. Table 5 shows the selected sites and the years under consideration.

Hence, the $NPV_{1st\ year}$ was calculated for 18 selected cases (2 PV technologies × 3 years × 3 locations). The $NPV_{1st\ year}$ expresses whether a PV power plant would have covered its annual costs in the first year of operation. Degradation effects of the PV modules in the first year were neglected. Equation (3) shows the applied definition of the $NPV_{1st\ year}$. An interest rate of 5% was used for the annualization of the investment.

$$NPV_{1^{st}\ year} = Market\ \ revenues_{1^{st}\ year} - \left(O\&M\ \ costs_{1^{st}\ year} + Annualized\ \ investment\right) \quad (3)$$

Fig. 14 (left) shows the $NPV_{1st\ year}$ in EUR/MWh_{ac}, while Fig. 14 (right) shows the $NPV_{1st\ year}$ in EUR/kW_{dc}. The grey rectangles also show the range of marginal system cost reduction, based on Fig. 13. The results show that there was no case with a positive $NPV_{1st\ year}$ - all sites and both PV technologies generated less market revenue than their annual costs. This finding is consistent with the fact that PV power plants in Germany still rely on some kind of support mechanism (i.e. FiT or market premium, depending on the size of the PV power plant [46]). Second, the $NPV_{1st\ year}$ of C-PV was in all cases higher than that of $VBPV_{east}$, while the gap of both technologies ($gap = NPV_{1^{st}\ year,C-PV} - NPV_{1^{st}\ year,VBPV_{east}}$) decreased steadily from 2008 to 2016. For example, the $NPV_{1st\ year}$ per MWh_{ac} in Stuttgart in 2008 was more than 4.13 times higher than the $NPV_{1st\ year}$ of $VBPV_{east}$, while in 2016 the same ratio was only 1.14. The situation did not change when considering the $NPV_{1st\ year}$ per kW_{dc}: The ratios in 2008 and 2016 were 4.08 and 1.13 respectively.

3.5.1. Consideration of cost-cutting effects in future support schemes

Since $VBPV_{east}$ had a cost-reducing effect on the German electricity system, but at the same time was less economically viable than C-PV, it seems sensible to introduce adapted support mechanisms in the medium term to facilitate the market entry of VBPV. Although the EEG 2017 (German Renewable Energy Sources Act) offers the possibility of considering the integration costs of a technology ("…*to provide for additions or deductions from the award price which reflect the costs of the integration of the installation into the electricity system*…") [46], to the authors' knowledge there is currently no such application in relation to PV power plants. There are also no official calculation methods for quantifying the integration costs of a technology. The analyses from this work can serve as a basis for discussion of a holistic and applicable calculation method.

3.6. Uncertainty of results

In this section we discuss the uncertainty of the presented results.

3.6.1. Electricity generation

The simulation model for power generation is an in-house tool of the IER and its structure and functionality was presented in [23]. The validation of the tool is in progress and will be published in the near future. Recent unpublished results show that the model underestimates electricity generation by 5–10%, whereby the degree of cloudiness has a high influence on the accuracy of the simulation. The weather data used can be considered reliable.

3.6.2. Financial input parameters

Wherever possible, all financial parameters (e.g. investment of the technologies, historical electricity prices) were taken from reliable sources. Although real interest rates change with time, place and funding institution, the interest rate was set at a fixed value (i = 5%) for all calculations for reasons of comparability.

3.6.3. Macroeconomic electricity system perspective

The analyses of the German electricity supply were carried out to identify cost-minimizing solutions for different scenarios, using a "greenfield" approach. The results from such models are not intended to reflect "reality" but to show how a more cost-effective system can be achieved. It is not the concrete figures that are important, but the trends. It is therefore impossible to say how much costs VBPV would save in the German electricity system, but based on the results it can be said that under certain boundary conditions VBPV can reduce costs. Here we would like to quote William Hogan "*It is not the individual results of a model that are so important: it is the improved user appreciation of the policy problem that is the greatest contribution of modelling.*" [47].

Finally, Table 6 gives an overview of the key parameters that are assumed to have a significant influence on the results presented. The influence of the individual parameters should be examined more closely in future studies.

4. Conclusions

While monofacial photovoltaics account for the lion's share of the

Table 5
Selected cases for the comparison of the business and electricity system perspective.

German location		Year
C4 (Jena)	Minimum electricity generation from $VBPV_{east}$ & C-PV.	2008: maximum VF for $VBPV_{east}$ & C-PV.
C1 (Hamburg)	Median electricity generation from $VBPV_{east}$ & C-PV.	2012: median VF for $VBPV_{east}$ & C-PV.
C7 (Stuttgart)	Maximum electricity generation from $VBPV_{east}$ & C-PV.	2016: minimum VF for $VBPV_{east}$ & C-PV.

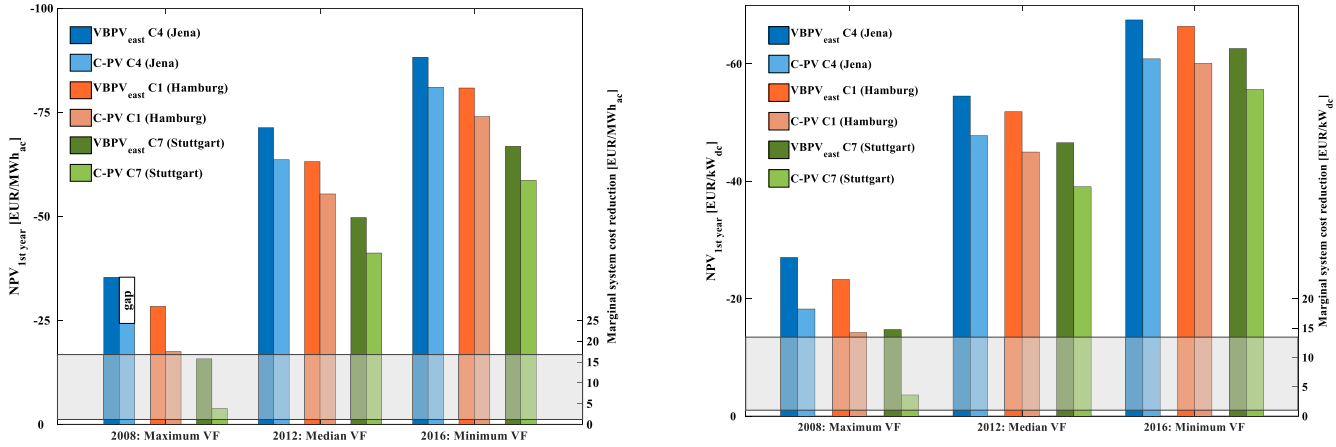

Fig. 14. The figure on the left shows the $NPV_{1st\ year}$ the power plants after the first year of operation in EUR/MWh_{ac} and the marginal system cost reduction that can be achieved. The right figure shows all values in EUR/kW_{dc}. The grey boxes show the achievable marginal system cost reduction, based on Fig. 13. C-PV always had a higher $NPV_{1st\ year}$ than $VBPV_{east}$, but the gap shrank over time.

capacity added worldwide, the importance of bifacial photovoltaics is growing rapidly. A special variant of bifacial systems are vertically installed module rows with a north-south axis (VBPV). This system design promises some advantages over conventional monofacial equator-oriented photovoltaic systems (C-PV). However, the current state of knowledge does not allow a comprehensive techno-economic analysis of VBPV compared to C-PV. In this paper we present a holistic analysis of VBPV with C-PV as a benchmark. The added value of this work helps to fill the knowledge gap in the techno-economic evaluation of VBPV, both from a business and macro-economic perspective. The results and findings of this work show that under certain conditions VBPV can offer significant advantages.

Electricity generation for VBPV and C-PV was simulated for twelve European sites. Two VBPV orientations were distinguished: either the more efficient front side was oriented to the west ($VBPV_{west}$) or to the east ($VBPV_{east}$). The results showed that both VBPV orientations generate slightly more electricity on an annual basis at a site latitude of more than approx. 50°. Investors and operators of PV systems in particular should therefore consider that VBPV can currently only achieve a higher energy yield in higher latitudes.

Seasonal differences were also found in the camel-shaped diurnal generation profile of VBPV. In locations with a rather humid climate and a high proportion of diffuse light, the two generation peaks were attenuated in autumn and winter. In contrast, in Seville, a site with a lot of direct light, the two generation peaks were clearly pronounced throughout the year. It is therefore important to note that the distinguishing feature of VBPV, namely increased electricity production in the mornings and afternoons, is attenuated in humid climates.

It was examined whether VBPV can achieve higher market revenues on day-ahead electricity markets. For this purpose, value factors (VF) of C-PV and VBPV were calculated for the investigated sites based on historical day-ahead market prices and simulated power generation. The most remarkable results were observed in the case of Germany, where both VBPV orientations have achieved higher VF than C-PV since 2012, while the VF of both PV technologies have declined. These results suggest that VBPV can achieve higher revenues than C-PV in markets with high PV penetration. This aspect is particularly important, because in the long-term renewable plants should be competitive without subsidies. Similarly, investors must recognize that further investment in C-PV in already saturated markets and expiring feed-in tariffs is no guarantee of profit.

To compare the impact of the site on electricity generation costs, the levelized costs of electricity (LCOE) were calculated. Due to the higher investments, VBPV had higher LCOE at all locations investigated. However, it is very likely that as the installed capacity of bifacial PV increases worldwide, costs of bifacial PV systems and their LCOE will decrease.

Finally, in order to achieve a sustainable, low-carbon and cost-effective European energy supply, renewable plants must not only be economical at the operational level, but their integration into the national electricity supply systems should incur as little additional system cost as possible. The cost reducing effects induced by VBPV in a national electricity system were examined using the case study of Germany. It was found that $VBPV_{east}$ can reduce overall system costs

Table 6
Decisive parameters to consider in future studies.

Parameter	In this work	Expected impact
Bifaciality	0.85	Since bifaciality is likely to increase over time, electricity generation and the profitability of VBPV may increase significantly.
Investment for mounting structures.	Equal for C-PV and VBPV.	VBPV systems must withstand higher wind loads, so the cost of VBPV mounting structures is likely to be higher in reality than for C-PV.
Installed PV capacity in Germany.	Status as of 31.12.2017 (Fig. 1).	When establishing a representative generation curve of C-PV technology for Germany, the capacity considered shall be updated. More installed C-PV capacity should increase the marginal system cost reduction induced by VBPV.
Dual use of the land used by VBPV.	No dual use considered.	Although VBPV has a much larger row spacing, the cost of leasing land could be lower compared to C-PV, because the space between the rows can be used for other purposes (e.g. agriculture, grazing).
Land lease	Same for all locations.	As the land rent can vary considerably even within one country, the calculated LCOE in this work most likely does not reflect the actual cost of the land.
Spatial resolution in E2M2.	Germany modelled as a single node.	The implementation of regional aspects (weather, grid capacities, electricity demand, installed C-PV capacity) would make it possible to determine preferred installation locations for VBPV.
Considered country in E2M2.	Germany.	In countries with little installed PV capacity, the cost reduction potentials in the electricity supply system could be lower.

and the need for electricity storage if high shares of renewable electricity and reduced CO_2 emissions are to be achieved, which is one of the objectives of the European Union for its future energy supply. At the same time, the comparison of the unsubsidized net present value in the first year of operation showed that VBPV is currently not able to compete with C-PV. Therefore, in the medium term, decision-makers should adapt support schemes in such a way that system cost cutting technologies can receive higher amounts of subsidies. This would help to reduce the overall costs of the European energy system transformation.

Data statement

The two models used for this work (simulation of the power generation of C-PV and VBPV and E2M2) cannot be shared due to their ongoing use in doctoral theses. All other data are freely available and were cited accordingly.

Funding

This work was supported by the German Federal Ministry of Education and Research (BMBF) and the German Federal Ministry for Economic Affairs and Energy (BMWi).

Appendix A

A.1. Glossary

See Table 7.

Table 7
Abbreviations.

Abbreviation	Full Term
CHP	Combined heat and power
C-PV	Conventional PV (monofacial, equator-oriented, optimally tilted according to [29])
DHI	Diffuse horizontal irradiance
DNI	Direct normal irradiance
E2M2	European electricity market model
EEG	Erneuerbare Energien Gesetz (German Renewable Energy Sources Act)
EG	Electricity generation
EPC	Engineering, procurement and construction
FiT	Feed-in-tariff
GAMS	General Algebraic Modeling System
LCOE	Levelized costs of electricity
MOE	Merit order effect
NOCT	Nominal operating cell temperature
O&M	Operation & maintenance
PV	Photovoltaics
RE	Renewably generated electricity
RET	Renewable energy technologies
TMY	Typical meteorological year
VF	Market value factor(s)

A.2. Technical and financial values for VBPV and C-PV

Where necessary, the US dollar was converted into euros at an average exchange rate over one year (June 2018 - June 2019) of 1.1423 USD/EUR [48] (see Table 8).

CRediT authorship contribution statement

Dimitrij Chudinzow: Supervision, Project administration, Conceptualization, Methodology, Writing - original draft, Data curation, Formal analysis, Visualization. **Sylvio Nagel:** Conceptualization, Methodology, Writing - original draft, Data curation, Formal analysis. **Joshua Güsewell:** Conceptualization, Methodology, Data curation, Formal analysis, Visualization. **Ludger Eltrop:** Writing - review & editing.

Declaration of competing interest

The authors declare that they have no known competing financial interests or personal relationships that could have appeared to influence this work.

Acknowledgement

The authors would like to thank Ms Irina Ochakovsky and Ms Audrey Dobbins for the linguistic corrections. Our thanks also go to the anonymous reviewers and editors for their constructive comments during the review process.

Table 8
Technical and financial values for VBPV and C-PV.

Parameter	Value	Reference
Annual degradation rate of both PV technologies	0.3%/year	[24]
Annual land lease	0.18 €/(m^2·year)	[49]
Annual O&M	0.0158 €/(W_{dc}·year)	[50]
EPC	13% of equipment costs	[41]
Installation labour	0.136 €/W_{dc}	[50]
Interest rate for LCOE analysis	5%	Own assumption
Inverter oversize for bifacial system	20% additional inverter capacity in relation to the total bifacial front side capacity.	[41]
Invest bifacial module	0.432 €/W_{dc}	[41]
Invest electrical components	0.131 €/W_{dc}	[50]
Invest inverter	0.07 €/W_{dc}	[50]
Invest monofacial module	0.389 €/W_{dc}	[41]
Invest racking	0.14 €/W_{dc}	[50]
Land area use C-PV	0.0198 m^2/W_{dc} (=1.98 ha/MW_{dc})	Own calculation
Land area use VBPV	0.0373 m^2/W_{dc} (=3.73 ha/MW_{dc})	Own calculation
Lifetime of all examined PV systems	30 years	[50]

A.3. Hourly-averaged specific electricity generation of all investigated sites in the four quarters of a year

See Fig. 15.

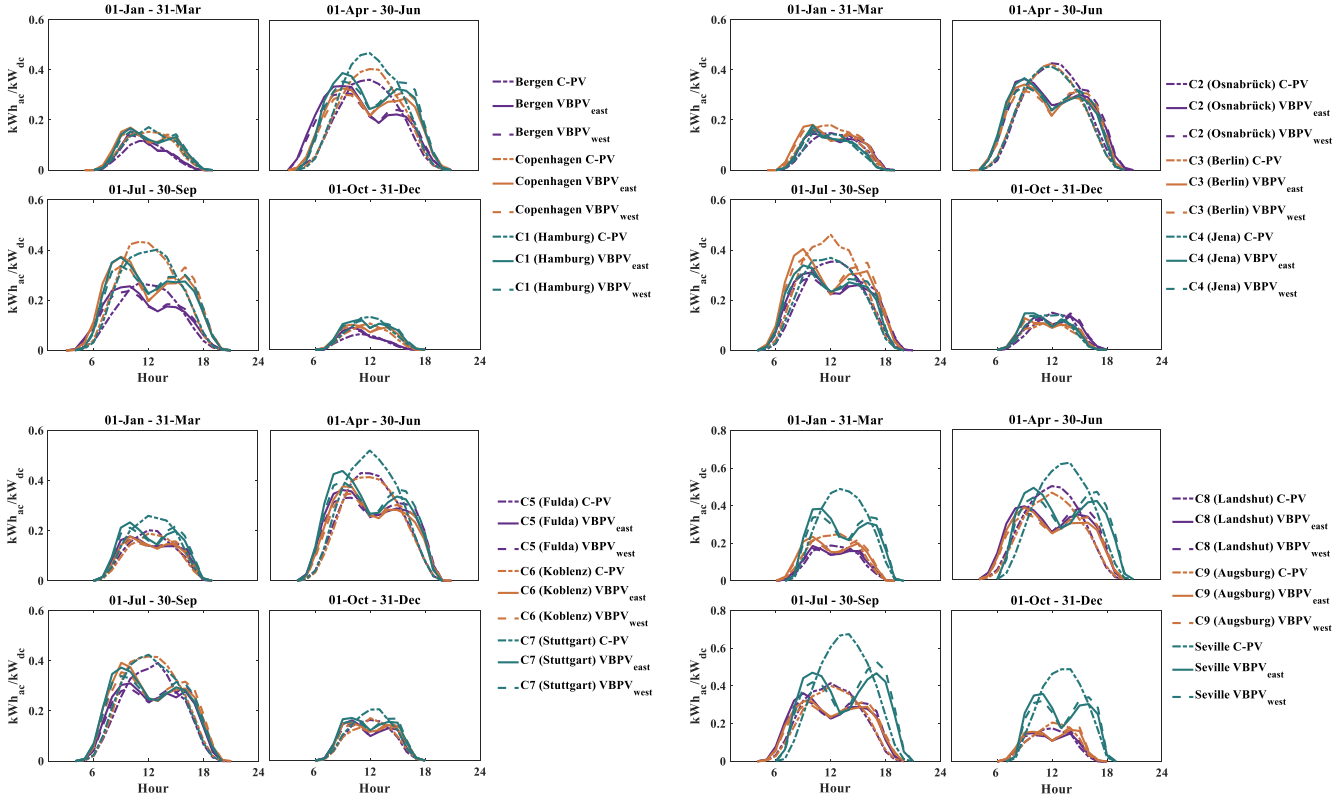

Fig. 15. Hourly-averaged specific electricity generation of all investigated sites in the four quarters of a year.

A.4. Calculated value factors for all investigated sites

See Fig. 16.

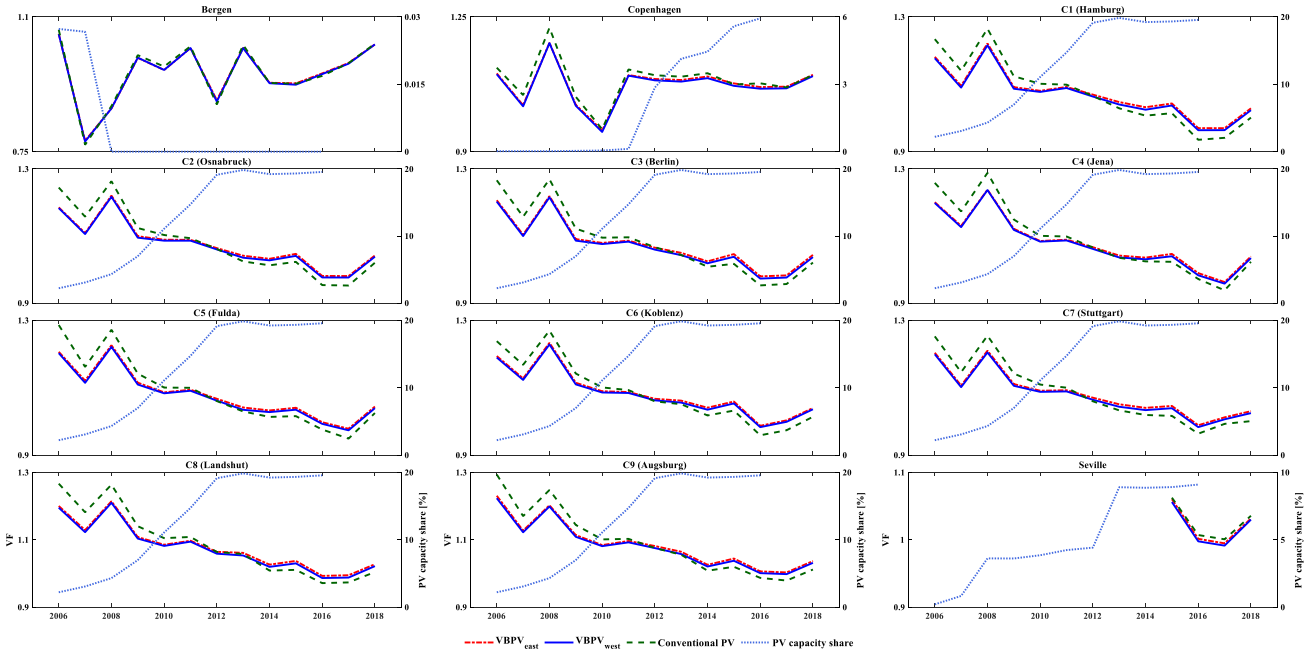

Fig. 16. Calculated market value factors (VF) and historical PV capacity shares for all sites. For improved readability, the limits of the Y-axes are different for each country.

A.5. Selected mathematical formulations in E2M2

1. Objective function

$\min C = \sum_{u \in U^{inv}} (C_u^{fix} + C_u^{grid}) + \sum_{u \in U} \sum_{t \in T} C_{u,t}^{var}$	[51]
$= \sum_{u \in U^{inv}} [P_u^{inv} \cdot (c_u^{inv} + c_u^{fixOaM} + c_u^{grid})] + \sum_{u \in U} \sum_{t \in T} [p_{u,t}^{gen} \cdot (c_{u,t}^{varOaM} + c_{u,t}^{fuel})]$	
C	Total system costs [€].
C_u^{fix}	Fixed costs of power plant u [€/MW].
$C_{u,t}^{var}$	Variable costs of power plant u [€/MWh].
C_u^{grid}	Grid expansion costs caused by power plant u [€].
c_u^{grid}	Specific costs of grid extension for integration of power plant u [€/MW]. The grid expansion costs for one additional MW of installed capacity of fluctuating renewable energies are determined by using the grid expansion costs calculated by Agora [35]. These were calculated in cost per energy unit [€/MWh] and for our purposes multiplied by the full-load hours of each technology to obtain the incremental cost per capacity [€/MW].
c_u^{fixOaM}	Specific fixed yearly operating and maintenance costs of power plant u [€/MW].
$c_{u,t}^{fuel}$	Specific fuel costs of power plant u [€/MWh].
c_u^{inv}	Specific capital costs of power plant u [€/MW].
$c_{u,t}^{varOaM}$	Specific variable operating and maintenance costs of power plant u [€/MWh].
P_u^{inv}	Capacity of invested power plant u [MW].
$p_{u,t}^{gen}$	Generated power of invested power plant u at time step t [MWh].
T	All time steps within scope.
t	Time step [1/h].
U	All power plants.
U^{inv}	Invested power plant.
u	Power plant.

2. Demand

$$\forall\, t \in T \bigwedge R \in U: \sum_{u \in U} (p_{u,t}^{gen} + p_{u,t}^{stor}) + p_t^{DSM} + p_t^{ImEx} - \sum_{r \in R} p_{r,t}^{curt} = p_t^{D}$$

R	All renewable power plants.
r	Renewable power plant.
$p_{u,t}^{stor}$	Delta of loading and unloading electricity storage u at time step t [MWh].
p_t^{DSM}	Delta of electricity used for demand side management at time step t [MWh].
$p_{r,t}^{curt}$	Amount of curtailed electricity at time step t from renewable power plant r that is not fed into the grid [MWh].
p_t^{ImEx}	Delta of electricity import and export at time step t [MWh].
p_t^{D}	Total demand of electricity at time step t [MWh],

3. Greenhouse Gas Emissions

$$\sum_{u \in U} \sum_{t \in T} \left(\frac{p_{u,t}^{gen}}{\eta_u} \cdot ghg_u \right) \leq GHG^{max}$$

η_u	Fuel conversion efficiency of power plant u [%].
ghg_u	Specific greenhouse gas emissions of used fuel of power plant u $[t_{CO_{2-eq}}/MWh_{fuel}]$.
GHG^{max}	Total maximum of permitted greenhouse gas emissions $[t_{CO_{2-eq}}]$.

4. Share of Renewables

$$\frac{\sum_{r \in U} \sum_{t \in T} (p_{r,t}^{gen} - p_{r,t}^{curt})}{\sum_{u \in U} \sum_{t \in T} p_{u,t}^{gen}} \geq RES^{min}$$

p_r^{gen}	Generated power of renewable power plant r at time step t [MWh].
RES^{min}	Minimal required renewable energy share [%].

A.6. Technical and financial inputs of fluctuating renewable energies in E2M2

See Table 9.

Table 9
Technical and financial inputs of fluctuating renewable energies in E2M2.

	Investment [€/kW_{el}]	Annual fixed costs [€/(kW_{el}·a)]	Costs for expansion of transmission/distribution grid [€/kW_{el}]	Full load hours [h/a]
Photovoltaic (C-PV)	1000	19	238/119	850
VBPV	Factor of C-PV	23	238/119	852_{east} 847_{west}
Wind onshore	1200	60	360/180	1750
Wind offshore	2800	112	2520/180	4000

Appendix B. Supplementary material

Supplementary data to this article can be found online at https://doi.org/10.1016/j.apenergy.2020.114782.

References

[1] European Commission. EU Energy in Figures: Statistical pocketbook 2018. [Online] Available: https://publications.europa.eu/en/publication-detail/-/publication/99fc30eb-c06d-11e8-9893-01aa75ed71a1/language-en/format-PDF/source-77059768. Accessed on: Feb. 13 2019.
[2] Agora Energiewende, Sandbag, editors. The European Power Sector in 2017: State of Affairs and Review of Current Developments.
[3] Jäger-Waldau A. PV Status Report 2018. [Online] Available: http://publications.jrc.ec.europa.eu/repository/bitstream/JRC113626/pv_status_report_2018_online.pdf. Accessed on: Mar. 12 2019.
[4] Hildebrandt H. 3 MWp vertical E-W oriented system in Germany. [Online] Available: http://bifipv-workshop.com/fileadmin/layout/images/Konstanz-2017/8_H._Hildebrand_NEXT_2_SUN_3MWp_vertican_E-W_oriented_system.pdf. Accessed on: Jan. 11 2019.
[5] Guo S, Walsh TM, Peters M. Vertically mounted bifacial photovoltaic modules: A global analysis. Energy 2013;61:447–54.
[6] Khan MR, Hanna A, Sun X, Alam MA. Vertical bifacial solar farms: physics, design, and global optimization. Available: http://arxiv.org/pdf/1704.08630.
[7] Appelbaum J. Bifacial photovoltaic panels field. Renewable Energy 2016;85:338–43.
[8] Tveten ÅG, Bolkesjø TF, Martinsen T, Hvarnes H. Solar feed-in tariffs and the merit order effect: A study of the German electricity market. Energy Policy 2013;61:761–70.
[9] Edenhofer O, Hirth L, Knopf B, Pahle M, Schlömer S, Schmid E, et al. On the economics of renewable energy sources. Energy Econ 2013;40:S12–23.
[10] Hirth L. The market value of variable renewables. Energy Econ 2013;38:218–36.
[11] Winkler J, Sensfuß F, Pudlik M. Analyse ausgewählter Einflussfaktoren auf den Marktwert Erneuerbarer Energien: Leitstudie Strommarkt. Arbeitspaket 2015;4.
[12] Fernahl A, Hartmann M, Lenck T, Federico T. Ermittlung des Marktwertes der deutschlandweiten Stromerzeugung aus regenerativen Kraftwerken: Studie für die vier deutschen Übertragungsnetzbetreiber im Auftrag der Amprion GmbH. Abschlusspräsentation. 2011.
[13] Hirth L. System-friendly renewables. [Online] Available: https://www.strommarkttreffen.org/1.1-2016-09-30-Hirth-System-friendly_renewables_Strommarkttreffen.pdf. Accessed on: Feb. 14 2019.
[14] Hartmann N. Role of storage technologies to integrate high shares of renewable electricity generation into the electricity system of Germany : simulation and optimization. 2013.
[15] Neuhoff K, May N, Richstein J. Anreize für die langfristige Integration von erneuerbaren Energien: Plädoyer für ein Marktwertmodell. DIW Wochenbericht, no. 42.2017, p. 929–952, https://www.diw.de/documents/publikationen/73/diw_01.c.567164.de/17-42-1.pdf, 2017.
[16] Fleischer B. The flexible use of bioenergy in the electricity market - A case study of Germany. Vienna, 2017.
[17] Sun N. Modellgestützte Untersuchung des Elektrizitätsmaktes: Kraftwerkseinsatzplanung und –investitionen. Dissertation, Institut für Energiewirtschaft und Rationelle Energieanwendung, Universität Stuttgart, Stuttgart; 2013.
[18] EEG-Anlagenstammdaten (master asset data). [Online] Available: https://www.netztransparenz.de/EEG/Anlagenstammdaten. Accessed on: May 01 2019.
[19] Mathworks, k-means description. [Online] Available: https://de.mathworks.com/help/stats/kmeans.html. Accessed on: May 02 2019.
[20] Open Power System Data: Time series. [Online] Available: https://data.open-power-system-data.org/time_series/2018-06-30. Accessed on: May 15 2019.
[21] ENTSO-E Transparency Platform. [Online] Available: https://transparency.entsoe.eu/transmission-domain/r2/dayAheadPrices/show. Accessed on: May 15 2019.
[22] JRC. Photovoltaic geographical information system. [Online] Available: http://re.jrc.ec.europa.eu/pvg_tools/en/tools.html. Accessed on: May 07 2019.
[23] Chudinzow D, Haas J, Díaz-Ferrán G, Moreno-Leiva S, Eltrop L. Simulating the energy yield of a bifacial photovoltaic power plant. Sol Energy 2019;183:812–22.
[24] Megacell. Datasheet BiSoN MBA-GG60 series 270-280Wp. [Online] Available: http://www.mega-group.it/wp-content/uploads/MBA-GG60-270_280B_rev3.pdf. Accessed on: Apr. 05 2018.
[25] ABB. ABB string inverters - TRIO-20.0/27.6-TL-OUTD 20 to 27.6 kW. [Online] Available: http://search-ext.abb.com/library/Download.aspx?DocumentID=BCD.00379&LanguageCode=en&DocumentPartId=&Action=Launch. Accessed on: Apr. 29 2019.
[26] PVsyst. Albedo coefficient. [Online] Available: http://files.pvsyst.com/help/

albedo.htm. Accessed on: Oct. 08 2018.
[27] Roekens-Guibert H. Next Generation Tedlar* PVF Film for Photovoltaic Module Backsheets. [Online] Available: http://www.chipscalereview.com/legacy/www.ea-nrw.de/pv/workshop2007/5Roekens_PVF.pdf. Accessed on: May 01 2019.
[28] Longi. Longi LR6-60-280M Datasheet. [Online] Available: https://www.solarsystems.pro/images/download/longiSolar/LR6-60_ENG.pdf. Accessed on: Mar. 19 2019.
[29] Jacobson MZ, Jadhav V. World estimates of PV optimal tilt angles and ratios of sunlight incident upon tilted and tracked PV panels relative to horizontal panels. Sol Energy 2018;169:55–66.
[30] Hirth L. The benefits of flexibility: The value of wind energy with hydropower. Appl Energy 2016;181:210–23.
[31] Open Power Systems Data: National generation capacity. [Online] Available: https://data.open-power-system-data.org/national_generation_capacity/. Accessed on: Jun. 06 2019.
[32] Renewable energy production in Norway. [Online] Available: https://www.regjeringen.no/en/topics/energy/renewable-energy/renewable-energy-production-in-norway/id2343462/. Accessed on: May 15 2019.
[33] APX Power Spot Exchange. APX Power NL Daylight saving time. [Online] Available: https://www.apxgroup.com/wp-content/uploads/APX-Power-NL-Exchange-Notice-50-long-clock-change-2015.pdf. Accessed on: Sep. 26 2019.
[34] Kost C, Shammugam S, Jülch V, Nguyen H-T, Schlegl T. Levelized cost of electricity renewable energy technologies. [Online] Available: https://www.ise.fraunhofer.de/content/dam/ise/en/documents/publications/studies/EN2018_Fraunhofer-ISE_LCOE_Renewable_Energy_Technologies.pdf. Accessed on: Jun. 27 2019.
[35] Fürstenwerth D, Pescia D, Litz P. The integration costs of wind and solar power: An overview of the debate on the effects of adding wind and solar photovoltaic into power systems; Dec. 2015.
[36] Hundt M, Barth R, Sun N, Brand H, Voß A. Herausforderungen eines Elektrizitätsversorgungssystems mit hohen Anteilen erneuerbarer Energien. IER - Institut für Energiewirtschaft und Rationelle Energieanwendung, Universität Stuttgart, Stuttgart; 2010.
[37] Umweltbundesamt. Entwicklung des Stromverbrauchs nach Sektoren (Development of electricity consumption by sector). [Online] Available: https://www.umweltbundesamt.de/daten/energie/stromverbrauch. Accessed on: Jan. 19 2020.
[38] Strogies M, Gniffke P. Berichterstattung unter der Klimarahmenkonvention der Vereinten Nationen und dem Kyoto-Protokoll 2017: Nationaler Inventarbericht zum Deutschen Treibhausgasinventar 1990 – 2015. Umweltbundesamt - UNFCCC-Submission, Dessau-Roßlau; 2017.
[39] Molin E, Stridh B, Molin A, Wackelgard E. Experimental yield study of bifacial PV modules in nordic conditions. IEEE J Photovolt 2018;8(6):1457–63.
[40] Shoukry I, Libal J, Kopecek R, Wefringhaus E, Werner J. Modelling of bifacial gain for stand-alone and in-field installed bifacial PV modules. Energy Procedia 2016;92:600–8.
[41] Rodríguez-Gallegos CD, Bieri M, Gandhi O, Singh JP, Reindl T, Panda SK. Monofacial vs bifacial Si-based PV modules: which one is more cost-effective? Sol Energy 2018;176:412–38.
[42] Lichner C. Next2Sun finanziert dritten bifazialen Solarpark über Energiegenossenschaft. [Online] Available: https://www.pv-magazine.de/2019/03/08/next2sun-finanziert-dritten-bifazialen-solarpark-ueber-energiegenossenschaft/. Accessed on: Jun. 27 2019.
[43] "Eine Insel mit zwei Bergen," Photon, https://next2sun.com/wp-content/uploads/PHOTON-Artikel.pdf, 2017.
[44] Baubeginn für Agri-PV-Anlage. [Online] Available: https://www.iwr.de/ticker/bifaciale-solaranlagen-baubeginn-fuer-agri-pv-anlage-artikel1892. Accessed on: Oct. 02 2019.
[45] Olson A, Jones R. Chasing grid parity: understanding the dynamic value of renewable energy. Electricity J. 2012;25(3): 17–27, http://www.sciencedirect.com/science/article/pii/S1040619012000541.
[46] Federal Ministry For Economic Affairs And Energy. Renewable Energy Sources Act (EEG 2017). [Online] Available: https://www.bmwi.de/Redaktion/EN/Downloads/renewable-energy-sources-act-2017.pdf%3F_blob%3DpublicationFile%26v%3D3. Accessed on: Sep. 23 2019.
[47] Hogan W. Energy modeling: building understanding for better use. In: Presented at the second lawrence symposium on systems and decision sciences, Berkeley, California; 1979.
[48] European Central Bank. ECB euro reference exchange rate. [Online] Available: https://www.ecb.europa.eu/stats/policy_and_exchange_rates/euro_reference_exchange_rates/html/eurofxref-graph-usd.en.html. Accessed on: Jun. 27 2019.
[49] Leipe F, Zill T. Ein Leitfaden für Kommunen: Solarparks auf Brachflächen in Thüringen. [Online] Available: http://www.thega.de/fileadmin/thega/pdf/projekte/solarparks/Leitfaden_Solarparks_gesamt.pdf. Accessed on: Jun. 07 2019.
[50] Fu R, Feldman D, Margolis R. U.S. Solar Photovoltaic System Cost Benchmark: Q1 2018. [Online] Available: https://www.nrel.gov/docs/fy19osti/72399.pdf. Accessed on: Feb. 13 2019.
[51] Fleischer B. Systemeffekte von Bioenergie in der Elektrizitäts- und Fernwärmewirtschaft - Eine modellgestützte Analyse langfristiger Energiewendeszenarien in Deutschland (unpublished PhD thesis); 2020.

5 Summary & conclusions

Against the background of anthropogenic climate change, renewable energies are playing an increasingly important role worldwide in reducing greenhouse gas emissions. Among the renewable energies, photovoltaics (PV) represent a key technology in numerous national transformation strategies for a sustainable energy supply. Among the different technological variants of PV, bifacial PV (B-PV) is a variant that has been little used until recent years, but which has several benefits over conventional, monofacial PV (C-PV). Compared to C-PV, B-PV offers the advantage that the irradiation hitting the back of the device can also be converted into electricity. On the one hand, this makes it possible to significantly increase the energy yield and reduce electricity generation costs. On the other hand, vertically installed bifacial PV modules with the sides facing east and west (VBPV) can be used to create a diurnal generation profile complementary to that of C-PV. This may be of particular importance for national power supply systems, as the complementary generation profile could reduce the integration costs of PV. The present work is located in this content nexus and the overall objective is to deepen the understanding of *how the energetic and economic advantages of bifacial PV systems can be exploited best* and to quantify these. At the beginning of the analyses it became apparent that there was no adequate energy yield model available for bifacial PV systems, which is indispensable for the analysis of the objective set. Consequently, there were three subordinate objectives in total. In the following, the analyses and findings for each objective are summarized and further research needs are outlined.

5.1 Development of an energy yield model for bifacial PV systems

For bifacial PV systems the adequate calculation of the absorption of ground-reflected irradiance (GRI) is of particular importance, because this irradiance contribution allows to significantly increase the energy yield. Due to the market dominance of monofacial PV systems for decades, only a few simulation tools for bifacial PV systems were available at the beginning of this work, so the know-how in this area was still limited.

In the first step, existing modelling approaches were reviewed, potential for improvement identified and implemented in a newly developed energy yield model. Compared to the status quo, the new model features, among other things, a three-dimensional representation of the PV field, a three-dimensional calculation of view factors when calculating GRI and a holistic treatment of all module rows. The model is also able to consider both non-tracking and single axis tracking PV systems with a north-south axis or an east-west axis. Using the new model, the influence of various parameters (shadow cast, reflectivity of the soil, “edge effects”,

seasonal course of the irradiation contributions) on the amount of irradiation absorbed could be investigated and quantified. For example, it has been shown that in a location such as San Felipe (Chile) with a very high proportion of direct irradiance, the presence of ground shadows reduces the annual energy yield by almost 4 %. This shows that the yield-reducing effect of ground shadows should be captured in sufficient detail in order to avoid overpredictions of the energy yield.

Based on a Swiss bifacial PV test site, the developed model was validated. It was shown that the angle-dependent **absorption of irradiation** on the front side is well represented by the simulation model. Only at a tilt angle of 90° do larger deviations occur. The angle-dependent **electricity generation** (front + rear side) is also well captured by the model, with larger deviations occurring at a tilt angle of 0° (module is parallel to the ground). At cloudy weather, the model tends to overestimate the electricity generation by approx. 5 %, at sunnier weather the electricity generation is underpredicted by 12 % on average. The highest underprediction of generated electricity was observed at a tilt angle of 0° with a 20 % deviation.

Also, the model was part of an international benchmark for bifacial PV simulation models conducted by the IEA in the year 2019. It has been shown that the variation of the simulation results of the 13 models analysed significantly depends on the plant design, location and weather conditions. The simulated energy yields of the model presented here fit in well with the results of the other models, although depending on the scenario, the model tends to underestimate the frontal energy yield. This could be due to the finite and relatively small size of the view fields and the approach used to take diffuse irradiation into account (isotropic sky diffuse model), which presumably underestimates the absorbed diffuse irradiation.

Recommendations for further research

The further development of energy yield models for bifacial PV systems will remain an important issue for industry and research for many years to come. Based on the experiences with model development and model application, the following key aspects should be considered in the future:

- For a more precise calculation of GRI it should be taken into account that bifacial modules are semi-opaque and scatter and transmit part of the incident light.
- A three-dimensional representation of further components (structure, inverter, torque tube in the case of tracked systems) and the consideration of these would lead to a more precise calculation of absorbed irradiation. But the computational effort has to be kept within a reasonable range.

- Ray tracing methods allow a more precise tracking of the ray path of light, but is also much more computationally intensive. A hybrid approach using view factors and ray tracing could combine the advantages of both methods and thus lead to more accurate results.

5.2 Improving the techno-economic performance of bifacial PV systems

The main advantage of bifacial PV power plants compared to C-PV is the ability to use irradiation on both sides of a module, thereby increasing the energy yield. In contrast to C-PV, the energy yield of B-PV depends to a greater extent on the field design. Installation parameters such as row spacing, module elevation, tilt angle (in the case of fixed-tilt systems, FT) and the reflectivity of the ground have a significant impact on the energy yield. Depending on whether the PV system has a fixed tilt or is uniaxially tracked, different parameters must be taken into account in order to achieve the lowest possible levelized cost of electricity (LCOE). A distinction was made between two variants of the tracked system: the module rows of a system with an east-west axis follow the elevation angle of the sun and those of a system with a north-south axis follow the azimuth angle of the sun, in this work both systems were called ”elevation-tracked” (ET) and ”azimuth-tracked” (AT).

The investigation of the annual energy yield and LCOE was carried out with the developed energy yield model for eight European cities, with Seville (Spain) being the southernmost and Bergen (Norway) the northernmost investigated city.

It has been found that AT has the highest energy yields at all sites, followed by ET and FT. By doubling the row distance from 5 m to 10 m and increasing the module elevation from 0.75 m to 1.5 m, FT can achieve an additional energy yield of approx. 5 % at all locations, whereby the additional energy yield decreases with decreasing latitude. With ET and AT, additional yields of up to 6 % can be achieved by simultaneously increasing the row spacing and module elevation. In the case of ET, the additional energy gain due to a larger row spacing decreases with decreasing latitude. In the case of FT, it was shown that if the tilt angle is chosen 5° smaller than the recommended latitude-dependent tilt angle for C-PV, the energy yield could be increased at all locations.

The most effective measure to increase the energy yield, which is associated with additional investments, is an enhancement of the soil reflectivity through the use of white gravel or white foil. This can increase the energy yield at all locations and for all plant designs by 8 % - 20 %.

The LCOE analysis showed that FT achieves the lowest LCOE in the six northernmost locations, followed by AT and ET. If the reflectivity of the soil is not increased and corresponds to that of grass, almost any change in installation parameters for FT leads to higher LCOE. However, if the soil is lightened, several combined measures will result in lower LCOE than in

the base configuration. Similar observations were made for ET and AT: A brightening of the soil in combination with different installation parameters can lead to a reduction in LCOE.

It was also found that if the row spacing is increased (leading to more land demand and higher land lease), the relative increase in LCOE of FT and ET is higher at low latitudes than at high latitudes. This leads to the conclusion that an investment in certain field configurations is more likely to pay off in higher latitudes i.e. less sunny locations. This was not found to be the case for AT.

Furthermore, it was calculated how expensive soil brightening measures may be at maximum in order not to increase the LCOE compared to the base configuration with the soil surface grass. It has been shown that constant LCOE is easier to achieve the smaller the row spacing and the higher the reflectivity of the brightened soil. Here it turned out that the additional investment in field configurations with a larger land requirement for all three investigated plant designs would be more economical at higher latitudes.

In this work, much emphasis was placed on investigating the influence of the location on the energy yield and the LCOE. To verify these results, the simulated annual energy yields were compared with those of another simulation model that has been developed and established in the meantime. The System Advisor Model, which is able to simulate bifacial PV systems since 2018, was used as a benchmark. It was found that the trend in the site-specific energy yield is determined by both models in a similar way, with the ratio of model results ranging from 85 % for the fixed-tilt design (FT) in Bergen to 108 % for the azimuth-tracking design (AT) in Stuttgart.

Recommendations for further research

- In the central and northern European regions, two-axis tracking monofacial PV systems are nowadays usually not economical. It seems reasonable to assume that this could change through the use of bifacial PV modules. Consequently, the economic viability of two-axis tracked bifacial PV systems should be investigated.

5.3 Analysis of vertical bifacial PV systems

Thanks to the two diurnal generation peaks, vertical bifacial photovoltaic power plants (VBPV) with a north-south axis represent an option to meet the challenges of a mismatch between electricity demand and the generation profile of C-PV. Despite this promising characteristic, it is hardly possible to assess the technical and economic properties of VBPV on the basis of existing studies. The added value of this work helps to fill the knowledge gap in the techno-economic evaluation of VBPV, both from a business perspective and an electricity

system perspective. The results and findings of this work show that under certain conditions VBPV can offer significant advantages.

Electricity generation for VBPV and C-PV was simulated for twelve European sites. Two VBPV orientations were distinguished: either the more efficient front side was oriented to the west ($VBPV_{west}$) or to the east ($VBPV_{east}$). The results showed that both VBPV orientations generate slightly more electricity on an annual basis at a site latitude of more than approx. 50°. Investors and operators of PV systems in particular should therefore consider that VBPV can currently only achieve a higher energy yield in higher latitudes.

Seasonal differences were also found in the camel-shaped diurnal generation profile of VBPV. In locations with a rather humid climate and a high proportion of diffuse light, the two generation peaks were attenuated in autumn and winter. In contrast, in Seville (Spain), a site with a lot of direct light, the two generation peaks were clearly pronounced throughout the year. It is therefore important to note that the distinguishing feature of VBPV, namely increased electricity production in the mornings and afternoons, is attenuated in humid climates.

It was examined whether VBPV can achieve higher market revenues on day-ahead electricity markets. For this purpose, value factors (VF) of C-PV and VBPV were calculated for the investigated sites based on historical day-ahead market prices and simulated power generation. The most remarkable results were observed in the case of Germany, where both VBPV orientations have achieved higher VF than C-PV since 2012, while the VF of both PV technologies have declined. The VF corresponding to this tipping point was 1.06. These results suggest that VBPV can achieve higher revenues than C-PV in markets with high PV penetration. This aspect is particularly important, because in the long-term renewable plants should be competitive without subsidies. Similarly, investors must recognize that further investment in C-PV in already saturated markets and expiring feed-in tariffs is no guarantee of profit.

To compare the impact of the site on electricity generation costs, the levelized costs of electricity (LCOE) were calculated. Due to the higher investments, VBPV had higher LCOE at all locations investigated. However, it is very likely that as the production capacities and installed capacity of bifacial PV systems increase worldwide, the costs of bifacial PV systems and their LCOE will decrease due to competition and learning curves.

Finally, in order to achieve a sustainable, low-carbon and cost-effective European power supply, renewable plants must not only be economical at the operational level, but their integration into the national electricity supply systems should incur as little integration costs as possible. The cost reducing effects induced by VBPV in a national electricity system were

examined with the case study of Germany using the cost-minimizing electricity market model E2M2. It was found that $VBPV_{east}$ can reduce overall system costs and the need for electricity storage if high shares of renewable electricity and reduced $CO_{2\text{-eq}}$ emissions are to be achieved, which is one of the objectives of the European Union for its future energy supply. $VBPV_{west}$ was not built by the model in any of the investigated scenarios. At the same time, the comparison of the unsubsidized net present value in the first year of operation showed that VBPV is currently not able to compete with C-PV, but the gap has been decreasing steadily since 2008.

Recommendations for further research

- The bifaciality ($\eta_{el,\ rear}/\eta_{el,\ front}$) is a decisive parameter for the presented results. Since the bifaciality of new module types is likely to increase, electricity generation, profitability and integration costs of VBPV may improve significantly. This should be investigated in the near future.
- Although VBPV has a much larger row spacing, the cost of leasing land could be lower compared to C-PV, because the space between the rows can be used for other purposes (e.g. agriculture, grazing). This should be investigated in the near future.
- The implementation of regional aspects (weather, grid capacities, electricity demand, installed C-PV capacity) would make it possible to determine preferred installation locations for VBPV.
- In countries with little installed C-PV capacity, the cost reduction potentials in the electricity supply system could be lower; this should be closely examined.

References

References

[1] L. Podlowski, *Bifacial PV Technology - Ready for Mass Deployment.* [Online]. Available: https://www.pi-berlin.com/wp-content/uploads/2019/10/White-Paper-Bifacial-PV-Technology-PI-Berlin.pdf (accessed: Apr. 17 2020).

[2] T. Dullweber *et al.,* "PERC+: industrial PERC solar cells with rear Al grid enabling bifaciality and reduced Al paste consumption," *Prog. Photovolt: Res. Appl.*, vol. 24, no. 12, pp. 1487–1498, 2016, doi: 10.1002/pip.2712.

[3] A. Cuevas, "The Early History of Bifacial Solar Cells," in *20th European Photovoltaic Solar Energy Conference : proceedings of the international conference held in Barcelona, Spain, 6 - 10 June 2005.* Accessed: Aug. 18 2020. [Online]. Available: https://www.tib.eu/en/search/id/BLCP%3ACN060220023/The-Early-History-of-Bifacial-Solar-Cells/

[4] A. Cuevas, "50 Per cent more output power from an albedo-collecting flat panel using bifacial solar cells," *Solar Energy*, vol. 29, no. 5, pp. 419–420, 1982, doi: 10.1016/0038-092X(82)90078-0.

[5] M. Maisch, "WoodMac: Bifacial module capacity will exceed 21 GW by 2024," *pv magazine*, 2019. [Online]. Available: https://www.pv-magazine.com/2019/09/26/woodmac-bifacial-module-capacity-will-exceed-21-gw-by-2024/

[6] *International Technology Roadmap for Photovoltaic (ITRPV): Results 2017 including maturity report 2018.* [Online]. Available: https://pv.vdma.org/documents/105945/26776337/ITRPV%20Ninth%20Edition%202018%20including%20maturity%20report%20201809 04_1536055215523.pdf/a907157c-a241-eec0-310d-fd76f1685b2a (accessed: Sep. 30 2019).

[7] L. Hirth, "Market value of solar power: Is photovoltaics cost-competitive?," *IET Renewable Power Generation*, vol. 9, no. 1, pp. 37–45, 2015, doi: 10.1049/iet-rpg.2014.0101.

[8] *PVSyst - Release notes.* [Online]. Available: https://www.pvsyst.com/release-notes-6-6x/ (accessed: Apr. 17 2020).

[9] *SAM - Release notes.* [Online]. Available: https://nrel.github.io/SAM/doc/releasenotes.html (accessed: Apr. 17 2020).

[10] S. Dubey, J. N. Sarvaiya, and B. Seshadri, "Temperature Dependent Photovoltaic (PV) Efficiency and Its Effect on PV Production in the World – A Review," *Energy Procedia*, vol. 33, pp. 311–321, 2013, doi: 10.1016/j.egypro.2013.05.072.

[11] *VDI-Wärmeatlas,* 11th ed. Berlin, Heidelberg: Springer, 2013.

[12] U. A. Yusufoglu *et al.,* "Simulation of Energy Production by Bifacial Modules with Revision of Ground Reflection," *Energy Procedia*, vol. 55, pp. 389–395, 2014, doi: 10.1016/j.egypro.2014.08.111.

[13] N. Lauzier, *MATLAB function that calculates view factors between two planar surfaces.* [Online]. Available: https://de.mathworks.com/matlabcentral/fileexchange/5664-view-factors (accessed: Jul. 14 2017).

[14] *CRediT (Contributor Roles Taxonomy) author statement.* [Online]. Available: https://www.elsevier.com/authors/journal-authors/policies-and-ethics/credit-author-statement (accessed: Apr. 24 2020).

[15] International Finance Corporation, *Utility-Scale Solar Photovoltaic Power Plants: A project developer's guide*.

[16] ATA Insights, *Webinar - Designing bifacial PV projects.* [Online]. Available: https://atainsights.com/recording-and-presentations-designing-bifacial-pv-projects-2020/ (accessed: Aug. 16 2021).

[17] LG, *Bifacial Design Guide.* [Online]. Available: http://www.lg-solar.com/downloads/brochures/Bifacial_design_guide_Full_ver.pdf (accessed: Jan. 25 2018).

[18] Hanwah Q-Cells, *Bifacial Design Guideline.* [Online]. Available: https://www.q-cells.us/dam/jcr:95c7dc96-f0bf-4bad-9124-928056ce6c78/Q_CELLS_White_Paper_Bifacial_Design_Guideline_2020-01_Rev01_EN.pdf (accessed: Aug. 16 2021).

[19] E. Bellini, "World now has 583.5 GW of operational PV," *pv magazine*, 2020. [Online]. Available: https://www.pv-magazine.com/2020/04/06/world-now-has-583-5-gw-of-operational-pv/

[20] National Renewable Energy Laboratory, *System Advisor Model (SAM)*, 2020. Accessed: Aug. 20 2020. [Online]. Available: https://sam.nrel.gov/

[21] Joint Research Centre, *Photovoltaic geographical information system.* [Online]. Available: http://re.jrc.ec.europa.eu/pvg_tools/en/tools.html (accessed: Feb. 21 2020).

[22] J. Stein *et al.,* "IEA PVPS Task 13 - Performance, Operation and Reliability of Photovoltaic Systems: Bifacial Photovoltaic Modules and Systems: Experience and Results from International Research and Pilot Applications," IEA PVPS, 2021. [Online]. Available: https://iea-pvps.org/wp-content/uploads/2021/04/IEA-PVPS-T13-14_2021-Bifacial-Photovoltaic-Modules-and-Systems-report.pdf

[23] Sandia National Laboratories, *Sky Diffuse Models.* [Online]. Available: https://pvpmc.sandia.gov/modeling-steps/1-weather-design-inputs/plane-of-array-poa-irradiance/calculating-poa-irradiance/poa-sky-diffuse/ (accessed: Aug. 16 2021).

[24] A. Jäger-Waldau, "PV Status Report 2018," European Commission, 2018. Accessed: Apr. 22 2020. [Online]. Available: http://publications.jrc.ec.europa.eu/repository/bitstream/JRC113626/pv_status_report_2018_online.pdf

[25] B. Fleischer, *Systemeffekte von Bioenergie in der Elektrizitäts- und Fernwärmewirtschaft - Eine modellgestützte Analyse langfristiger Energiewendeszenarien in Deutschland*, 2019. Accessed: Aug. 21 2020. [Online]. Available: https://elib.uni-stuttgart.de/handle/11682/10818

Previously published research reports at the IER

Contact:

Universität Stuttgart
Institut für Energiewirtschaft und Rationelle Energieanwendung
Bibliothek

Tel.: +49 711 685 87861
Fax: +49 711 685 87873
E-Mail: bib@ier.uni-stuttgart.de

Orders are also possible via Internet: www.ier.uni-stuttgart.de and https://elib.uni-stuttgart.de.

Band 146 N. Seckinger
Methodische Weiterentwicklung dynamischer, prospektiver Treibhausgasemissionsfaktoren zur Analyse von Technologien der Sektorkopplung
2022

Band 145 M. Unger
Systematische Analyse von Druckluftleckagen
2021

Band 144 Friedrich et al.
Messung und Bewertung der Schadstoffemissionen von Holzfeuerungen in Innenräumen
2020

Band 143 N. Li
Long-term Exposure of European Population Subgroups to PM2.5 and NO_2
August 2020, 152 Seiten

Band 142 M. Miller
Wege zur Ermittlung von Energieeffizienzpotenzialen von Informations- und Kommunikationstechnologien
Februar 2020, 391 Seiten

Band 141 R. Flatau
Integrierte Bewertung interdependenter Energieeffizienzmaßnahmen – Eine modellgestützte Analyse am Beispiel von Querschnittstechnologien
Juli 2019, 216 Seiten

Band 140 B. Fleischer
Systemeffekte von Bioenergie in der Elektrizitäts- und Fernwärmewirtschaft – Eine modellgestützte Analyse langfristiger Energiewendeszenarien für Deutschland

April 2019, 190 Seiten

Band 139 B. Mousavi
Analysis of the relative roles of supply-side and demand-side measures in tackling global climate change – Application of a hybrid energy system model
Januar 2019, 167 Seiten

Band 138 S. Bothor
Prognose von Netzverlusten
August 2019, 152 Seiten

Band 137 C. Schieberle
Development of a stochastic optimization approach to determine costefficient environmental protection strategies: Case study of policies for the future European passenger transport sector with a focus on railbound and on-road activities
Mai 2019, 218 Seiten

Band 136 J. Welsch
Modellierung von energiespeichern und Power-to-X im deutschen und europäischen Energiesystem
Dezember 2018, 158 Seiten

Band 135 E. M. Stenull
Stand und Entwicklungspotenziale der landwirtschaftlichen Biogasnutzung in Baden-Württemberg – ein regionalspezifischer Vergleich
Juni 2017, 171 Seiten

Band 134 J.-C. Brunke
Energieeinsparpotenziale von energieintensiven Produktionsprozessen in Deutschland - Eine Analyse mit Hilfe von Energieeinsparkostenkurven
August 2017, 353 Seiten

Band 133 S. Wolf
Integration von Wärmepumpen in industrielle Produktionssysteme – Potenziale und Instrumente zur Potenzialerschließung
Juni 2017, 177 Seiten

Band 132 S. Marathe
Recognising the Change in Land Use Patterns and its Impacts on Energy Demand and Emissions in Gauteng, South Africa
April 2017, 202 Seiten

Band 131 T. Haasz
Entwicklung von Methoden zur Abbildung von Demand Side Management in einem optimierenden Energiesystemmodell – Fallbeispiele für Deutschland in den Sektoren Industrie, Gewerbe, Handel, Dienstleistungen und Haushalte
April 2017, 177 Seiten

Band 130 M. Steurer
Analyse von Demand Side Integration im Hinblick auf eine effiziente und umweltfreundliche Energieversorgung
April 2017, 230 Seiten

Band 129 S. Bubeck
Potenziale elektrischer Energieanwendungstechniken zur rationellen Energieanwendung
Januar 2017, 255 Seiten

Band 128 R. Beestermöller
Die Energienachfrage privater Haushalte und ihre Bedeutung für den Klimaschutz – Volkswirtschaftliche Analysen zur deutschen und europäischen Klimapolitik mit einem technologiefundierten Allgemeinen Gleichgewichtsmodell
Januar 2017, 211 Seiten

Band 127 M. Ohl
Analyse der Einsatzpotenziale von Wärmeerzeugungstechniken in industriellen Anwendungen
August 2016, 202 Seiten

Band 126 W. Genius
Grüne Bilanzierung - Internalisierung von Umwelt- und Gesundheitsschäden im Rahmen der Input-Output-Rechnung
April 2015, 243 Seiten

Band 125 E. Heyden
Kostenoptimale Abwärmerückgewinnung durch integriert-iteratives Systemdesign (KOARiiS) - Ein Verfahren zur energetisch-ökonomischen Bewertung industrieller Abwärmepotenziale
2016, 121 Seiten

Band 124 K. Ohlau
Strategien zur wirksamen Minderung von Fluglärm in Deutschland - Minderungsmaßnahmen und langfristige Perspektiven
2015, 192 Seiten

Band 123 T. Telsnig
Standortabhängige Analyse und Bewertung solarthermischer Kraftwerke am Beispiel Südafrikas
September 2015, 285 Seiten

Band 122 M. Henßler
Ganzheitliche Analyse thermochemischer Verfahren bei der Nutzung fester Biomasse zur Kraftstoffproduktion in Deutschland
April 2015, 243 Seiten

Band 121 B. Fais
Modelling policy instruments in energy system models - the example of renewable electricity generation in Germany
Januar 2015, 194 Seiten

Band 120 M. Blesl
Kraft-Wärme-Kopplung im Wärmemarkt Deutschlands und Europas – eine Energiesystem- und Technikanalyse
August 2014, 204 Seiten

Band 119 S. Kempe
Räumlich detaillierte Potenzialanalyse der Fernwärmeversorgung in Deutschland mit einem hoch aufgelösten Energiesystemmodell
Juli 2014, 204 Seiten

Band 118 B. Thiruchittampalam
Entwicklung und Anwendung von Methoden und Modellen zur Berechnung von räumlich und zeitlich hochaufgelösten Emissionen in Europa
April 2014, 238 Seiten

Band 117 T. Kober
Energiewirtschaftliche Anforderungen an neue fossil befeuerte Kraftwerkemit CO_2-Abscheidung im liberalisierten europäischen Elektrizitätsmarkt
März 2014, 158 Seiten

Band 116 S. Wissel
Ganzheitlich-integrierte Betrachtung der Kernenergie im Hinblick auf eine nachhaltige Energieversorgung
Februar 2014, 230 Seiten

Band 115 R. Kuder
Energieeffizienz in der Industrie – Modellgestützte Analyse des effizienten Energieeinsatzes in der EU-27 mit Fokus auf den Industriesektor
Februar 2014, 286 Seiten

Band 114 J. Tomaschek
Long-term optimization of the transport sector to address greenhouse gas reduction targets under rapid growth – Application of an energy system model for Gauteng province, South Africa
Dezember 2013, 263 Seiten

Band 113 B. Rühle
Kosten regionaler Energie- und Klimapolitik - Szenarioanalysen mit einem Energiesystemmodell auf Bundesländerebene
November 2013, 196 Seiten

Band 112 N. Sun
Modellgestützte Untersuchung des Elektrizitätsmarktes - Kraftwerkseinsatzplanung und -investitionen
August 2013, 173 Seiten

Band 111 J. Lambauer
Auswirkungen von Basisinnovationen auf die Energiewirtschaft und die Energienachfrage in Deutschland - Am Beispiel der Nano und Biotechnologie

März 2013, 303 Seiten

Band 110 R. Barth
Ökonomische und technisch-betriebliche Auswirkungen verteilter Elektrizitätserzeugung in Verteilungsnetzen - eine modellgestützte Analyse am Beispiel eines Mittelspannungsnetzes
März 2013, 234 Seiten

Band 109 D. Bruchof
Energiewirtschaftliche Verkehrsstrategie - Möglichkeiten und Grenzen alternativer Kraftstoffe und Antriebe in Deutschland und der EU-27
März 2012, 226 Seiten

Band 108 E. D. Özdemir
The Future Role of Alternative Powertrains and Fuels in the German Transport Sector - A model based scenario analysis with respect to technical, economic and environmental aspects with a focus on road transport
Januar 2012, 194 Seiten

Band 107 U. Kugler
Straßenverkehrsemissionen in Europa - Emissionsberechnung und Bewertung von Minderungsmaßnahmen
Januar 2012, 236 Seiten

Band 106 M. Blesl, D. Bruchof, U. Fahl, T. Kober, R. Kuder, B. Götz, A. Voß
Integrierte Szenarioanalysen zu Energie- und Klimaschutzstrategien in Deutschland in einem Post-Kyoto-Regime
Februar 2011, 200 Seiten

Band 105 O. Mayer-Spohn
Parametrised Life Cycle Assessment of Electricity Generation in Hard-Coal-Fuelled Power Plants with Carbon Capture and Storage
Dezember 2009, 210 Seiten

Band 104 A. König
Ganzheitliche Analyse und Bewertung konkurrierender energetischer Nutzungspfade für Biomasse im Energiesystem Deutschland bis zum Jahr 2030
Juli 2009, 194 Seiten

Band 103 C. Kruck
Integration einer Stromerzeugung aus Windenergie und Speichersystemen unter besonderer Berücksichtigung von Druckluft-Speicherkraftwerken
Mai 2008, 162 Seiten

Band 102 U. Fahl, B. Rühle, M. Blesl, I. Ellersdorfer, L. Eltrop, D.-C. Harlinghausen, R. Küster, T. Rehrl, U. Remme, A. Voß
Energieprognose Bayern 2030
Oktober 2007, 296 Seiten

Band 101 U. Remme, M. Blesl, U. Fahl
Global resources and energy trade: An overview for coal, natural gas, oil and uranium
Juli 2007, 108 Seiten

Band 100 S. Eckardt
Energie- und Umweltmanagement in Hotels und Gaststätten: Entwicklung eines Softwaretools zur systematischen Prozessanalyse und Management-unterstützung
Mai 2007, 152 Seiten

Band 99 U. Remme
Zukünftige Rolle erneuerbarer Energien in Deutschland: Sensitivitätsanalysen mit einem linearen Optimierungsmodell
August 2006, 336 Seiten

Band 98 L. Eltrop, J. Moerschner, M. Härdtlein, A. König
Bilanz und Perspektiven der Holzenergienutzung in Baden-Württemberg
Mai 2006, 102 Seiten

Band 97 B. Frey
Modellierung systemübergreifender Energie- und Kohlenstoffbilanzen in Entwicklungsländern
Mai 2006, 148 Seiten

Band 96 K. Sander
Potenziale und Perspektiven stationärer Brennstoffzellen
Juni 2004, 256 Seiten

Band 95 M. A. dos Santos Bernardes
Technische, ökonomische und ökologische Analyse von Aufwindkraftwerken
März 2004, 228 Seiten

Band 94 J. Bagemihl
Optimierung eines Portfolios mit hydro-thermischem Kraftwerkspark im börslichen Strom- und Gasterminmarkt
Februar 2003, 138 Seiten

Band 93 A. Stuible
Ein Verfahren zur graphentheoretischen Dekomposition und algebraischen Reduktion von komplexen Energiesystemmodellen
November 2002, 156 Seiten

Band 92 M. Blesl
Räumlich hoch aufgelöste Modellierung leitungsgebundener Energieversorgungssysteme zur Deckung des Niedertemperaturwärmebedarfs
August 2002, 282 Seiten

Band 91 S. Briem, M. Blesl, M. A. dos Santos Bernardes, U. Fahl, W. Krewitt, M. Nill, S. Rath-Nagel, A. Voß

Grundlagen zur Beurteilung der Nachhaltigkeit von Energiesystemen in Baden-Württemberg
August 2002, 138 Seiten

Band 90 B. Frey, M. Neubauer
Energy Supply for Three Cities in Southern Africa
Juli 2002, 96 Seiten

Band 89 A. Heinz, R. Hartmann, G. Hitzler, G. Baumbach
Wissenschaftliche Begleitung der Betriebsphase der mit Rapsölmethylester befeuerten Energieversorgungsanlage des Deutschen Bundestages in Berlin
Juli 2002, 212 Seiten

Band 88 M. Sawillion
Aufbereitung der Energiebedarfsdaten und Einsatzanalysen zur Auslegung von Blockheizkraftwerken
Juli 2002, 136 Seiten

Band 87 T. Marheineke
Lebenszyklusanalyse fossiler, nuklearer und regenerativer Stromerzeugungstechniken
Juli 2002, 222 Seiten

Band 86 B. Leven, C. Hoeck, C. Schaefer, C. Weber, A. Voß
Innovationen und Energiebedarf - Analyse ausgewählter Technologien und Branchen mit dem Schwerpunkt Stromnachfrage
Juni 2002, 224 Seiten

Band 85 E. Laege
Entwicklung des Energiesektors im Spannungsfeld von Klimaschutz und Ökonomie - Eine modellgestützte Systemanalyse
Januar 2002, 254 Seiten

Band 84 S. Molt
Entwicklung eines Instrumentes zur Lösung großer energiesystemanalytischer Optimierungsprobleme durch Dekomposition und verteilte Berechnung
Oktober 2001, 166 Seiten

Band 83 D. Hartmann
Ganzheitliche Bilanzierung der Stromerzeugung aus regenerativen Energien
September 2001, 228 Seiten

Band 82 G. Kühner
Ein kosteneffizientes Verfahren für die entscheidungsunterstützende Umweltanalyse von Betrieben
September 2001, 210 Seiten

Band 81 I. Ellersdorfer, H. Specht, U. Fahl, A. Voß
Wettbewerb und Energieversorgungsstrukturen der Zukunft

August 2001, 172 Seiten

Band 80 B. Leven, J. Neubarth, C. Weber
Ökonomische und ökologische Bewertung der elektrischen Wärmepumpe im Vergleich zu anderen Heizungssystemen
Mai 2001, 166 Seiten

Band 79 R. Krüger, U. Fahl, J. Bagemihl, D. Herrmann
Perspektiven von Wasserstoff als Kraftstoff im öffentlichen Straßenpersonenverkehr von Ballungsgebieten und von Baden-Württemberg
April 2001, 142 Seiten

Band 78 A. Freibauer, M. Kaltschmitt (eds.)
Biogenic Greenhouse Gas Emissions from Agriculture in Europe
Februar 2001, 248 Seiten

Band 77 W. Rüffler
Integrierte Ressourcenplanung für Baden-Württemberg
Januar 2001, 284 Seiten

Band 76 S. Rivas
Ein agro-ökologisches regionalisiertes Modell zur Analyse des Brennholzversorgungssystems in Entwicklungsländern
Januar 2001, 200 Seiten

Band 75 M. Härdtlein
Ansatz zur Operationalisierung ökologischer Aspekte von "Nachhaltigkeit" am Beispiel der Produktion und Nutzung von Triticale (×*Triticosecale* Wittmack)-Ganzpflanzen unter besonderer Berücksichtigung der luftgetragenen N-Freisetzungen
September 2000, 168 Seiten

Band 74 T. Marheineke, W. Krewitt, J. Neubarth, R. Friedrich, A. Voß
Ganzheitliche Bilanzierung der Energie- und Stoffströme von Energieversorgungstechniken
August 2000, 118 Seiten

Band 73 J. Sontow
Energiewirtschaftliche Analyse einer großtechnischen Windstromerzeugung
Juli 2000, 242 Seiten

Band 72 H. Hermes
Analysen zur Umsetzung rationeller Energieanwendung in kleinen und mittleren Unternehmen des Kleinverbrauchersektors
Juli 2000, 188 Seiten

Band 71 C. Schaefer, C. Weber, H. Voss-Uhlenbrock, A. Schuler, F. Oosterhuis, E. Nieuwlaar, R. Angioletti, E. Kjellsson, S. Leth-Petersen, M. Togeby, J. Munksgaard
Effective Policy Instruments for Energy Efficiency in Residential Space

Heating - an International Empirical Analysis (EPISODE)
Juni 2000, 146 Seiten

Band 70 U. Fahl, J. Baur, I. Ellersdorfer, D. Herrmann, C. Hoeck, U. Remme, H. Specht, T. Steidle, A. Stuible, A. Voß
Energieverbrauchsprognose für Bayern
Mai 2000, 240 Seiten

Band 69 J. Baur
Verfahren zur Bestimmung optimaler Versorgungsstrukturen für die Elektrifizierung ländlicher Gebiete in Entwicklungsländern
Mai 2000, 154 Seiten

Band 68 G. Weinrebe
Technische, ökologische und ökonomische Analyse von solarthermischen Turmkraftwerken
April 2000, 212 Seiten

Band 67 C.-O. Wene, A. Voß, T. Fried (eds.)
Experience Curves for Policy Making - The Case of Energy Technologies
April 2000, 282 Seiten

Band 66 A. Schuler
Entwicklung eines Modells zur Analyse des Endenergieeinsatzes in Baden-Württemberg
März 2000, 236 Seiten

Band 65 A. Schäfer
Reduction of CO_2-Emissions in the Global Transportation Sector
März 2000, 290 Seiten

Band 64 A. Freibauer, M. Kaltschmitt (eds.)
Biogenic Emissions of Greenhouse Gases Caused by Arable and Animal Agriculture - Processes, Inventories, Mitigation
März 2000, 148 Seiten

Band 63 A. Heinz, R. Stülpnagel, M. Kaltschmitt, K. Scheffer, D. Jezierska
Feucht- und Trockengutlinien zur Energiegewinnung aus biogenen Festbrennstoffen. Vergleich anhand von Energie- und Emissionsbilanzen sowie anhand der Kosten
Dezember 1999, 308 Seiten

Band 62 U. Fahl, M. Blesl, D. Herrmann, C. Kemfert, U. Remme, H. Specht, A. Voß
Bedeutung der Kernenergie für die Energiewirtschaft in Baden-Württemberg - Auswirkungen eines Kernenergieausstiegs
November 1999, 146 Seiten

Band 61 A. Greßmann, M. Sawillion, W. Krewitt, R. Friedrich
Vergleich der externen Effekte von KWK-Anlagen mit Anlagen zur getrennten Erzeugung von Strom und Wärme
September 1999, 138 Seiten

Band 60 R. Lux
Auswirkungen fluktuierender Einspeisung auf die Stromerzeugung konventioneller Kraftwerkssysteme
September 1999, 162 Seiten

Band 59 M. Kayser
Energetische Nutzung hydrothermaler Erdwärmevorkommen in Deutschland - Eine energiewirtschaftliche Analyse -
Juli 1999, 184 Seiten

Band 58 C. John
Emissionen von Luftverunreinigungen aus dem Straßenverkehr in hoher räumlicher und zeitlicher Auflösung - Untersuchung von Emissionsszenarien am Beispiel Baden-Württembergs
Juni 1999, 214 Seiten

Band 57 T. Stelzer
Biokraftstoffe im Vergleich zu konventionellen Kraftstoffen - Lebensweganalysen von Umweltwirkungen
Mai 1999, 212 Seiten

Band 56 R. Lux, J. Sontow, A. Voß
Systemtechnische Analyse der Auswirkungen einer windtechnischen Stromerzeugung auf den konventionellen Kraftwerkspark
Mai 1999, 322 Seiten

Band 55 B. Biffar
Messung und Synthese von Wärmelastgängen in der Energieanalyse
Mai 1999, 236 Seiten

Band 54 E. Fleißner
Statistische Methoden der Energiebedarfsanalyse im Kleinverbrauchersektor
Januar 1999, 306 Seiten

Band 53 A. Freibauer, M. Kaltschmitt (Hrsg.)
Approaches to Greenhouse Gas Inventories of Biogenic Sources in Agriculture
Januar 1999, 252 Seiten

Band 52 J. Haug, B. Gebhardt, C. Weber, M. van Wees, U. Fahl, J. Adnot, L. Cauret, A. Pierru, F. Lantz, J.-W. Bode, J. Vis, A. van Wijk, D. Staniaszek, Z. Zavody
Evaluation and Comparison of Utility's and Governmental DSM-Programmes for the Promotion of Condensing Boilers
Oktober 1998, 156 Seiten

Band 51 M. Blesl, A. Schweiker, C. Schlenzig
Erweiterung der Analysemöglichkeiten von *NetWork* - Der Netzwerkeditor
September 1998, 112 Seiten

Band 50 S. Becher
Biogene Festbrennstoffe als Substitut für fossile Brennstoffe - Energie- und Emissionsbilanzen
Juli 1998, 200 Seiten

Band 49 P. Schaumann, M. Blesl, C. Böhringer, U. Fahl, R. Kühner, E. Läge, S. Molt, C. Schlenzig, A. Stuible, A. Voß
Einbindung des ECOLOG-Modells '*E³Net*' und Integration neuer methodischer Ansätze in das *IKARUS*-Instrumentarium (*ECOLOG II*)
Juli 1998, 110 Seiten

Band 48 G. Poltermann, S. Berret
ISO 14000ff und Öko-Audit - Methodik und Umsetzung
März 1998, 184 Seiten

Band 47 C. Schlenzig
PlaNet: Ein entscheidungsunterstützendes System für die Energie- und Umweltplanung
Januar 1998, 230 Seiten

Band 46 R. Friedrich, P. Bickel, W. Krewitt (Hrsg.)
External Costs of Transport
April 1998, 144 Seiten

Band 45 H.-D. Hermes, E. Thöne, A. Voß, H. Despretz, G. Weimann, G. Kamelander, C. Ureta
Tools for the Dissemination and Realization of Rational Use of Energy in Small and Medium Enterprises
Januar 1998, 352 Seiten

Band 44 C. Weber, A. Schuler, B. Gebhardt, H.-D. Hermes, U. Fahl, A. Voß
Grundlagenuntersuchungen zum Energiebedarf und seinen Bestimmungsfaktoren
Dezember 1997, 186 Seiten

Band 43 J. Albiger
Integrierte Ressourcenplanung in der Energiewirtschaft mit Ansätzen aus der Kraftwerkseinsatzplanung
November 1997, 168 Seiten

Band 42 P. Berner
Maßnahmen zur Minderung der Emissionen flüchtiger organischer Verbindungen aus der Lackanwendung - Vergleich zwischen Abluftreinigung und primären Maßnahmen am Beispiel Baden-Württembergs
November 1997, 238 Seiten

Band 41 J. Haug, M. Sawillion, U. Fahl, A. Voß, R. Werner, K. Weiß, J. Rösch, W. Wölfle
Analysis of Impediments to the Rational Use of Energy in the Public Sector and Implementation of Third Party Financing Strategies to improve Energy Efficiency
August 1997, 122 Seiten

Band 40 U. Fahl, R. Krüger, E. Läge, W. Rüffler, P. Schaumann, A. Voß
Kostenvergleich verschiedener CO_2-Minderungsmaßnahmen in der Bundesrepublik Deutschland
August 1997, 156 Seiten

Band 39 M. Sawillion, B. Biffar, K. Hufendiek, R. Lux, E. Thöne
MOSAIK - Ein EDV-Instrument zur Energieberatung von Gewerbe und mittelständischer Industrie
Juli 1997, 172 Seiten

Band 38 M. Kaltschmitt
Systemtechnische und energiewirtschaftliche Analyse der Nutzung erneuerbarer Energien in Deutschland
April 1997, 108 Seiten

Band 37 C. Böhringer, T. Rutherford, A. Pahlke, U. Fahl, A. Voß
Volkswirtschaftliche Effekte einer Umstrukturierung des deutschen Steuersystems unter besonderer Berücksichtigung von Umweltsteuern
März 1997, 82 Seiten

Band 36 P. Schaumann
Klimaverträgliche Wege der Entwicklung der deutschen Strom- und Fernwärmeversorgung - Systemanalyse mit einem regionalisierten Energiemodell
Januar 1997, 282 Seiten

Band 35 R. Kühner
Ein verallgemeinertes Schema zur Bildung mathematischer Modelle energiewirtschaftlicher Systeme
Dezember 1996, 262 Seiten

Band 34 U. Fahl, P. Schaumann
Energie und Klima als Optimierungsproblem am Beispiel Niedersachsen
November 1996, 124 Seiten

Band 33 W. Krewitt
Quantifizierung und Vergleich der Gesundheitsrisiken verschiedener Stromerzeugungssysteme
November 1996, 196 Seiten

Band 32 C. Weber, B. Gebhardt, A. Schuler, T. Schulze, U. Fahl, A. Voß, A. Perrels, W. van Arkel, W. Pellekaan, M. O'Connor, E. Schenk, G. Ryan
Consumers' Lifestyles and Pollutant Emissions
September 1996, 118 Seiten

Band 31 W. Rüffler, A. Schuler, U. Fahl, H.W. Balandynowicz, A. Voß
Szenariorechnungen für das Projekt *Klimaverträgliche Energieversorgung in Baden-Württemberg*
Juli 1996, 140 Seiten

Band 30 C. Weber, B. Gebhardt, A. Schuler, U. Fahl, A. Voß
Energy Consumption and Air-Borne Emissions in a Consumer Perspective
September 1996, 264 Seiten

Band 29 M. Hanselmann
Entwicklung eines Programmsystems zur Optimierung der Fahrweise von Kraft-Wärme-Kopplungsanlagen
August 1996, 138 Seiten

Band 28 G. Schmid
Die technisch-ökonomische Bewertung von Emissionsminderungsstrategien mit Hilfe von Energiemodellen
August 1996, 184 Seiten

Band 27 A. Obermeier, J. Seier, C. John, P. Berner, R. Friedrich
TRACT: Erstellung einer Emissionsdatenbasis für TRACT
August 1996, 172 Seiten

Band 26 T. Hellwig
OMNIUM - Ein Verfahren zur Optimierung der Abwärmenutzung in Industriebetrieben
Mai 1998, 118 Seiten

Band 25 R. Laing
CAREAIR - ein EDV-gestütztes Instrumentarium zur Untersuchung von Emissionsminderungsstrategien für Dritte-Welt-Länder dargestellt am Beispiel Nigerias
Februar 1996, 221 Seiten

Band 24 P. Mayerhofer, W. Krewitt, A. Trukenmüller, A. Greßmann, P. Bickel, R. Friedrich
Externe Kosten der Energieversorgung
März 1996, Kurzfassung, 40 Seiten

Band 23 M. Blesl, C. Schlenzig, T. Steidle, A. Voß
Entwicklung eines Energieinformationssystems
März 1996, 76 Seiten

Band 22 M. Kaltschmitt, A. Voß
Integration einer Stromerzeugung aus Windkraft und Solarstrahlung in den konventionellen Kraftwerksverbund
Juni 1995, Kurzfassung, 51 Seiten

Band 21 U. Fahl, E. Läge, W. Rüffler, P. Schaumann, C. Böhringer, R. Krüger, A. Voß
Emissionsminderung von energiebedingten klimarelevanten Spurengasen in der Bundesrepublik Deutschland und in Baden-Württemberg
September 1995, 454 Seiten

Band 20 M. Fischedick
Erneuerbare Energien und Blockheizkraftwerke im Kraftwerksverbund - Technische Effekte, Kosten, Emissionen
Dezember 1995, 196 Seiten

Band 19 A. Obermeier
Ermittlung und Analyse von Emissionen flüchtiger organischer Verbindungen in Baden-Württemberg
Mai 1995, 208 Seiten

Band 18 N. Kalume
Strukturmodule - Ein methodischer Ansatz zur Analyse von Energiesystemen in Entwicklungsländern
Dezember 1994, 113 Seiten

Band 17 T. Müller
Ermittlung der SO_2- und NO_x-Emissionen aus stationären Feuerungsanlagen in Baden-Württemberg in hoher räumlicher und zeitlicher Auflösung
November 1994, 142 Seiten

Band 16 A. Wiese
Simulation und Analyse einer Stromerzeugung aus erneuerbaren Energien in Deutschland
Juni 1994, 223 Seiten

Band 15 M. Sawillion, T. Hellwig, B. Biffar, R. Schelle, E. Thöne
Optimierung der Energieversorgung eines Industrieunternehmens unter Umweltschutz- und Wirtschaftlichkeitsaspekten - Wertanalyse-Projekt
Januar 1994, 154 Seiten

Band 14 M. Heymann, A. Trukenmüller, R. Friedrich
Development prospects for emission inventories and atmospheric transport and chemistry models
November 1993, 105 Seiten

Band 13 R. Friedrich
Ansatz zur Ermittlung optimaler Strategien zur Minderung von Luftschadstoffemissionen aus Energieumwandlungsprozessen
Juli 1992, 292 Seiten

Band 12 U. Fahl, M. Fischedick, M. Hanselmann, M. Kaltschmitt, A. Voß
Abschätzung der technischen und wirtschaftlichen Minderungspotentiale energiebedingter CO_2-Emissionen durch einen verstärkten Erdgaseinsatz in der Elektrizitätsversorgung Baden-Württembergs unter besonderer Berücksichtigung konkurrierender Nutzungsmöglichkeiten
August 1992, 471 Seiten

Band 11 M. Kaltschmitt, A. Wiese
Potentiale und Kosten regenerativer Energieträger in Baden-Württemberg
April 1992, 320 Seiten

Band 10 A. Reuter
Entwicklung und Anwendung eines mikrocomputergestützten Energieplanungsinstrumentariums für den Einsatz in Entwicklungsländern
November 1991, 170 Seiten

Band 9 T. Kohler
Einsatzmöglichkeiten für Heizreaktoren im Energiesystem der Bundesrepublik Deutschland
Juli 1991, 162 Seiten

Band 8 M. Mattis
Kosten und Auswirkungen von Maßnahmen zur Minderung der SO_2- und NO_x-Emissionen aus Feuerungsanlagen in Baden-Württemberg
Juni 1991, 188 Seiten

Band 7 M. Kaltschmitt
Möglichkeiten und Grenzen einer Stromerzeugung aus Windkraft und Solarstrahlung am Beispiel Baden-Württembergs
Dezember 1990, 178 Seiten

Band 6 G. Schmid, A. Voß, H.W. Balandynowicz, J. Cofala, Z. Parczewski
Air Pollution Control Strategies - A Comparative Analysis for Poland and the Federal Republic of Germany
Juli 1990, 92 Seiten

Band 5 T. Müller, B. Boysen, U. Fahl, R. Friedrich, M. Kaltschmitt, R. Laing, A. Voß, J. Giesecke, K. Jorde, C. Voigt
Regionale Energie- und Umweltanalyse für die Region Neckar-Alb
Juli 1990, 484 Seiten

Band 4 T. Müller, B. Boysen, U. Fahl, R. Friedrich, M. Kaltschmitt, R. Laing, A. Voß, J. Giesecke, K. Jorde, C. Voigt
Regionale Energie- und Umweltanalyse für die Region Hochrhein-Bodensee
Juni 1990, 498 Seiten

Band 3 D. Kluck
Einsatzoptimierung von Kraftwerkssystemen mit Kraft-Wärme-Kopplung
Mai 1990, 155 Seiten

Band 2 M. Fleischhauer, R. Friedrich, S. Häring, A. Haugg, J. Müller, A. Reuter, A. Voß, H.-G. Wystrcil
Grundlagen zur Abschätzung und Bewertung der von Kohlekraftwerken ausgehenden Umweltbelastungen in Entwicklungsländern
Mai 1990, 316 Seiten

Band 1 U. Fahl
KDS - Ein System zur Entscheidungsunterstützung in Energiewirtschaft und Energiepolitik
März 1990, 265 Seiten

Content

Bifacial photovoltaic systems (B-PV) offer the advantage over conventional, monofacial photovoltaic systems that the irradiation incident on the rear side can also be converted into electricity. This makes it possible to significantly increase the energy yield and reduce electricity generation costs. In addition, vertically installed bifacial PV systems (VBPV) facing east and west can provide a complementary generation profile to conventional PV systems with two generation peaks. This can help to increase the economic efficiency of market-oriented PV systems and reduce the integration costs in power supply systems.

Despite these promising features, B-PV has long played a minor role in research, development and application, leaving knowledge gaps in the areas of “energy yield simulation”, “field design” and “integration into power systems”. In order to close the identified knowledge gaps, a new energy yield model was developed, which enables a more precise and holistic calculation of the ground-reflected irradiance. With the help of this model, numerous irradiation- and field design-related influences on the energy yield were investigated and evaluated. Based on a Swiss bifacial PV test site, the developed model was validated.

Furthermore, the model was used to investigate the energy yields and electricity generation costs at various European locations of non-tracking and single-axis tracking bifacial PV systems and recommendations for the optimal field design were derived.

Finally, the profitability and system-friendliness of VBPV was analysed by coupling the developed model with the cost-minimising electricity market model E2M2.

IER Institut für Energiewirtschaft und
Rationelle Energieanwendung
Universität Stuttgart
Heßbrühlstr. 49a
70565 Stuttgart